

**UNIVERSITA' DEGLI STUDI DI NAPOLI**  
**"FEDERICO II"**



DOTTORATO DI RICERCA IN "SCIENZA DEL FARMACO"  
XXVII CICLO 2012-2015

**ISOLATION AND STRUCTURAL ELUCIDATION OF  
BIOACTIVE SECONDARY METABOLITES  
FROM MARINE AND TERRESTRIAL ORGANISMS**

Dr. Annamaria Sinisi

Tutor

Prof. O. Taglialatela-Scafati

Coordinatore

Prof.ssa M. V. D'Auria

La vraie générosité envers l'avenir consiste

à tout donner au présent.

(A. Camus)

# INDEX

<b>INDEX OF FIGURES</b> .....	<b>IV</b>
<b>INDEX OF SCHEMES</b> .....	<b>V</b>
<b>INDEX OF TABLES</b> .....	<b>V</b>
<b>Abstract</b> .....	<b>VII</b>
<b>Abstract (in italiano)</b> .....	<b>VIII</b>
<b>Publications of the candidate during the PhD period</b> .....	<b>XI</b>
<b>CHAPTER 1 - INTRODUCTION</b> .....	<b>1</b>
1.1 NATURE AS INSPIRATION	1
1.1.1 An historical perspective	2
1.1.2 The marine environment	5
1.2 TECHNIQUES AND METHODS	6
1.2.1 Isolation procedures	7
1.2.2 Mass Spectrometry	9
1.2.3 Nuclear Magnetic Resonance	11
1.2.4 Determination of stereochemistry	12
1.2.4.1 Murata's Method	14
1.2.4.2 Marfey's Method	18
1.2.5 General Experimental Section	21
References	23
<b>CHAPTER 2 -BIOACTIVE MACROLIDES, DEPSI-PEPTIDES AND STEROLS FROM THE SPONGE <i>THEONELLA SWINHOEI</i></b> .....	<b>25</b>
2.1 PORIFERA: A TREASURE TROVE OF SECONDARY METABOLITES	25
2.2 <i>THEONELLA SWINHOEI</i>	30
2.3 ISOLATION AND PURIFICATION	32
2.4 MACROLIDES FROM <i>THEONELLA SWINHOEI</i>	33
2.5 DEPSIPEPTIDES FROM <i>THEONELLA SWINHOEI</i>	41
2.6 ANTIPROLIFERATIVE ACTIVITY OF SWINHOLIDES AND THEONELLAPEPTOLIDES.	47
2.7. 4-METHYLENESTEROLS: TYPICAL <i>THEONELLA</i> METABOLITES	52
2.8 PXR MODULATION ACTIVITY OF <i>THEONELLA</i> STEROIDS	53
2.9 EXPERIMENTAL SECTION	61
2.9.1 Animal material, Extraction and Isolation	61
2.9.2 Spectroscopic data for the isolated compounds	62
2.9.3. Evaluation of antiproliferative activity	63

2.9.4. Luciferase assay	63
2.9.5 Real Time PCR	64
2.9.6 Computational Details	65
References	66
<b>CHAPTER 3 -HALOINDOLES FROM <i>IOTROCHOTA PURPUREA</i>.....</b>	<b>72</b>
3.1 HALOGENATED METABOLITES FROM SPONGES	73
3.1.1 Bromoindole alkaloids	74
3.2 ISOLATION AND STRUCTURAL ELUCIDATION OF BROMOINDOLE DERIVATIVES	75
3.3 ANTIKINASE ACTIVITY	77
3.4 EXPERIMENTAL SECTION	78
3.4.1 Animal material, Extraction and Isolation	78
3.4.2 Spectroscopic data for isolated compounds	79
3.4.3 Protein kinases assays	79
References	81
<b>CHAPTER 4 -ANTIMALARIAL AND ANTI-INFLAMMATORY SESQUITERPENE LACTONES FROM <i>VERNONIA AMYGDALINA</i> .....</b>	<b>85</b>
4.1 TRANSMISSION BLOCKING ACTIVITY	87
4.1.1 The burden of malaria	87
4.1.2 The antimalarial potential of plants	91
4.1.3 Antimalarial activity of Vernonia amygdalina extracts	92
4.2 MICHAEL-RELATED BIOACTIVITY OF SESQUITERPENES LACTONES	98
4.2.1 Structure elucidation of new sesquiterpenes lactones	99
4.2.2. Michael related bioactivity: NF-Kb and STAT3 inhibition.	101
4.3 CONCLUSIONS	106
4.4 EXPERIMENTAL SECTION	106
4.4.1 Plant material, extraction and isolation	106
4.4.2 Spectroscopic data for isolated compounds.	108
4.4.3 Cysteamine assay	109
4.4.4 Cytotoxicity assays	110
4.4.5 Transcriptional assays	110
4.4.6 Cell cycle analysis	111
4.4.7 Assessment of transmission blocking activity in vivo	111
References	113
<b>CHAPTER 5 -CONCLUSIONS .....</b>	<b>118</b>
<b>CHAPTER 6 -SPECTRAL DATA.....</b>	<b>119</b>

Spectral data for CHAPTER 2	119
Spectral data for CHAPTER 3	131
Spectral data for CHAPTER 4	133
<b><i>Acknowledgements</i></b> .....	<b>143</b>

## INDEX OF FIGURES

Figure 1.1 ESI mass spectrometry .....	10
Figure 1.2 Ion trajectories in an Orbitrap mass spectrometer. ....	11
Figure 1.3 Values of $^3J_{\text{HH}}$ coupling for the six staggered rotamers corresponding to two different diastereomers <i>erythro</i> and <i>threo</i> .....	15
Figure 1.4 Structure of L-FDAA .....	19
Figure 1.5 Structure of D and L aminoacids L-FDAA derivatives. ....	20
Figure 2.1 Some examples of Porifera. ....	25
Figure 2.2 A sponge body structure.....	26
Figure 2.3 Microscope image of spicules.....	27
Figure 2.4 Schematic diagram of symbiotic relationships between sponges and microorganisms. A, extracellular exosymbiosis; B, extracellular endosymbiosis; C, intracellular symbiosis; and D, intranuclear symbiosis. ....	28
Figure 2.5 A specimen of the sponge <i>Theonella sp.</i> collected in the area of Bunaken Marine Park of Manado (Indonesia).....	30
Figure 2.6 Some molecules from <i>Theonella swinhoei</i> . ....	31
Figure 2.7 Comparison between the resonances of isoswinholide B (5) and swinholide A (1) in selected regions. $\Delta\delta$ (isoswinholide B – swinholide A) is reported in ppm.....	35
Figure 2.8 Key COSY and HMBC correlation detected for the C-1/C-8 moiety of swinholide K (6).....	39
Figure 2.9 Application of the Murata's method to the C-5/C-6 and C-6/C-7 bonds of swinholide K (6).....	39
Figure 2.10 COSY and key KMBC correlations (left) and MS/MS fragmentations of 8 and its ring-opened methanolysis product, respectively. ....	43
Figure 2.11 Crystal structure of actin in complex with swinholide A. ....	48
Figure 2.12 Anti-proliferative activity of theonellapeptolides 7-9 on hepatic carcinoma cell line.* .....	49
Figure 2.13 Anti-proliferative activity of swinholides (1-6) on hepatic carcinoma cell line.* .....	51
Figure 2.14 Transactivation assay performed on HepG2 cells transiently transfected with full-length FXR,RXR, $\beta$ gal and the canonical FXRE containing 3 inverted repeats (IR1). * .....	56
Figure 2.15 Concentration response-curves for 17 and 21.* .....	58

Figure 2.16 Real-Time PCR analysis of mRNA relative expression of the PXR target genes CYP3A4, MDR1, MPR3 in HepG2 cells treated with Rifaximin (10 $\mu$ M), 17 and 21 (10 $\mu$ M).*	59
Figure 2.17 Representation of the binding mode of the agonist prenicasterol 17 (violet sticks in A) and 21 (cyan sticks in B) predicted by docking calculations in the PXR LBD (PBD code 3HVL).*	60
Figure 3.1 <i>Iotrochota purpurea</i>	72
Figure 3.2 Key HMBC correlation for matemone B (7).	77
Figure 4.1 The malaria cell cycle	88
Figure 4.2 Proportion of mature ookinetes with respect to total early sporogonic stage.*	95
Figure 4.3 Selected 2D NMR correlations of vernomygdalin (15). <i>left</i> : COSY (boldened lines) and HMBC correlations (arrows); <i>right</i> : ROESY correlations.	100
Figure 4.4 Results of the cysteamine assay for vernolide (8) and vernodalol (9). The reactive Michael acceptor moiety is marked in red.	102
Figure 4.5 Comparative cysteamine assay of a ca. equimolecular mixture of vernolide (8) and vernodalol (9). A) reference mixture B) spectrum obtained after the addition of a stoichiometric amount (1.0 equivalent) of cysteamine.	103
Figure 4.6 Vernolide induces cell cycle arrest*	105

## INDEX OF SCHEMES

Scheme 1.1 Modified Kupchan's partitioning methodology.	8
Scheme 1.2 Identification of the single conformer with a correct configuration from the staggered rotamers with threo (syn) and erythro (anti) arrangements through the combined use of measured $^3J_{\text{HH}}$ and $^{2,3}J_{\text{CH}}$ values.	17

## INDEX OF TABLES

Table 2.1 $^1\text{H}$ (700 MHz) and $^{13}\text{C}$ (175 MHz) NMR data of isoswinholide B (5) in $\text{CD}_3\text{OD}$ .	36
Table 2.2 $^1\text{H}$ (700 MHz) and $^{13}\text{C}$ (175 MHz) NMR data of swinholide K (6) in $\text{CD}_3\text{OD}$ .	40
Table 2.3 $^1\text{H}$ (500 MHz) and $^{13}\text{C}$ (125 MHz) NMR data of sulfinyltheonellaepetolide in $\text{CD}_3\text{OD}$ (8).	45

Table 2.4 $^1\text{H}$ (500 MHz) and $^{13}\text{C}$ (125 MHz) NMR data of theonellapeptolide If (9) in $\text{CD}_3\text{OD}$ . .....	47
Table 2.5 $\text{IC}_{50}$ and efficiency (as % of growth inhibition .....	50
Table 4.1 Inhibitory activity of ethylacetate phase fractions from <i>V. amygdalina</i> leaves against early sporogonic stages. ....	93
Table 4.2 Impact of vernolide and vernodalol on the development of early sporogonic stages in vitro .....	94
Table 4.3 Activity of <i>V. amygdalina</i> extracts, fractions and pure compounds on cell viability of a human colon cancer and endothelial cell line.....	97
Table 4.4 Activity of <i>V. amygdalina</i> sesquiterpenoids on inhibition of NF- $\kappa$ B and STAT3, activation of Nrf2 and cytotoxicity in DU145 cells. ....	104

## Abstract

Natural products have historically been a rich source of “lead compounds” in drug discovery. The investigation of terrestrial plants and marine organisms aimed at searching new biologically active compounds is a central issue of this kind of studies, through structure elucidation combined with biological evaluation. My research work, described in this PhD thesis, falls within this research field and was addressed at three different topics: - i) isolation and structural elucidation of cytotoxic macrolides and depsipeptides and sterols active on PXR receptors from sponge *Theonella swinhoei*; ii) isolation and structural elucidation of metabolites modulating kinase activity from sponge *Iotrochota purpurea*; iii) isolation and analysis of correlation between reactivity and bioactivity for antimalarial and anti-inflammatory metabolites from the African plant *Vernonia amygdalina*. The structure elucidation of new molecules was performed using advanced spectroscopic techniques (2D-NMR and MS) and advanced methods of stereochemical determination (Murata’s method and Marfey’s method).

The chemical investigation of spongal metabolites carried out during my PhD was financed by the European project “Bluegenics”. Several structurally interesting bioactive molecules have been isolated from *Theonella* sp., namely swinholides (cyclic 44-member macrolides) and theonellapeptolides (cyclic tridecadepsipeptides with a large amount of non-ribosomal amino acids), both featuring *in vitro* antiproliferative activity and providing important information regarding structure-activity relationship. The class of 4-methylensterols, typical of *Theonella* sponges, showed activity on nuclear receptor PXR, shedding light on structure-activity relationships useful for synthesis of lead compounds to be used for therapy of metabolic diseases.

Regarding the second topic, the isolation of haloindole derivatives, by bioguided approach, allowed their evaluation for antikinase activity, which could have an important impact on the manipulation of cell proliferation, diabetes, and neurodegenerative disorders.

Finally, a bioguided analysis of *Vernonia amygdalina*, a plant from Africa used as foodstuff and as drugs in the folk medicine, allowed the characterization of plant extracts for stage specific effects on gametocytes and sporogonic stages

of *Plasmodium* and identification of compounds responsible for antimalarial activity. In particular, leaves of *V. amygdalina* contain sesquiterpene lactones vernolide and vernodalol featuring this kind of activity; thus, they have a potential for drug discovery and for the development of standardized *V. amygdalina* based phytomedicines. The second aim of the investigation on *V. amygdalina* was the isolation and structural elucidation of a series of sesquiterpene compounds with Michael related bioactivity, capable of shedding light on the molecular mechanisms underlying the anti-inflammatory and anticancer activities detected for the extract. On these series, cysteamine assay proved to be a tool to build a sort of Michael-oma profile of this class of metabolites, identifying the most reactive site in polyfunctional compounds and ranking them in terms of reactivity. Considering the correlation between thia-Michael acceptor reactivity and modulation of important biological target, sesquiterpene lactones were evaluated on transcription factors NF- $\kappa$ B, STAT3 and Nrf2 involved in cancer initiation and progression, concluding that vernolide is the major anti-inflammatory constituent of extracts and elucidating the anticancer activity reported.

## **Abstract (in italiano)**

I composti di origine naturale costituiscono storicamente una ricchissima fonte di "lead compound" utili al processo di drug discovery. In questo ambito, la ricerca di nuove molecole biologicamente attive da piante ed organismi marini costituisce un capitolo centrale, attraverso la determinazione strutturale combinata alla valutazione dell'attività biologica. Il lavoro di ricerca descritto in questa tesi di dottorato si è inserito in questo campo, ed è stato indirizzato a tre diversi topic: i) isolamento e determinazione strutturale di macrolidi e depsipeptidi citotossici e steroli attivi sui recettori PXR dalla spugna *Theonella swinhoei*; ii) isolamento e determinazione strutturale di metaboliti aventi attività modulatrice sulle chinasi dalla spugna *Iotrochota purpurea*; iii) isolamento e analisi della correlazione tra bioattività e reattività per metaboliti antimalarici ed antinfiammatori dalla pianta *Vernonia amygdalina*. La determinazione

strutturale delle nuove molecole isolate è stata effettuata utilizzando metodologie spettroscopiche avanzate (2D-NMR e MS) e tecniche per la determinazione della stereochimica (metodi di Marfey e di Murata).

L'analisi chimica di metaboliti provenienti da spugne condotta durante il mio dottorato è stata finanziata dal progetto europeo Bluegenics. Diverse molecole bioattive, molto interessanti da un punto di vista strutturale, sono state isolate da *Theonella sp.*: swinholidi (macrolidi ciclici a 44 termini) e theonellapeptolidi (tridecadepsipectidi ciclici ricchi in aminoacidi non ribosomiali), che hanno mostrato *in vitro* un'azione antiproliferativa che ha fornito importanti informazioni riguardo alle relazioni tra struttura delle macromolecole ed attività. La classe dei 4-metilensteroli, molecole caratteristiche delle spugne *Theonella sp.*, hanno mostrato un'attività modulatrice sui recettori nucleari PXR, facendo luce sulle relazioni tra struttura e attività utili alla sintesi di lead compounds per la terapia di disturbi metabolici.

Riguardo il secondo topic, l'isolamento di derivati aloindolici, tramite un approccio bioguidato, ha permesso la valutazione dell'attività antichinastica, che potrebbe avere un forte impatto sulla modulazione di proliferazione cellulare, diabete e disordini neurodegenerativi.

Infine, l'analisi fitochimica della pianta africana *Vernonia amygdalina*, utilizzata come alimento e come farmaco nella medicina tradizionale, ha condotto alla caratterizzazione degli estratti per gli effetti stadio-specifici sulle fasi gametocitica e sporogonica del ciclo vitale di *Plasmodium* e l'identificazione dei composti responsabili dell'attività antimalarica. In particolare, le foglie di *V. amygdalina* contengono i lattoni sesquiterpenici vernolide e vernodalolo dotati di questo tipo di attività, evidenziando il potenziale della pianta per il drug discovery e per lo sviluppo di un fitofarmaco basato su estratti standardizzati. Il secondo obiettivo è stato l'isolamento e la determinazione strutturale di una serie di composti sesquiterpenici, aventi bioattività correlata alla reattività di Michael, utile a far luce sui meccanismi molecolari che sono alla base delle attività antinfiammatoria ed anticancro già riportate in letteratura per gli estratti di questa pianta. Su questa serie di molecole, è stata, quindi, validata l'utilità del

saggio della cisteamina nella creazione di un profilo Michael-oma di questa classe di metaboliti, identificando il sito più reattivo nei composti polifunzionali e stabilendo un ranking di reattività tra questi composti. In considerazione della correlazione tra reattività di tipo thia-Michael e modulazione di importanti target biologici, è stata effettuata la valutazione dei lattoni sesquiterpenici sui fattori di trascrizione NF- $\kappa$ B, STAT3 e Nrf2, coinvolti nelle fasi iniziali e nel progredire delle patologie cancerose, individuando nel vernolide il composto con maggiore attività antinfiammatoria dell'estratto e dando una spiegazione all'attività anticancro riportata per la pianta.

## Publications of the candidate during the PhD period

1. Sinisi A., Calcinai B., Cerrano C., Dien H.A., Zampella A., D'Amore C., Renga B., Fiorucci S., Tagliatela-Scafati O., Isoswinholide B and swinholide K, potently cytotoxic dimeric macrolides from *Theonella swinhoei*, *Bioorganic & Medicinal Chemistry*, **2013**, *21*, 5332-5338.
2. Sinisi A., Calcinai B., Cerrano C., Dien H.A., Zampella A., D'Amore C., Renga B., Fiorucci S., Tagliatela-Scafati O., New tricaepptides of the theonellapeptolide family from the Indonesian sponge *Theonella swinhoei*, *Bellstein Journal of Organic Chemistry*, **2013**, *9*, 1643-1651.
3. Sepe V., D'Amore C., Ummarino R., Renga B., D'Auria M. V., Novellino E., Sinisi A., Tagliatela-Scafati O., Nakao Y., Limongelli V., Zampella A., Fiorucci S., Insights on pregnane-X-receptor modulation. Natural and semisynthetic steroids from *Theonella* marine sponges, *European Journal of Medicinal Chemistry*, **2014**, *73*, 126-134.
4. Anokwuru, C., Sinisi A., Amidou, S., Tagliatela-Scafati, O., Antibacterial and antioxidant constituents of *Acalypha wilkesiana*, *Natural Product Research*, **2015**, DOI: 10.1080/14786419.2014.983105
5. Sinisi A., Virgilio A., Russo V., Gerardo S., Santoro A., Galeone A., Tagliatela-Scafati O., Roperto F., Ptaquiloside, the major carcinogen of bracken fern, in the pooled raw milk of healthy sheep and goats: an underestimated, global concern of food safety, *Journal of Agricultural and Food Chemistry*, in press.
6. Abay S., Lucantoni L., Dahiya N., Dori G., Dembo E. G., Esposito F., Lupidi G., Ogboi S., Ouédraogo R. K., Sinisi A., Tagliatela-Scafati O., Yerbanga S. R., Bramucci M., Quassinti L., Ouédraogo J., Christophides G. and Habluetzel A., Plasmodium transmission blocking activities of *Vernonia amygdalina* extracts and isolated compounds, *Malaria Journal*, submitted.
7. Sinisi A., Millàn E., Abay S., Habluetzel A., Appendino G., Muñoz E., Tagliatela-Scafati O., Poly-electrophilic sesquiterpene lactones from

*Vernonia amygdalina*: new members and differences in their mechanism of thiol-trapping and in bioactivity, *Journal of Natural Products*, submitted.

# CHAPTER 1 - INTRODUCTION

---

## 1.1 NATURE AS INSPIRATION

Natural products can be considered the foundation of the pharmaceutical industry. Despite a period in which pharmaceutical companies cut back on their use of natural products in drug discovery, there are many promising drug candidates in the current development pipeline that are of natural origin and today natural product-based drug discovery is experiencing a renaissance. Technical drawbacks associated with natural product research have been lessened, and there are better opportunities to explore the biological activity of previously inaccessible sources of natural products. With the increasing acceptance that the chemical diversity of natural products is well suited to provide the core scaffolds for future drugs, there will be further developments in the use of novel natural products and chemical libraries based on natural products in drug discovery campaigns. In particular, the marine environment, a rich source of structurally unique, bioactive metabolites, has produced a number of drug candidates that are currently in clinical trials. In the everexpanding search for sources of new chemical diversity, the exploration of deep-sea fauna has emerged as a new frontier in drug discovery and development.

Natural products have inspired many developments in organic chemistry, leading to advances in synthetic methodologies and to the possibility of preparing analogues of the original lead compound with improved pharmacological or pharmaceutical properties. Natural product scaffolds have also been well recognized as being 'privileged' structures in terms of their ability to be the basis for successful drugs. Such scaffolds are being used as cores of compound libraries made by combinatorial techniques. With the application of various techniques to create analogues and derivatives of natural products, it becomes possible to derive novel compounds that can be patented, even when the original structure was previously disclosed.

Plants and marine organisms produce many biologically active substances for defense and other ecological purposes, and so these substances are uniquely tailored to fit into a biological receptor of some kind: this is one of the several

reasons why natural products have proved to be such a prolific source of bioactive agents. Natural products are often large molecules with built-in chirality and are thus uniquely suited to bind to complex proteins and other biological receptors. As a result of these considerations, there is a high correlation between the properties of drugs and those of natural products.

The research work described in this PhD thesis has been performed at the Department of Pharmacy of Università di Napoli "Federico II" and, for a semester, at CNRS-Paris. It was addressed at different aspects of the research on marine and terrestrial natural products, with special attention to the "core activity" of natural product chemistry, i.e. isolation and structure elucidation of new bioactive compounds.

The activity described in this PhD thesis followed three different research projects:

- a) Isolation and structural elucidation of cytotoxic macrolides and depsipeptides and PXR-modulating steroids from Indonesian sponge *Theonella swinhoei*.
- b) Isolation and structural elucidation of metabolites modulating kinase activity from Indonesian sponge *Iotrochota purpurea*.
- c) Isolation and analysis of correlation between reactivity and bioactivity for antimalarial and anti-inflammatory metabolites from African plant *Vernonia amygdalina*.

The results obtained during my Ph.D. have been reported in seven papers (listed at the end of this chapter) already published or submitted for publication.

### **1.1.1 An historical perspective<sup>1-2</sup>**

For centuries China led the world in the use of natural products for healing. Shen Nung Pen Ts'ao is a detailed report of Chinese herbs which lists 385 materials. Pen Ts'ao Ma catalogue, written by Li-Chen during the Ming Dynasty, (1573–1620) mentions 1898 herbal drugs and 8160 prescriptions. The number of medicinal herbs used in 1979 in China numbered 5967. One of the most famous Chinese folk herbs is the ginseng (*Panax ginseng*) root, used for treatment of various diseases. The active principles were thought to

be the saponins called ginsenosides. The extract of the Ginkgo tree, *Ginkgo biloba* L., another popular medicine, can improve memory and sharpen mental alertness. The Indian hemp plant, *Cannabis sativa*, has been used since 3000 BC, and it is also used as marijuana or hashish. Its constituent,  $\Delta^9$ -THC (tetrahydrocannabinol) is responsible for its mind-altering effect. Mechoulam has been the principal scientist in this field and the first to elucidate the structure of  $\Delta^9$ -THC. During the 17th century, the Jesuits brought with them from South America the bark of the cinchona *Cinchona officinalis* (called quina-quina by the Indians) for the treatment of malaria. In 1820, active compound quinine has been isolated from the China tree. Alkaloids are the major constituents of the herbal plants and the extracts used for centuries, but it was not until the early nineteenth century that the active principles were isolated in pure form, for example morphine (1816), atropine (1819). It was a century later that the structures of these compounds were finally elucidated. Modern methods used to separate complex organic mixtures can separate samples rapidly and efficiently in the picogram range. This has been impossible until recently. Among the recent outstanding contributions to the chemistry of natural products is the conformational analysis designed by Derek Barton. Using conformational analysis, he determined the structures of many key terpenoid. Robert B. Woodward was involved in the structural determinations of penicillin, strychnine, patalin, terramycin, aureomycin and the synthesis of Vitamin B12. His paper published in 1941-42 on empirical rules for estimating the absorption maxima of enones and dienes made the general organic chemical community realize that UV could be used for structural studies, thus launching the beginning of the spectroscopic revolution which soon brought on the applications of IR, NMR and MS. As chemical techniques improved, the active constituents were isolated from plants, were structurally characterized, and in due course, many were synthesized in the laboratory. Sometimes, more active or better tolerated drugs were produced by chemical modification (semi- synthesis), or by total synthesis of analogues of the active principles.

The investigation on the biosynthesis, a metabolic sequences leading to various selected classes of natural products, is of pivotal importance in

Natural Product Chemistry. The term natural product is generally used to mean a secondary metabolite: a small molecule that is not essential to the growth and development of the producing organism. Such compounds are found only in specific organisms, or group of organisms, and are an expression of the individuality of species. Well over 300,000 secondary metabolites probably exist. Unraveling the biosynthetic pathways by which natural products are made is difficult and time-consuming work, but is fundamental to understand how organisms function at the molecular level. The molecules are sometimes complex, but the building blocks for their biosynthesis derived from primary metabolism. It has been established that the primary synthetic process in nature is photosynthesis by which green plants utilize the energy of the sun for the production of organic compounds from carbon dioxide. The initial products of photosynthesis are carbohydrates. Further metabolic alterations lead to the formation of a pool of organic compounds of low molecular weight and simple structures such as carboxylic- and amino acids, which are vital for the living organisms. They form the synthetic starting materials for specific, genetically controlled, enzymatically catalyzed reactions that lead to the complex compounds that characterize the secondary metabolism of plants and mammals. In many cases, a suitable cofactor, e.g.  $\text{NAD}^+$ , PLP, HSCoA, as well as the substrate, may also be bound to participate in the transformation. Enzymes have the power to effect these transformation more efficiently and more rapidly than the chemical analogy, and also under very much milder conditions. Where relevant, they also carry out reactions in stereospecific manner. Some of the important reaction frequently encountered are alkylation, oxidation and reduction, decarboxylation, aldol and Claisen reactions.

The reaction pathway leading to a particular natural product is called the biosynthetic pathway and the corresponding event is known as biogenesis. By far the most important building blocks employed in the biosynthesis of secondary metabolites are derived from the intermediates acetyl coenzyme A (acetyl-CoA), shikimic acid, mevalonic acid, and 1-deoxyxylulose 5-phosphate. These are utilized respectively in the acetate, shikimate, mevalonate, and deoxyxylulose phosphate pathways.

### **1.1.2 The marine environment**

The study of marine natural products is considerably far behind that of compounds of terrestrial origin due to the difficulty in collection and identification of marine organisms. However, in spite of these difficulties, the marine environment has proven to be a very rich source of extremely potent compounds that have demonstrated significant activities in antitumor, anti-inflammatory, analgesia, immuno-modulation, allergy, and antimicrobial assays.<sup>3</sup> Bioactive products have been isolated from animals and plants as well as from marine microorganisms such as bacteria and fungi, protozoa and chromista.

The oceans cover more than 70% of the earth's surface and contain more than 300,000 described species of plants and animals.<sup>4-5</sup> Macroscopic organisms have adapted to all regions of the oceans, including polar, temperate, and tropical areas. The diversity in species is extraordinarily rich on coral reefs, where there are around 1,000 species per m<sup>2</sup> in some areas, with the Indo-Pacific Ocean having the world's greatest tropical marine biodiversity. The number and the activity of the natural products is directly related to the level of biodiversity of a marine area. The most interesting and promising marine natural products are small- to medium- molecular weight compounds produced principally by marine invertebrates (sponges, tunicates, soft corals) and microbes that have stimulated interdisciplinary studies by chemists, biologists and pharmacologists. The incredible potential of even a single marine organism to produce a large array of secondary metabolites can be interpreted by considering the common features of the secondary metabolism in all the living organisms as well as some peculiar features of the marine environment. Secondary metabolites play an essential role for the adaptation of the producer organism to the environment, mainly, but not uniquely, in terms of defence; they are practically the sole tool in the hands of organisms at lower evolutionary levels or lacking of mechanical or morphological way for protecting themselves (this is the case of sessile organisms as plants, algae, and the marine invertebrates sponges, tunicates, and bryozoans).

For all the reasons above summarized, it is not surprising that a thorough chemical analysis of a single marine invertebrate, carried out with non-destructive modern spectroscopic techniques (allowing the stereostructure elucidation of molecules isolated in the low milligram range) can afford tens, when not hundreds, of secondary metabolites. These products provide a rich source of chemical diversity that can be fruitfully used as a “natural combinatorial library”, frequently more rich and chemically diverse than the libraries obtained through the use of synthetic combinatorial chemistry. Ideally, this “natural library” can be screened in order to find lead compounds to be used as inspiration to design and develop new potentially useful therapeutic agents and to gain the first information about the structure-activity relationships.

In spite of the difficulties associated with the limited availability of the compounds under investigation, which is strictly related to the limited supply of the biological material correctly protected for environmental concerns, some interesting results have been obtained. Through the combined efforts of marine natural product chemists and pharmacologists, an astounding array of promising compounds have been identified. Some of these molecules are either at advanced stages of clinical trials or have been selected as promising candidates for extended pre-clinical evaluation. The majority of these products fall within the area of antimicrobial and cancer therapies. Just to cite an example, ecteinascidin 743 (ET-743): the Spanish company PharmaMar licensed the compound from the University of Illinois before 1994. It is sold by Zeltia and Johnson and Johnson under the brand name Yondelis. It is approved for use in Europe, Russia and South Korea for the treatment of advanced soft tissue sarcoma. It is also undergoing clinical trials for the treatment of breast, prostate, and paediatric sarcomas.

## **1.2 TECHNIQUES AND METHODS**

Recently, natural products chemistry has undergone explosive growth due to advances in isolation techniques, synthetic and biosynthetic approaches as well as spectroscopic and chromatographic methods. For the discovery of new compounds from natural source it is important to characterize these

new compounds in a non-destructive way, with submilligram samples. The study of natural compounds can be divided in the following steps:

- ✓ Isolation and purification from biologic material;
- ✓ Structural determination;
- ✓ Determination of absolute and relative configuration

### ***1.2.1 Isolation procedures***

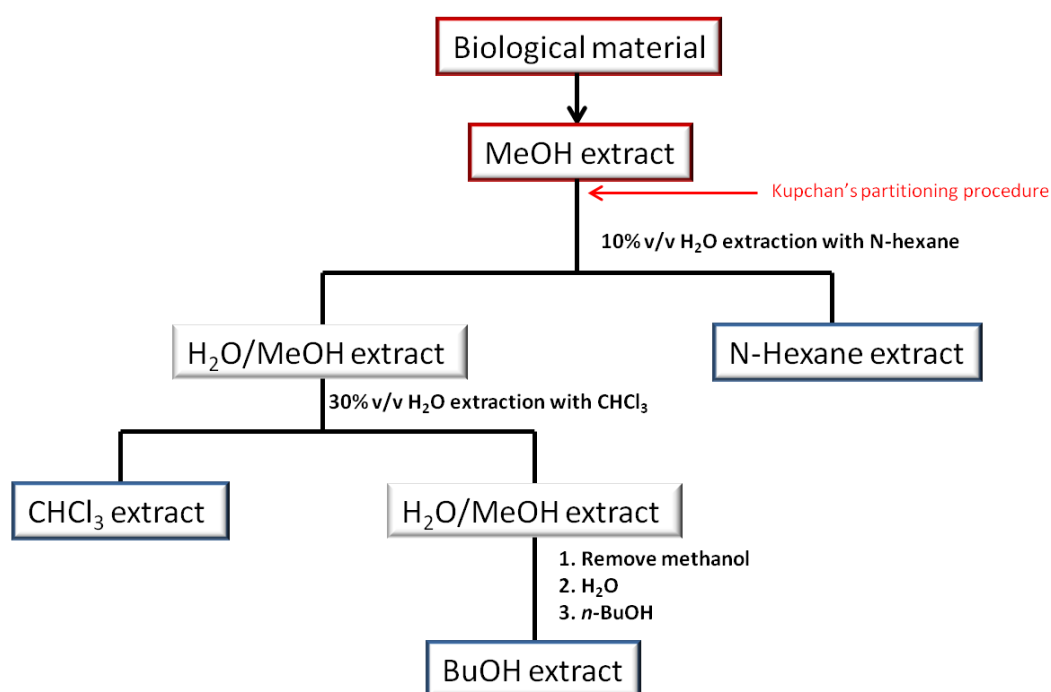
The isolation of natural products from the producing organisms poses numerous problems, because these compounds may only be present in infinitesimal quantities. The nature of the separation problem varies considerably, from the isolation of small quantities (milligrams or less) for structure determination purposes to the isolation of very much larger amounts (hundred milligram to gram quantities) for comprehensive biological testing, for semi-synthetic work or even for production of therapeutic agents. For these purposes, a good selection of different techniques is really important. The problem of separation and isolation of new metabolites from natural sources was solved with the development of techniques, such as the various analytical and preparative chromatographic methods.

First, biological materials is extracted with an organic solvent, such as methanol. Then, the crude extract is partitioned between solvent with different polarity. In some cases, a modified Kupchan's partitioning methodology<sup>6</sup> has been used in this research. In this procedure, the composition of aqueous phase is adjusted sequentially as follows (**Scheme 1.1**).

- The methanol extract is dissolved in a mixture of 10% H<sub>2</sub>O/MeOH and partitioned against n-hexane; hexane extract obtained is rich in lipophilic compounds.
- The water content (% v/v) of the MeOH extract is adjusted to 30% and partitioned against CHCl<sub>3</sub>; in this extract compounds with medium polarity were usually found.

- MeOH is removed from the aqueous phase by evaporation, and then the aqueous phase is extracted with *n*-BuOH; this final extract contains polar compounds.

In this way, four extracts (n-hexane, CHCl<sub>3</sub>, n-BuOH and H<sub>2</sub>O extracts) can be obtained. Crude extracts are further fractionated through sequential chromatographic techniques. The initial stages of a separation procedure involve methods with a high loading capacity and cheap stationary phases - these have traditionally been column chromatography with silica gel or liquid-liquid methods. Subsequent steps employ techniques which require smaller samples - HPLC, for example.



**Scheme 1.1** Modified Kupchan's partitioning methodology.

MPLC (Medium Pressure Liquid chromatography) is a preparative liquid-solid chromatography: medium pressure is used to force liquid mobile phase through the solid stationary phase. MPLC is more efficient in resolution than the open-column and the separation involves a considerable gain in time. The solid stationary phase can be a normal phase, like silica gel, or bonded phase (RP-8, RP-18). The technique makes use of pressures of *ca.* 5-40 bar and can easily accommodate much larger sample loads (100 mg-100 g) than are generally applied in other separations.

High Performance (or High Pressure) Liquid Chromatography (HPLC) , both normal-phase and reverse-phase, is the most widely used chromatographic method, and finds application in the preparative separation of samples to “pilot” the preparative isolation of natural products (optimization of the experimental conditions, checking of the different fractions throughout the separation). On the whole, however, HPLC is commonly applied as the last step in purification processes affording pure compounds in high yields.

Finally the structure of isolated compounds is characterized and molecules are submitted to pharmacological assays.

### **1.2.2 Mass Spectrometry**

Mass Spectrometry is an analytical technique, particularly used in organic chemistry, which allows to measure molecular masses of unknown compounds and thus to determine their elementary formula. Unlike spectroscopic techniques, mass spectrometry is a destructive technique, and it is not based on the interaction between radiations and matter. Any molecule has first to be ionized and transferred to gas phase in the ion source and then it is transmitted to the mass analyzer where its mass properties are measured. These three fundamental steps of the process occur in three different parts of the mass spectrometer, namely *ionisation source*, *analyser*, and *detector*. In order to obtain a mass spectrum, ions in a gas-phase must be produced in the ion source. They are subsequently accelerated, by an electric field, until they get to a specific speed and they are transferred to the mass analyzer, which separate different ions on the base of their mass/charge ( $m/z$ ) ratio. The separated ions are then measured on the detector and the results displayed.

Most of compounds described in the following chapters have been analyzed by *Electrospray Ionisation* (ESI) mass spectrometry through an *Orbitrap* system.

ESI mass spectrometry allows the determination of non-volatile molecules to be analyzed directly from the liquid phase (**Fig.1.1**). The electrospray process is governed by a large number of chemical and physical parameters that

together determine the quality of the process. Its start and end can be defined by an electrical circuit that drives the spray of liquid-charged droplets.

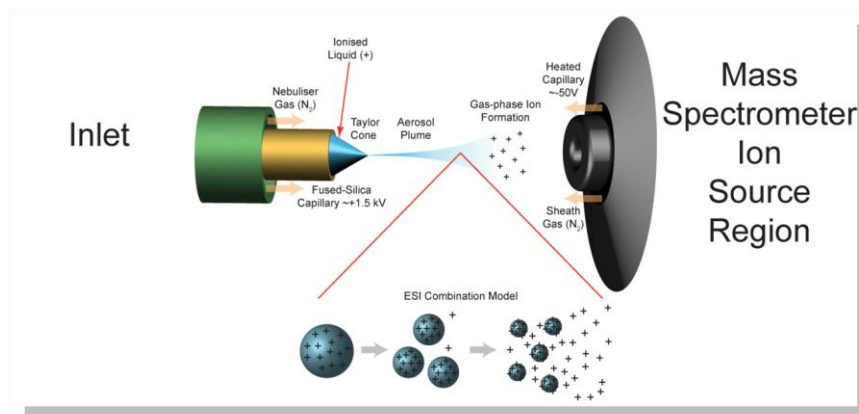


**Figure 1.1** ESI mass spectrometry

In this process, the biomolecule starts out as an entity or complex, usually charged and dissolved in a water-rich environment. At the end of the process the same biomolecule is represented and harvested through the orifice of a mass analyser as a series of 'naked' multicharged ions. In a vacuum, the biomolecular ions then are selectively analysed according to their mass/charge ratio. Because of the electric potential of the capillary, each droplet of the spray carries an excess positive or negative charge, and this causes extensive protonation or deprotonation of the molecules of the sample, which become ions. An uncharged carrier gas such as nitrogen is used to help the liquid to nebulize and the neutral solvent in the droplets to evaporate.

Orbitrap is a new type of mass analyzer introduced by Makarov.<sup>7</sup> The LTQ-Orbitrap combines the most advanced Ion Trap and Fourier Transform technologies into a single instrument with unprecedented analytical power and versatility. The instrument provides a high mass resolution, accurate mass determinations, and MS<sup>n</sup> for routine high-throughput analysis.

In an Orbitrap, ions are injected tangentially into the electric field between the electrodes and trapped because their electrostatic attraction to the inner electrode is balanced by centrifugal forces. Thus, ions cycle around the central electrode in rings. In addition, the ions also move back and forth along the axis of the central electrode. Therefore, ions of a specific mass-to-charge ratio move in rings which oscillate along the central spindle (**Fig.1.2**).

The frequency of these harmonic oscillations is independent of the ion velocity and is inversely proportional to the square root of the mass-to-charge ratio ( $m/z$ ).

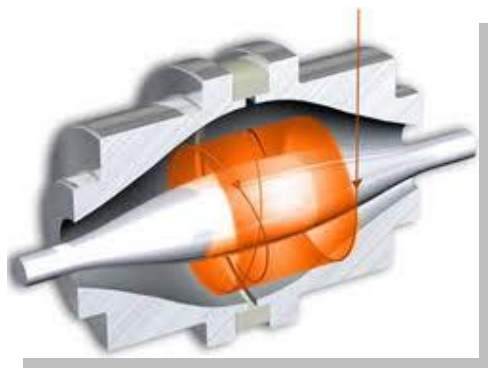


**Figure 1.2** Ion trajectories in an Orbitrap mass spectrometer.

By sensing the ion oscillation similar as in the FT-MS (Fourier transform mass spectrometry), the trap can be used as a mass analyzer. Orbitraps have a high mass accuracy (1-2 ppm), a high resolving power (up to 200,000). Currently, there are two commercial LTQ-Orbitrap instruments, the Discovery and XL models. One of the primary differences is that the XL has a linear octopole collision cell (absent in the Discovery model), in which collisional activation and fragmentation can be performed. Although this feature provides additional versatility to MS/MS experiments, the analytical performance and fundamental principles of operation of the Orbitrap analyzers in both instruments are identical.<sup>8</sup>

### **1.2.3 Nuclear Magnetic Resonance** <sup>9-10-11</sup>

Nuclear Magnetic Resonance (NMR) spectroscopy is a powerful and theoretically complex analytical tool used for structure elucidation of the isolated secondary metabolites. It involves re-orientations of nuclear spins with respect to an applied static magnetic field. In addition to standard  $^1\text{H}$  and  $^{13}\text{C}$  NMR spectra, 2D NMR experiments have been largely used in the course of my research activity. They are superior to their 1D NMR counterparts both for the information on the connection of nuclei and for the easier assignment of nuclei resonating in crowded regions of the spectra (signal overlapping is much less likely in two dimensions than in one).

The COSY (COrrrelation SpectroscopY) experiments allow a determination of the connectivity of a molecule by revealing which protons are spin-spin coupled. In spite of the many modifications which have been proposed along the years, the very basic sequence composed of two  $\pi/2$  pulses separated by the evolution period  $t_1$  is still the best choice if one is simply dealing with the presence or the absence of a given coupling, but not with the value of the relevant coupling constant.

The HSQC (Heteronuclear Single Quantum Correlation) experiment is 2D NMR heteronuclear correlation experiment, in which only one-bond proton-carbon couplings ( $^1J_{CH}$ ) are observed. The HSQC experiment correlates the chemical shift of proton with the chemical shift of the directly bonded carbon.

The HMBC (Heteronuclear Multiple Bond Correlation) experiment is a heteronuclear two-and three-bond  $^1\text{H}$ - $^{13}\text{C}$  correlation experiment; its sequence is less efficient than HSQC because the involved  $^{2,3}J_{CH}$  couplings are smaller (3-10Hz). Moreover, while  $^1J_{CH}$  are all quite close to each other,  $^{2,3}J_{CH}$  can be very different, making necessary the optimization of the experiment for each type of coupling. As a consequence, in many HMBC spectra not all of the correlation peaks which could be expected from the structure of the molecule are present. Cross peaks are between protons and carbons that are two or three bonds away while direct one-bond cross-peaks are suppressed. This experiment, finally, allow the connection of the fragments and the assembling of the structure of the molecules.

#### **1.2.4 Determination of stereochemistry**

The determination of absolute and relative stereochemistry is a key step for the characterization of natural products. The knowledge of the stereochemical details of a compound is tightly linked with molecular recognition and biological activity. In the human system, enantiomeric drugs may give rise to different interactions, thus behaving very differently in their activity, toxicology, adsorption, metabolism, pharmacokinetics and bioavailability.<sup>12</sup> So, the knowledge of the three-dimensional disposition of a molecule is important to understand the biological activity, the interaction

drug-receptor, but also to synthesize improved analogues of natural products.

Many natural compounds have one or more chiral centers. In the configuration determination, establishing the relative configuration of chiral centers is usually the first step. NMR can be very useful, especially through evaluation of chemical shifts ( $\delta$ ), coupling constants ( $J$ ) and NOE effects. The chemical shifts of protons are influenced by their chemical surroundings, so the protons of two diastereomers have different values.

The Karplus's equation<sup>13</sup> describes the influence of relative arrangements of protons in a molecule on the values of coupling constants ( $J_{H-H}$ ).

$${}^3J = A\cos\theta^2 + B\cos\theta + C$$

This equation evidences that the values of homonuclear ( ${}^3J_{H-H}$ ) and heteronuclear ( ${}^3J_{C-H}$ ) coupling constants are related to the value of the dihedral angle  $\theta$  between atoms. The superscript "3" indicates that a  ${}^1H$  atom is coupled to another  ${}^1H$  atom three bonds away, via H-C-C-H bonds. The magnitude of these coupling constants are generally smallest (0-1,5 Hz) when the torsion angle is close to  $90^\circ$  and largest at angles of  $0$  and  $180^\circ$ . In some cases the axial-axial coupling constant for an antiperiplanar  $180^\circ$  H-C-C-H configuration may be more than 9.5 Hz. Indeed for rigid cyclohexanes it is around 9-13 Hz, because the dihedral angle is close to  $180^\circ$ , where the orbitals overlap most efficiently.

NOE (Nuclear Overhauser Enhancement) effect<sup>14</sup> can give additional information about relative configuration of stereogenic centers. This effect can be observed upon irradiation on a specific signal, during the acquisition of the spectra: the relaxation times of all the protons surrounding the irradiated proton (distance  $\leq 2.5 \text{ \AA}$ ), even though not belonging to the same spin system, are influenced and thus, their height of signals changes. The NOE effect establishes a spatial relationship between substituents of fixed molecules, but this effect is dependent from the dimensions of the molecule. The ROESY (Rotating-frame Overhauser Spectroscopy) experiment is a chemical shift homonuclear correlation which can detect ROEs (Rotating-frame Overhauser Effect). ROE is similar to NOE, being related to dipolar coupling between nuclei, and depending on the geometric distance between

the nuclei. While NOE is positive for small molecules and negative for macromolecules, ROE is always positive. Therefore, the ROESY experiment is particularly useful for mid-size molecules, which would show a NOE close to zero.

The two following sub-paragraph will provide further details about two methods used for determination of configuration in this research work.

#### **1.2.4.1 Murata's Method**

NMR is certainly one of the most powerful instrumental techniques for the analysis of the relative stereochemistry of organic compounds. Even more, the application of NMR techniques to the problem of determining the relative spatial orientation of substituents has become a routine task in modern organic chemistry laboratories.

Cyclic compounds with small (three to six membered) rings display a predictable conformation behavior that allows the knowledge of their configuration to be extracted from simple NMR parameters, such as proton-proton  $J$ -coupling values and NOE intensities. A much more challenging task is the assignment of relative (and absolute) configuration in the case of flexible system, such as open (polysubstituted) chain and/or macrocyclic compounds for which a clear-cut, definite stereochemical strategy is not yet available.

In acyclic systems, all coupling constants are observed as a weighted average of each conformer and for this reason, the dihedral angles obtained from these data provide a much more reliable constraint information regarding the major conformer than NOE data. However, the use of the sole homonuclear coupling constants ( $^3J_{H-H}$ ) for relative stereochemistry assignments in flexible system is not feasible since they don't allow to distinguish among all the spatial arrangements of the substituents linked to a two-carbon fragments, as it would be needed for the identification of the rotamer with the correct configuration (**Figure 1.3**).

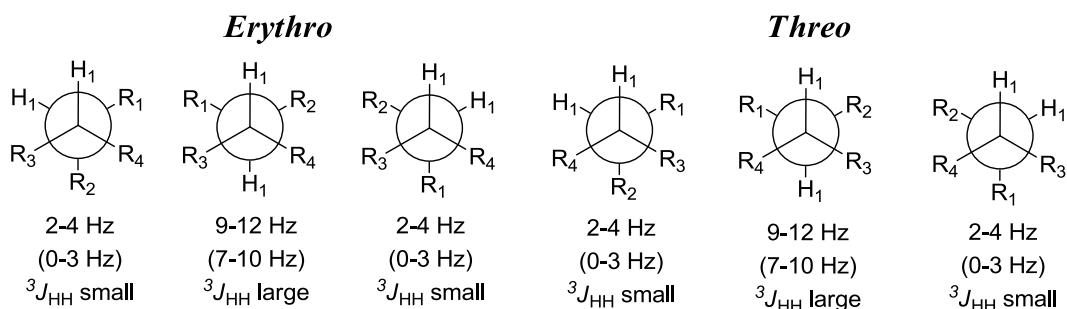


**Figure 1.3** Values of  $^3J_{HH}$  coupling for the six staggered rotamers corresponding to two different diastereomers *erythro* and *threo*

In other words, even if we restrict our attention just to staggered conformations, in absence of additional information on the geometry of the system, one angular constraint for each C2 segment is not sufficient to solve the problem, since more solutions can be consistent with the experimental data. The situation changes dramatically, though, when additional angular information on a stereochemically undetermined C2 fragment is provided from heteronuclear coupling constant ( $^2,^3J_{CH}$ ). Along these lines, Murata et al.<sup>15</sup> have reported a method for the assignment of the relative configuration of acyclic compounds based on the combined use of homonuclear proton-proton coupling constants  $^3J_{H-H}$ , heteronuclear proton-carbon coupling constants  $^2,^3J_{H-C}$  and NOE data.

This model is basically applicable to acyclic structures having stereogenic carbons bearing hydroxyl, alkoxy or methyl substituents. Every chiral molecule containing consecutive or alternate stereochemical centers can be ideally divided in two carbon fragment. This simplification allows the determination, for each single fragment, of the predominant rotamer with the exact configuration, among the six possible staggered conformers through the use of the *J*-based NMR approach, see **Scheme 1.2**. For the sake of simplicity, let us compare every single couple of vicinal asymmetric carbons to those belonging to a 2,3-disubstituted butane system. The strategy followed for a 2,3-disubstituted butane can then be applied to a large variety of natural and synthetic products in which the substituents are methoxy, hydroxy and methyl groups. A 2,3-disubstituted butane can have two relative diastereomeric configurations, named *syn* (or *threo*) and *anti* (or *erythro*). Each of these two configurations can be arranged in three staggered

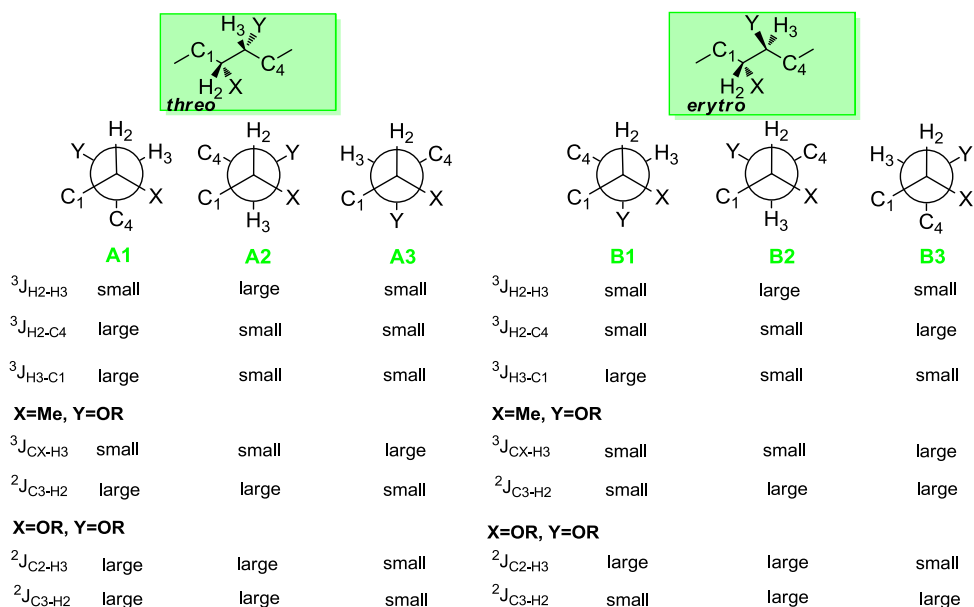
rotamers, for a total of six possible conformers, as shown in **Scheme 1.2** (A1, A2, A3, B1, B2, B3). Every single rotamer shows its own homonuclear and heteronuclear coupling constant pattern. Assuming that we have a sufficient number of experimental coupling constraints, these  $^3J_{\text{H-H}}$  and  $^{2,3}J_{\text{C-H}}$  will allow to univocally identify four of the six rotamers, namely A1, A3, B1, B3. The two rotamers A2 and B2, characterized by an anti position of the two vicinal protons, have to be distinguished on the basis of NOE (or ROE) data because they show the same coupling constant pattern.

The first step in the determination of the relative configuration of two vicinal methines consists in the evaluation of the homonuclear proton-proton coupling constant of the C2 fragment of interest (**Scheme 1.2**), in order to assess whether or not it exists in a predominant conformation.

Small  $^3J_{\text{H-H}}$  (0-4 Hz) will indicate a gauche arrangement of H2 and H3 protons. In this case the relative configuration can be safely obtained from three or four additional angular constraints deriving from the heteronuclear coupling constants values. These  $^{2,3}J_{\text{C-H}}$  values, indeed, will allow to establish the arrangement (*gauche* or *anti*) of H2 with regard to substituent Y and C4 and the arrangement of H3 with regard to substituent X and C1 and will therefore allow to choose the correct gauche rotamer among A1, A3 (*threo*), B1 and B3 (*erythro*) (**Schemes 1.2**).

Large  $^3J_{\text{H-H}}$  values (8-12 Hz) indicate anti disposition of the protons. Nevertheless the  $^{2,3}J_{\text{C-H}}$  values are the same for both rotamers A2 (*threo*) and B2 (*erythro*) (**Schemes 1.2**) and so they don't allow to distinguish them. In this case it is necessary to use NOE data regarding protons on carbons C1 and C4 and possibly protons on substituents Y and X. An NOE effect between protons on C1 and C4 and/or an NOE effect between protons on Y and X suggest the rotamer A2 in **Scheme 1.2**, while an NOE between protons on C1 and on Y and/or an NOE between protons on C4 and on X are suggestive of the rotamer B2. Intermediate values of  $^3J_{\text{H-H}}$  (4-8 Hz) are usually indicative of an interconversion between two or more conformers that is fast on the NMR scale. In this case, it would be still possible to identify the alternating conformers on the basis of the homonuclear and heteronuclear coupling constant value and to assign the relative configuration, but the methodology

is being pushed to the limit and therefore much more care has to be put in its application. In addition, the registration of NMR spectra at a low temperature can be of help in case of complex conformational equilibria, due to the population increase of the most stable conformer.



**Scheme 1.2** Identification of the single conformer with a correct configuration from the staggered rotamers with threo (syn) and erythro (anti) arrangements through the combined use of measured  $^3J_{HH}$  and  $^2,^3J_{CH}$  values.

For small molecules, the homonuclear  $^3J_{H-H}$  can be easily determined through the analysis of a 1D proton spectrum. Nevertheless, the use of more sophisticated 2D NMR techniques, such as E.COSY<sup>16</sup> or P.E.COSY<sup>17</sup>, is mandatory when the direct measurement of the  $J$  values in the proton spectra of medium and high molecular weight products is prevented by severe signal overcrowding.

Heteronuclear long range  $^2,^3J_{C-H}$  values have become widely available after the introduction of inverse detection NMR techniques<sup>18</sup> and the implementation of pulse-field-gradient (PFG) hardware in commercial NMR spectrometers. These values are determined, in the original method proposed by Murata, by 2D hetero half-filtered TOCSY (HETLOC),<sup>19-20</sup> phase sensitive HMBC (PS-HMBC)<sup>21-22</sup> experiments and, in a recent application of the methodology, HSQC-TOCSY spectra have also been used for this purpose.

However, the extensive use of  $J_{C-H}$  couplings in the analysis of the relative configuration has been hampered due to the difficulties arising from the need to make reliable judgments on the size (*large*, *medium* or *small*) of a given heteronuclear  $J$  coupling value in the absence of a desirable wealth of literature data and of efficient empirical rules, unlike the case of  $^1H-^1H$   $J$  values, and due to the impossibility to deal with cases in which the dominant conformation of the C2 fragment under investigation is represented by an anti arrangement between protons. Indeed, in this particular instance, the sole pattern, however extensive, of homo- and heteronuclear  $J$ -couplings does not allow us to distinguish between the two possible relative configurations (*erythro* and *threo*).

#### 1.2.4.2 Marfey's Method

Indirect methods, to determinate the absolute configuration, involve the formation of covalent diastereomeric derivates by reacting the enantiomers with a chiral derivatizing agent (CDA). Thus the diastereomeric derivatives may be resolved by using conventional achiral columns in HPLC, both normal and reversed phase.

The most widely used method to determinate the absolute stereochemistry of ribosomal amino acids is the Marfey's method.<sup>23</sup> This method consists of the derivatization of amino acid residues, obtained by complete acid hydrolysis of peptide, with a chiral agent FDAA (1-fluoro-2,4-dinitrophenyl-L-alaninamide, **Figure 1.4**) and then the comparison of retention times of these derivates from parent peptide with the retention time of appropriate standards D and L through HPLC.

This method is enough easy for ribosomal amino acids, commercially available, and consist of four phases:

- a) Hydrolysis of parent peptide with HCl 6 N;
- b) Derivatization of the hydrolyzed with L-FDAA;
- c) Derivatization of both standards, D and L, with L-FDAA. It is possible to derivatize L-amino acid with D-FDAA, if the D-standard isn't commercially available or is too expensive.
- d) Analysis through HPLC of retention times.



**Figure 1.4** Structure of L-FDAA

However, it is difficult to apply this chromatographic method to a peptide containing unusual amino acids without having their standard samples. Another limitation is the possibility to make mistake valuing the  $t_R$  of the derivatives in HPLC. The last problem can be solved using LC-MS that allowed to identify the peak through the  $m/z$  ratio.

Recently a new method was developed, known as “advanced Marfey’s method”,<sup>24</sup> useful to determinate the absolute configuration of non-conventional amino acids, not commercially available, and is based on the elution time of amino acids derivatized with L-FDAA. This method was tested on a number of proteogenic or not amino acids and showed the L-aminoacid-L-FDAA is always eluted from the column before its corresponding D-isomer. Now it is well recognized, according to the NMR and UV measurement, that D- and L-aminoacid-L-FDAA derivatives can be resolved due to the difference in their hydrophobicity which is derived from the *cis* or *trans* type arrangement of two more hydrophobic substituents at both  $\alpha$ -carbons of an introduced amino acid and L-FDAA; the D-isomer (with a *cis* type arrangement) interacts more strongly with RP silica gel and has the longer retention time compared to the less hydrophobic L-amino acid-L-FDAA, which has a *trans* type arrangement (**Figure 1.5**).

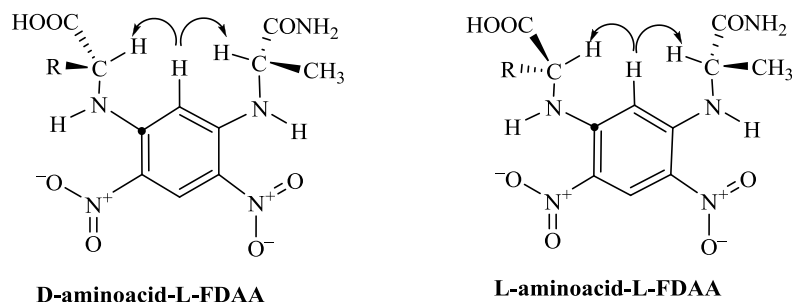


**Figure 1.5** Structure of D and L aminoacids L-FDAA derivatives.

The advanced Marfey's method is an useful tool to determinate the absolute configuration of non ribosomal amino acids. It consists of four steps:

- The amino acid obtained from hydrolysis of the peptide is divided into two portions;
- Derivatization of amino acid with L-FDAA;
- Derivatization of amino acid with D-FDAA;
- Analysis of  $t_R$  through LC-MS.

The peaks of any amino acids in peptides are identified without a standard sample using mass spectrometry, and the absolute configuration of a desired amino acid is deduced from its corresponding enantiomer.

This method is applicable to determinate the absolute configuration of the  $\alpha$  chiral center of  $\alpha$ -amino acid and to determine the absolute configuration of  $\alpha$ -amino acid with more chiral centers, only if the relative configuration is known.

The method cannot be used for  $\beta$  or  $\gamma$ -aminoacids and for aminoacids with more chiral centers, if it the relative configuration is unknown.

The advanced Marfey's method is a nonempirical one, but it has some drawbacks, since it relies on the elution order of amino acid derivative with L-FDAA to determine its absolute configuration. It is clear that the nature of the amino acid side-chain is responsible for this behavior. So, some aminoacids do not follow the elution order in column and the isomer L-amino acid-L-FDAA has a longer retention time compared to the D-amino acid-L-FDAA, or the two derivatives have  $t_R$  too similar. The aminoacids with ionizable side-chain, like Asp and Glu, pose problems of derivatization. Amino acids like tyrosine and histidine or containing two amino groups such as ornithine and

lysine can form both mono- and di-substituted Marfey's derivatives thus doubling the number of peaks in a chromatogram for these amino acids.

### **1.2.5 General Experimental Section**

Optical rotations ( $\text{CHCl}_3$ ) were measured at 589 nm on a P2000 Jasco polarimeter or Perkin-Elmer 243 B polarimeter. NMR spectra were obtained on Varian Inova 700 MHz, 500 MHz and 400 MHz spectrometer ( $^1\text{H}$  at 700 MHz,  $^{13}\text{C}$  at 175 MHz) equipped with a Sun hardware, or on Bruker Avance 3HD 400 or 600 (USA), J in Hz, spectra referred to  $\text{CD}_3\text{OD}$  ( $\delta_{\text{H}} = 3.32$ ,  $\delta_{\text{C}} = 55.0$ ) or  $\text{CDCl}_3$  ( $\delta_{\text{H}} = 7.26$ ,  $\delta_{\text{C}} = 77.0$ ) or DMSO ( $\delta_{\text{H}} = 2.50$ ,  $\delta_{\text{C}} = 39.5$ ) as internal standard. Homonuclear  $^1\text{H}$  connectivities were determined by the COSY experiment. One-bond heteronuclear  $^1\text{H}$ - $^{13}\text{C}$  connectivities were determined with the HSQC experiment. Through-space  $^1\text{H}$  connectivities were evidenced using a ROESY experiment with a mixing time of 250 ms. Two and three bond  $^1\text{H}$ - $^{13}\text{C}$  connectivities were determined by gradient 2D HMBC experiments optimized for a  $^2,^3J = 9$  Hz. The phase sensitive (PS)-HMBC spectra were recorded with the delay set at 40 ms and a data size of 2K (F2)  $\times$  128 (F1) points. Low- and high-resolution ESIMS spectra were obtained on a LTQ OrbitrapXL (Thermo Scientific) mass spectrometer. Medium pressure liquid chromatography was performed on a Büchi apparatus using a silica gel (230-400 mesh) column; silica gel 60 (70-230 mesh) and RP-18 used for gravity column chromatography was purchased from Macherey-Nagel. Flash chromatographies were performed with a Buchi C615/601 pump system using silica gel cartridges (40-63  $\mu\text{m}$ ) (Buchi®, Swintzerland). Preparative HPLC were performed on a LaChrom-Merck Hitachi HPLC system, pump L-7100, UV detector L-7400 using a C-18 column (Knauer, 300  $\times$  8 mm, prefilled with C-18 Eurosphere, flow rate 5 mL/min, UV detection at 280 nm). Analytic HPLC were achieved on a Knauer apparatus equipped with a refractive index detector or on an Alliance apparatus (model 2695, Waters, USA) equipped with photodiode array detector (model 2998, Waters), an evaporative light-scattering detector (model Sedex 80, Sedere, France) and the software Empower; LUNA (Phenomenex, normal phase, SI60, 250  $\times$  4 mm), LUNA (Phenomenex, C-18, 100-5, 250  $\times$  4.5 mm), GEMINI

(Phenomenex, C6-Phenyl, 5  $\mu\text{m}$ , 250 x 4.6 mm) columns were used, with 0.7 or 1 mL/min as flow rate.

## References

---

- <sup>1</sup> Bankova V., *Chemistry Central Journal*, **2007**, 1, 1.
- <sup>2</sup> Nakanishi, K.; A historical perspective of natural products chemistry in Barton D and Nakanishi K (eds.), *Comprehensive Natural Products Chemistry*, Vol. 2, XXI–XXXVIII, Elsevier Publishers, **1995**.
- <sup>3</sup> Pomponi, SA.; *J Biotechnol*, **1999**, 70, 5–13.
- <sup>4</sup> Newman, D.J.; Cragg, G. M.; *J. Nat. Prod.*, **2004**, 67 (8), 1216–1238.
- <sup>5</sup> Jimeno, JM.; *Anticancer Drugs*, **2002**, 13 (suppl 1), S15–19.
- <sup>6</sup> Kupchan S. M., Britton R. W., Ziegler M. F., Sigel C. W. *J. Org. Chem.*, **1973**, 38, 178.
- <sup>7</sup> Hu, Q.; Noll, R. J.; Li, H.; Makarov, A.; Hardmanand, M.; Cooks, R. G.; *J. Mass Spectrom.*, **2005**, 40, 430–443.
- <sup>8</sup> Perry, R. H.; Cooks, R. G.; Noll, R. J.; *Mass Spectrometry Reviews*, **2008**, 27, 661– 69.
- <sup>9</sup> Bax, A.; Two Dimensional Nuclear Magnetic Resonance in Liquids, Delft University Press, Dordrecht, **1982**.
- <sup>10</sup> Palmer III, A. G.; Cavanagh, J.; Wright, P. E.; Rance, M.; *J. Magn. Reson*, **1991**, 151-170.
- <sup>11</sup> Bax, A.; Summers, M. F.; *J. Am. Chem. Soc*, **1986**, 2093.
- <sup>12</sup> Jamali, F.; Mehahvar, R.; Pautto, F.M. *J. Pharm. Sci.*, **1989**, 78, 685.
- <sup>13</sup> Karplus, M.; *J. Chem. Phys.*, **1959**, 11.
- <sup>14</sup> Sanders, J. K. M.; Mersh, J. D.; *Prog. NMR Spectrosc.*, **1982**, 353.
- <sup>15</sup> Matsumori, N.; Kaneno, D.; Murata, M.; Nakamura, H.; Tachibana, K. *J. Org.Chem.*, **1999**, 64, 866.

- 
- <sup>16</sup> Griesenger, C.; Sorensen, O. W.; Ernst, R. R. *J. Am. Chem. Soc.*, **1985**, *107*, 6394.
- <sup>17</sup> Mueller, L. *J. Magn. Reson.*, **1987**, *72*, 191.
- <sup>18</sup> Biamonti, C.; Rios, C. B.; Lyons, B. A.; Montelione, G. T. *Adv. Biophys. Chem.*, **1994**, *4*, 51.
- <sup>19</sup> Kurz, M.; Schmieder, P.; Kessler, H. *Angew. Chem. Int. Ed. Engl.*, **1991**, *30*, 1329.
- <sup>20</sup> Wollborn, U.; Leibfritz, D. *J. Magn. Reson.*, **1992**, *98*, 142.
- <sup>21</sup> Zhu, G.; Live, D.; Bax, A. *J. Am. Chem. Soc.*, **1994**, *116*, 8370.
- <sup>22</sup> Boyd, J.; Soffe, N.; John, B.; Plant, D.; Hurd, R. *J. Magn. Res.*, **1992**, *98*, 660.
- <sup>23</sup> Marfey, P. *Carlsberg Res. Commun.*, **1984**, *49*, 591-596.
- <sup>24</sup> Fujii, K.; Harada, K. et al. *Anal. Chem.*, **1997**, *69*, 3346-3352.

## CHAPTER 2 -BIOACTIVE MACROLIDES, DEPSI- PEPTIDES AND STEROLS FROM THE SPONGE *THEONELLA SWINHOEI*

---

A substantial part of the research work during my PhD involved chemical analysis of marine invertebrates, particularly sponges, very rich sources of secondary metabolites. Sponges *Theonella swinhoei* and *Iotrochota purpurea* have been the object of my study.

### 2.1 PORIFERA: A TREASURE TROVE OF SECONDARY METABOLITES

Sponges (*phylum* Porifera) are the most primitive of the multicellular animals. Neither true tissues nor organs are present and the cells display a considerable degree of independence. All the members of the phylum are sessile and exhibit little detectable movement.

Sponges are aquatic sessile filter feeders and live permanently attached to a location in the water. Sponges can be found in nearly all aquatic environment (marine and fresh water; shallow and deep; tropical and Antarctic), wherever there are substrata for sponge attachment and growth.<sup>1</sup>

They can show a variety of sizes, colors, and shapes, including arborescent (tree-like), flabellate (fan-shaped), caliculate (cup shaped), tubular (tube shaped) and amorphous (shapeless) (**Figure 2.1**).



**Figure 2.1** Some examples of Porifera.

The outer dermal membrane is composed of two cell layers of specialized cells named pinacocytes, which digest food particles too large to enter the ostia. The body wall is approximately two cell layers thick with a gel like substance named mesohyl, the gelatinous matrix within the sponge made of collagen. The body wall is perforated by many pores and channels (ostia), through which water enters the animal, passing into the spongocoel, and exiting it through a large opening, the osculum (**Figure 2.2**). The interior cells are called choanocytes and contain a central flagellum surrounded by a collar of microvilli which are connected by a thin membrane. By cooperatively moving their flagella, choanocytes generate a flow of water through the sponges pores, into the spongocoel, and out through the osculum. This improves both respiratory and digestive functions for the sponge, pulling in oxygen and nutrients and allowing a rapid expulsion of carbon dioxide and other waste products.

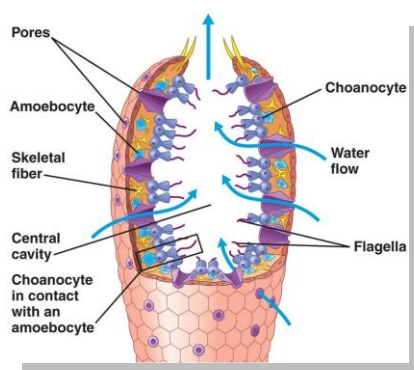


**Figure 2.2** A sponge body structure.

Body plans range from simple through to complex, produced by varying degrees of infolding of the body wall and complexity of water canals throughout the sponge. The simplest body structure in sponges is a tube or vase shape known as asconoid. This refers to a sessile tubular structure. Water, along with particulate matter, flows through small pores. The ostia lead to flagellated choanoderm which pick up particulate matter, while the water is pushed up and out of the tube at the osculum.

Synconoids also take on tubular structure but have an internal tissue which generates a much greater surface area for the absorption of nutrients. Folds in the internal tissue create a sort of zigzag pattern in which the internal openings are referred to as choanocyte chambers. The external openings are

incurrent canals. The body of the sponges is reinforced by the skeleton, collagen fibers and spicules (**Figure 2.3**). Sponges use various materials to reinforce their mesohyl and in some cases to produce skeletons and this form the main basis for classifying sponges.

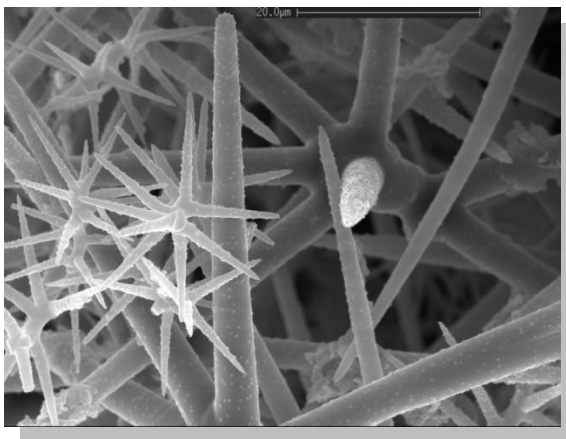


**Figure 2.3** Microscope image of spicules.

Demosponges reinforce the mesohyl with fibers of a special form of collagen called spongin, most also produce spicules of silica, and a few secrete massive external frameworks of calcium carbonate. Although glass sponges also produce spicules made of silica, their bodies mainly consist of syncytia that in some ways behave like many cells sharing a single external membrane, and in others like individual cells with multiple nuclei.

Demosponges constitute about 90% of all known sponge species, including all freshwater ones, and have the widest range of habitats.

Sponges, lacking any physical defence from their predators, rely on chemical defense mediated by secondary metabolites, which are essential for their survival. The chemicals also probably play a role in competition among sponges and other organisms, as they are released by sponges to ensure themselves space in the marine ecosystem.

Sponges are very fertile host animals for diverse symbiotic microorganisms: the symbionts locate both intra- and extra cellularly (**Figure 2.4**), and each symbiotic microorganism seems to have a specific habitat in the host sponge. Extracellular symbionts are present on the outer layers of sponges as exosymbionts, or in the mesohyl as endosymbionts. Intracellular or intranuclear symbionts permanently reside in host cells or nuclei.

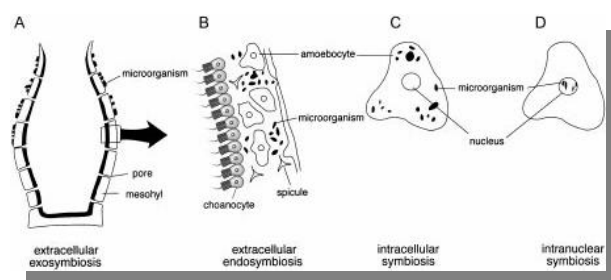


**Figure 2.4** Schematic diagram of symbiotic relationships between sponges and microorganisms. A, extracellular exosymbiosis; B, extracellular endosymbiosis; C, intracellular symbiosis; and D, intranuclear symbiosis.

A number of promising compounds have been identified from marine sponges that possess pronounced biological activity and are already at advanced stages of clinical trials, mostly for the treatment of cancer, or have been selected as promising candidates for extended preclinical evaluation.<sup>2</sup> The types of compounds characterized from marine organisms are diverse and represent many different classes, structurally complex with unique functionalities, including cyclic peptides, terpenes and steroids, and macrolides.

**Cyclic Peptides** are polypeptide chains whose amino and carboxyl terminus are themselves linked together with a peptide bond that forms a circular chain. The unusual properties of cyclic peptides are due both to their circular structure and their unusual mode of biosynthesis, which frequently incorporates uncommon amino acids. As result, the presence of non-ribosomal amino acids produces pronounced effects on the pharmacological activities of these metabolites. For example, N-alkylation and the lack of N and C termini enhance the hydrophobicity, thus determining a more facile crossing of biological membranes and an improved stability to enzymatic degradation. Cyclization reduces peptide conformational flexibility that results in a higher receptor affinity. All these features make cyclopeptides promising lead compounds in drug discovery.

Cyclic depsipeptides are cyclic peptides in which one or more of the peptide (amide) bonds are replaced by other bonds. Other functional groups, different from the usual amino and carboxyl group, are linked together, closing the polypeptide chain, including ester, lactone, thioester bonds.

The biosynthesis of natural cyclic peptides is interesting to biologists, since it frequently involves *non-ribosomal peptide synthetases*. Most peptides are made by bacteria. Nonribosomal peptide synthetases (NRPSs) and polyketide synthases (PKSs) are multi-enzymatic, multi-domain megasynthases involved in the biosynthesis of nonribosomal peptides and polyketides.<sup>3-4-5</sup>

**Terpenes and steroids** are a large and varied class of natural compounds, structurally different each other. They derive from C5 isoprene units linked together head to tail. Several modes of cyclization are conceivable and lead to various skeletons just like the cyclization of polyketide chains. The terpenes are classified according to the number of C5 units: monoterpenes, C10; sesquiterpenes C15; diterpenes, C20; sesterterpenes, C25; triterpenes, C30; and tetraterpenes C40. The prominent biological activity of marine terpenes is evident in their ecological role in the marine environment, and makes them interesting as potential drugs. Steroids are terpenes having a tetracyclic ring system and comprise a large number of ubiquitous compounds which are divided into subgroups, mainly according to side chain functionality: sterols, sapogenins, cardiac aglycones, bile acids, adrenal steroids and sex hormones. Sterols isolated from sponges are sometimes very complex mixtures of highly functionalized compounds, many of which have no terrestrial counterpart.

**Macrolides** are a group of compounds that stems from the presence of a macrolide ring, usually a large macrocyclic lactone ring to which one or more sugars may be attached. Marine macrolides provide a fascinating range of structural and functional diversity, which may find application as specific molecular probes for the investigation of the cytoskeleton and cell cycle events. In fact, many macrolides isolated from sponges disrupt the organization of microfilaments, interacting with actin in the cell cytoskeleton, and represent a promising mechanism of action for developing novel anticancer drugs.

## 2.2 THEONELLA SWINHOEI

Sponges of the order Lithistida are an evolutionary ancient lineage that is typically found in deeper waters and caves of tropical oceans. Lithistid sponges have a structurally massive, rigid or “rock-like” morphology. This polyphyletic order is grouped together because their skeletons consist of fused or interlocked spicules, called desmas.

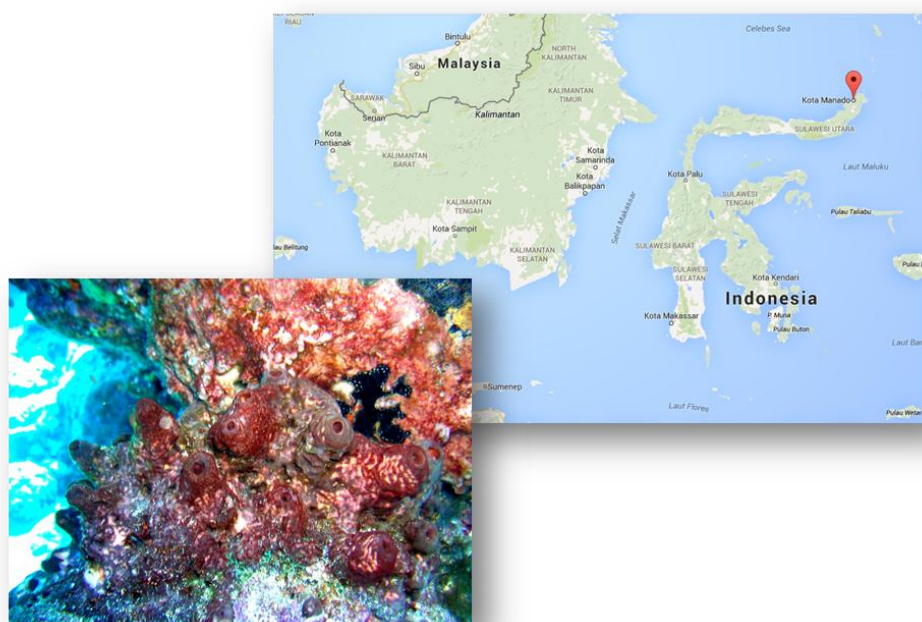


**Figure 2.5** A specimen of the sponge *Theonella sp.* collected in the area of Bunaken Marine Park of Manado (Indonesia).

Over half of the compounds reported for lithistid sponges were isolated from *Theonella* (family Theonellidae). *Theonella* species have been reported to contain a wide variety of diverse secondary metabolites with intriguing structures and promising biological activities, which have been calculated to represent more than nine biosynthetic classes<sup>6</sup> (**Figure 2.6**). In particular, *Theonella swinhoei* represents one of the most prolific source of innovative and bioactive metabolites. More than one hundred metabolites have been reported from the single extraordinary prolific species *Theonella swinhoei*, including non-ribosomal polypeptides/depsipeptides, polyketide macrolides (as the cytotoxic swinholide A, **1**<sup>7</sup>), polyene derivatives (exemplified by

aurantosides<sup>8</sup>), and uncommon steroids (4-methylene steroids<sup>9</sup> and truncated side-chain sulfated steroids<sup>10</sup>), recently demonstrated to act as modulator of nuclear receptors FXR and PXR.<sup>11</sup>

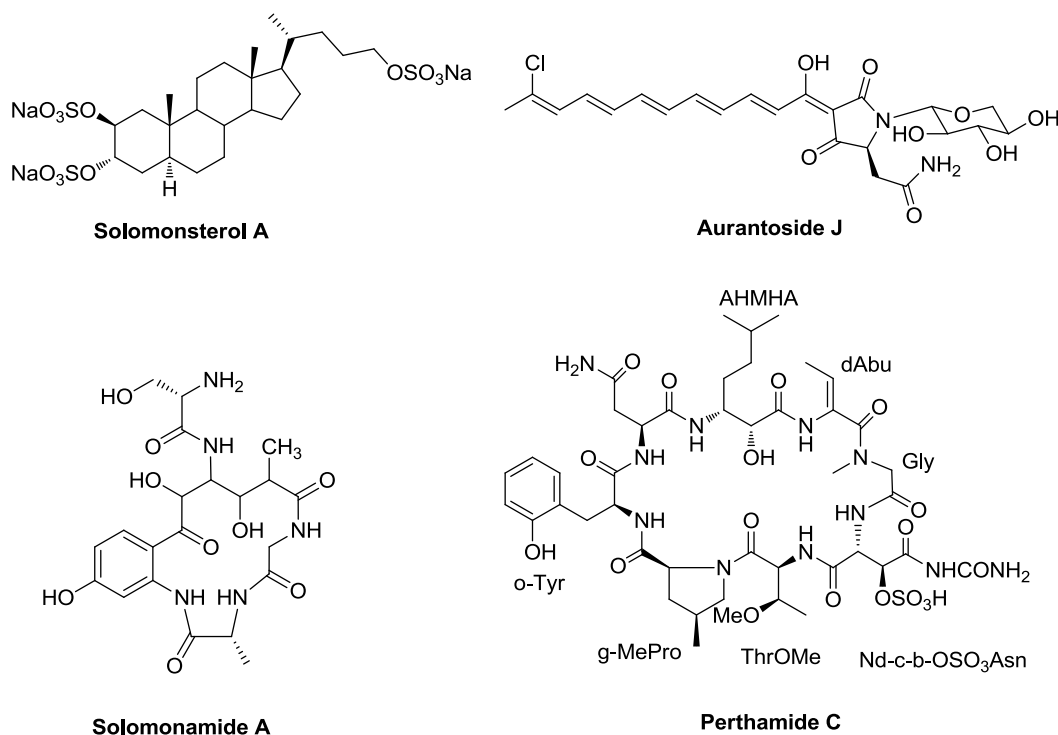


**Figure 2.6** Some molecules from *Theonella swinhoei*.

However, among bioactive metabolites found from worldwide collections of *Theonella swinhoei*, surely the peptides represent the most significant group. The diverse array of *Theonella* derived peptides range from acyclic peptides such as polytheonamides<sup>12</sup>, koshikamides A1 and A2<sup>13-14</sup>; cyclic peptides, exemplified by cyclotheonamides<sup>15-16</sup>, kombamide<sup>17</sup>, orbiculamide<sup>18</sup>, keramamides<sup>19</sup>, cupolamide<sup>20</sup>, oriamide<sup>21</sup>, perthamides<sup>22</sup> and solomonamides<sup>23</sup>, large-ring bicyclic peptides, such as theonellamides; depsipeptides headed by theonellapeptolides<sup>24</sup>; and glycopeptides<sup>25</sup>. As for other peptides of marine origin, the most striking feature of these metabolites is the preponderance of non-ribosomal amino acids, including the D configured, N-methylated and alkylated.

The exceptional chemical diversity found in the metabolites of *Theonella* sponges may in part be due to the biosynthetic capacity of bacteria that they host<sup>26</sup>. This hypothesis has been convincingly supported in the case of

swinholide A, omnamides and theopederins. In 2005, Gerwich<sup>27</sup> reported the direct isolation of swinholide A and related derivatives from two different cyanobacteria, demonstrating that marine cyanobacteria possess the metabolic capacity to produce this skeletal class. As concerning omnamides and theopederins, from the highly complex metagenome of *Theonella swinhoei*, was identified a prokaryotic gene cluster<sup>28</sup>, likely responsible for the biosynthesis of these two metabolites.<sup>29</sup> A bacterial family, named *Entotheonella* sp., has been identified through single-cell- and metagenomics-based discovery as the responsible for most of the biosynthetic work producing the typical *Theonella* metabolites.<sup>30</sup>

The existence of some different chemotypes of *T. swinhoei* has been postulated<sup>7</sup>, but a detailed understanding of the genetic bases for the observed chemical variation is made problematic by the complexity of the microbial community associated with this sponge<sup>31</sup>.

In the course of a project directed to the chemical investigation and evaluation of the marine invertebrates from Indonesian Sea, in collaboration with the Sam Ratulangi University (Manado, Indonesia), my research group had previously analyzed a red/yellow specimen of *T. swinhoei* collected in North Sulawesi (Indonesia) which proved to be rich in aurantosides<sup>32</sup> and 4-methylene steroids,<sup>33</sup> while polyketide macrolides and peptide-based derivatives were extremely rare if not absent. During Ph.D. period, chemical analysis of a brown-colored specimen of *T. swinhoei*, collected in the same area of the previous, has been undertaken, and an extremely different secondary metabolite composition was detected. The analysis of this sponge afforded to the isolation of new compounds, belonging to different chemical classes. The variety of compounds isolated reaffirms the biological richness of *Theonella swinhoei*, that may be considered a cornucopia of metabolites.

## 2.3 ISOLATION AND PURIFICATION

*Theonella swinhoei* (order Lithistida, family Theonellidae) was collected in the Bunaken Marine Park of Manado (North Sulawesi, Indonesia) in January 2010 and frozen immediately after collection. The frozen material was repeatedly extracted with methanol and the crude extract was subjected to a modified

Kupchan's partitioning procedure to obtain *n*-hexane, CHCl<sub>3</sub> and *n*-BuOH extracts.

The CHCl<sub>3</sub> extract was chromatographed by silica gel MPLC; fractions from MPLC were further purified by HPLC on reversed-phase column. The study of chloroform extract afforded the known swinholides A (**1**), B (**2**), D (**3**) and isoswinholide A (**4**), along with two new members of this family, named isoswinholide B (**5**) and swinholide K (**6**); the known theonellapeptolide Id (**7**) and the new analogues sulfinyltheonellapeptolide (**8**) and theonellapeptolide If (**9**); four already known (**12-15**) and one new compound (**16**) belonging to the 4-methylensterols family.

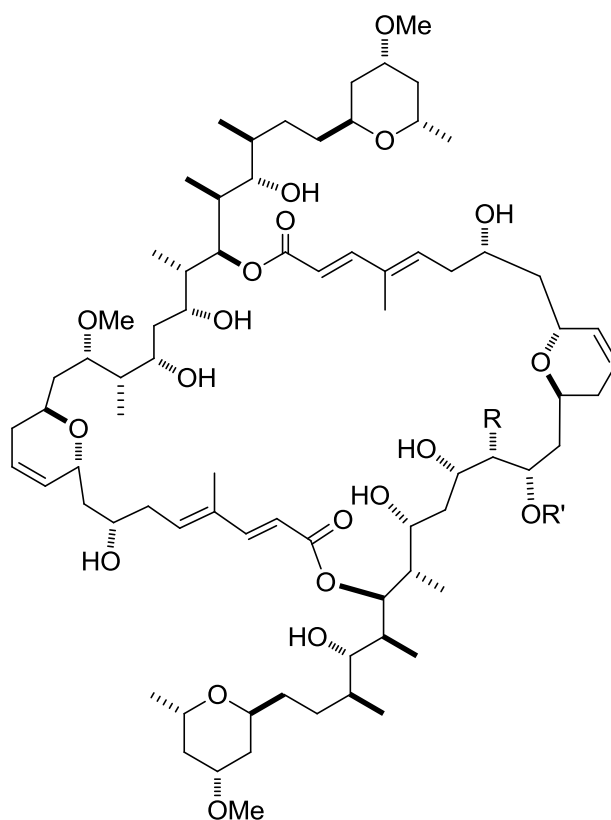
## 2.4 MACROLIDES FROM *THEONELLA SWINHOEI*

The known swinholides A (**1**), B (**2**), D (**3**) and isoswinholide A (**4**), along with two new members of this family, named isoswinholide B (**5**) and swinholide K (**6**) were obtained. The known compounds were identified on the basis of the identity of their spectroscopic data with those published in the literature.<sup>34-35-36</sup>

The whole series of compounds was evaluated on HepG2 cells (hepatocarcinoma cell line), revealing that the new swinholide K (**6**) is a potent cytotoxin, while isoswinholide B (**5**) is at least 100 times less active than its parent compound **1**.

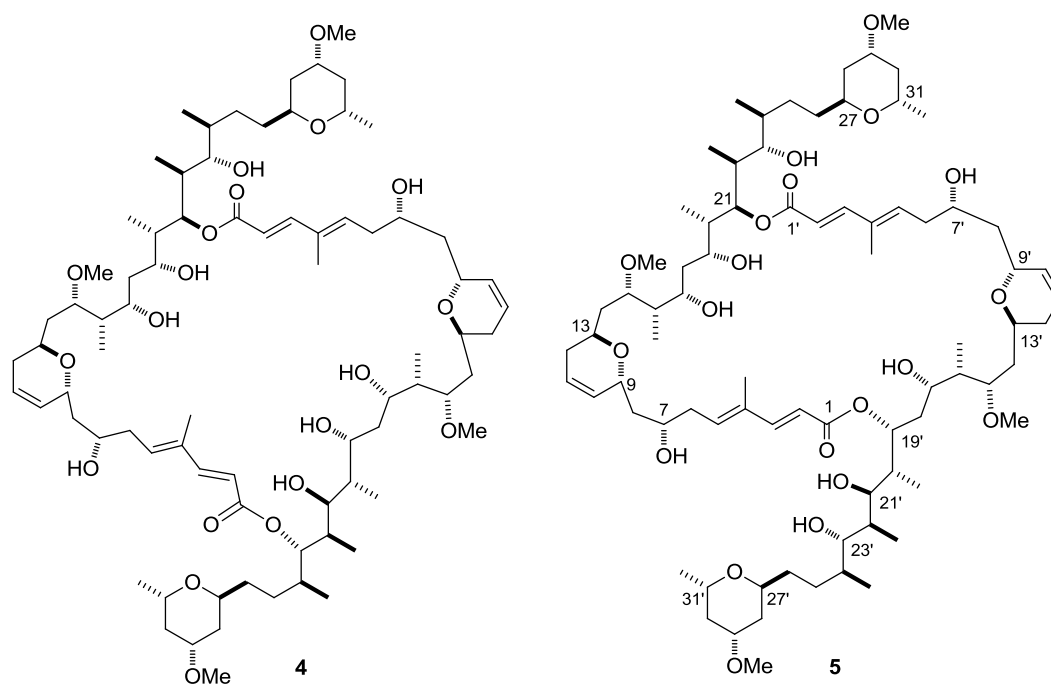
Isoswinholide B (**5**) was isolated as an optically active white powder for which HR-ESIMS indicated the molecular formula C<sub>78</sub>H<sub>132</sub>O<sub>20</sub>, identical to that of the parent compound swinholide A (**1**). The <sup>1</sup>H NMR profile of **5** (CD<sub>3</sub>OD, **Table 2.1**) soon suggested its belonging to the swinholide family; however, the marked splitting of many signals was indicative of a lack of symmetry between the two C<sub>39</sub> units of the dilactone system. In swinholides B,<sup>31</sup> C,<sup>31</sup> D<sup>7</sup> and G<sup>7</sup> this effect is due to methylation or demethylation at a single center, while in swinholides E,<sup>7</sup> I<sup>37</sup> and J<sup>30</sup> it is ascribable to the presence of an additional oxygen atom on the carbon backbone. Both these kinds of structural changes should be excluded in the case of **5** on the basis of molecular formula consideration; in addition, an inspection of the <sup>1</sup>H NMR spectrum aided by the 2D HSQC experiment revealed that all the expected

methyl groups (four linking oxygen, ten linking  $sp^3$  methines and two linking  $sp^2$  unprotonated carbons) were actually present in the structure of **5**.



- 1** R = Me R' = Me  
**2** R = H R' = Me  
**3** R = Me R' = H

Careful inspection of 2D COSY and TOCSY spectra of **5** allowed the definition of two large spin systems (from H-5 to 31-Me and from H-5' to 31'-Me), extended to H-2/2' and H-3/3' on the basis of the long-range couplings showed by 4-Me/4'-Me (**Table 2.1**), thus defining a backbone identical to that of swinholide A, including the trans geometry of the disubstituted double bond ( $J_{H-2/H-3} = J_{H-2'/H-3'} = 15.9$  Hz).



As evidenced by the careful comparison of the proton resonances assigned for 5 with those reported for swinholide A (**1**),<sup>30</sup> the main differences lie in the dienolate region of one unit and in the H-17/H-23 region of the other unit (**Figure 2.7**). On the contrary, as for swinholide A, proton resonances and coupling constants from position 25 to position 31 were practically identical for the two units, indirectly suggesting that these regions should not be involved in the loss of symmetry.

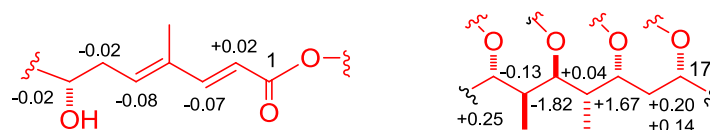


**Figure 2.7** Comparison between the resonances of isoswinholide B (**5**) and swinholide A (**1**) in selected regions.  $\Delta\delta$  (isoswinholide B – swinholide A) is reported in ppm

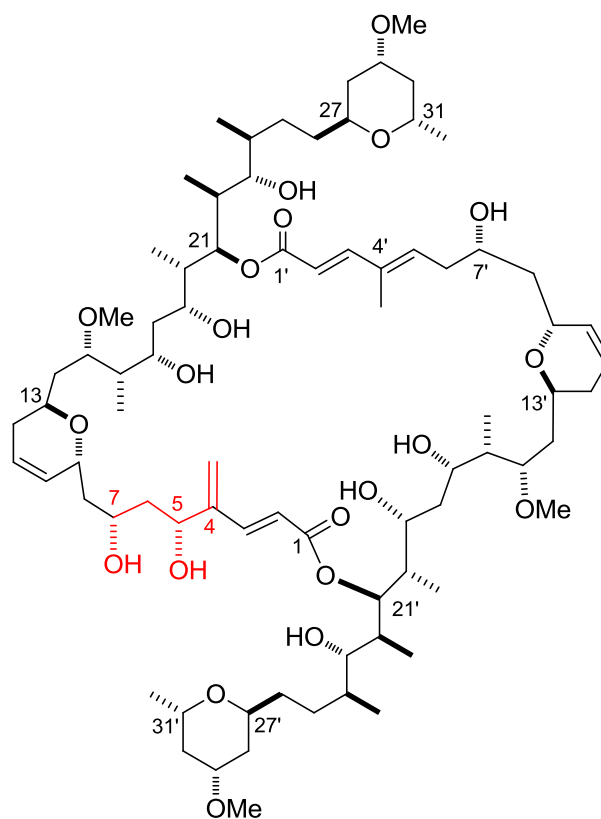
**Table 2.1**  $^1\text{H}$  (700 MHz) and  $^{13}\text{C}$  (175 MHz) NMR data of isoswinholide B (**5**) in  $\text{CD}_3\text{OD}$ 

Pos.	$\delta_{\text{H}}$ mult ( $J$ in Hz)	$\delta_{\text{C}}$ (type)	Pos.	$\delta_{\text{H}}$ ( $J$ in Hz)	$\delta_{\text{C}}$ (type)
1	-	169.4 (C)	1'	-	170.3 (C)
2	5.86 d (15.9)	115.0 (CH)	2'	5.89 d (15.9)	115.0 (CH)
3	7.36 d (15.9)	149.9 (CH)	3'	7.44 d (15.9)	149.9 (CH)
4	-	135.1 (C)	4'	-	135.1 (C)
4-Me	1.80 s	11.4 (CH <sub>3</sub> )	4'-Me	1.80 s	11.4 (CH <sub>3</sub> )
5	6.06 t (7.0)	139.3 (CH)	5'	6.18 t (6.8)	139.1 (CH)
6	2.38 ovl	37.5 (CH <sub>2</sub> )	6'	2.43 ovl	37.5 (CH <sub>2</sub> )
7	4.00 ovl	67.2 (CH)	7'	4.11 m	66.7 (CH)
8	1.37 m, 1.75 m	40.0 (CH <sub>2</sub> )	8'	1.33 m, 1.76 m	40.0 (CH <sub>2</sub> )
9	4.47 ovl	69.1 (CH)	9'	4.47 ovl	69.1 (CH)
10	5.66 ovl	129.8 (CH)	10'	5.66 ovl	129.8 (CH)
11	5.82 m	123.6 (CH)	11'	5.82 m	123.6 (CH)
12	1.96 m	31.6 (CH <sub>2</sub> )	12'	2.01 m	31.1 (CH <sub>2</sub> )
13	3.55 m	63.9 (CH)	13'	3.60 m	64.4 (CH)
14	1.57 m, 1.83 m	37.2 (CH <sub>2</sub> )	14'	1.59 m/1.87 m	35.7 (CH <sub>2</sub> )
15	3.77 m	78.1 (CH)	15'	3.79 m	77.3 (CH)
15-OMe	3.33 s	55.8 (CH <sub>3</sub> )	15'-OMe	3.35 s	55.8 (CH <sub>3</sub> )
16	1.53 m	43.9 (CH)	16'	1.59 m	41.9 (CH)
16-Me	0.84 d (7.0)	8.4 (CH <sub>3</sub> )	16'-Me	0.85 d (6.8)	8.4 (CH <sub>3</sub> )
17	3.62 m	73.1 (CH)	17'	3.61 m	69.8 (CH)
18	1.60 m, 1.76 m	39.1 (CH <sub>2</sub> )	18'	1.83 m, 1.88 m	38.3 (CH <sub>2</sub> )
19	3.99 ovl	71.9 (CH)	19'	5.65 m	74.2 (CH)
20	1.91 m	39.3 (CH)	20'	1.98 m	36.9 (CH)
20-Me	0.91 d (7.0)	13.2 (CH <sub>3</sub> )	20'-Me	0.94 d (7.0)	8.6 (CH <sub>3</sub> )
21	5.40 m	75.1 (CH)	21'	3.64 m	73.0 (CH)
22	1.93 m	37.7 (CH)	22'	1.85 m	37.9 (CH)
22-Me	0.94 d (7.0)	8.8 (CH <sub>3</sub> )	22'-Me	0.95 d (7.0)	8.8 (CH <sub>3</sub> )
23	3.12 dd (2.0, 9.7)	76.2 (CH)	23'	3.36 ovl	78.2 (CH)
24	1.73 m	34.6 (CH)	24'	1.67 m	33.0 (CH)
24-Me	0.98 d (6.5)	16.7 (CH <sub>3</sub> )	24'-Me	0.93 d (6.5)	16.1 (CH <sub>3</sub> )
25	1.28 m, 1.42 m	24.2 (CH <sub>2</sub> )	25'	1.28 m, 1.42 m	24.2 (CH <sub>2</sub> )
26	1.30 m, 1.94 m	29.0 (CH <sub>2</sub> )	26'	1.30 m, 1.94 m	29.0 (CH <sub>2</sub> )
27	3.97 ovl	72.4 (CH)	27'	3.97 ovl	72.4 (CH)
28	1.53 m, 1.87 m	35.7 (CH <sub>2</sub> )	28'	1.53 m, 1.87 m	35.7 (CH <sub>2</sub> )
29	3.63 m	74.1 (CH)	29'	3.63 m	74.1 (CH)
29-OMe	3.34 s	54.2 (CH <sub>3</sub> )	29'-OMe	3.34 s	54.2 (CH <sub>3</sub> )
30	1.11 ovl, 1.91 ovl	39.5 (CH <sub>2</sub> )	30'	1.11 ovl, 1.91 ovl	39.5 (CH <sub>2</sub> )
31	3.76 m	65.7 (CH)	31'	3.76 m	65.7 (CH)
31-Me	1.19 d (6.1)	20.8 (CH <sub>3</sub> )	31'-Me	1.19 d (6.1)	20.8 (CH <sub>3</sub> )

Extensive analysis of HSQC and HMBC spectra allowed the assignment of all the carbon resonances of **5** (Table 2.1) and the definitive confirmation of the structure of the two C39 halves, both identical to that of the symmetric swinholide A. This implied that compound **5** should differ from **1** only in one or both the lactonization positions. The HMBC cross-peaks H-21/C-1' and H-19'/C-1 unambiguously identified the oxygens at C-19' and C-21 as those

involved in the formation of the two lactone functionalities. Thus, compound **5** is a new member of the swinholide family, named isoswinholide B, showing the unprecedented 21/19' lactonization pattern. The single isoswinholide known before was isoswinholide A (**4**), showing lactonization at O-21 and O-23'. Interestingly, acidic treatment of swinholide A with p-TsOH afforded the symmetric 23/23'-diolide and 19,19' diolide, and the desymmetrized 23,17'-diolide, but no traces of isoswinholide B were detected.<sup>38</sup> On the other hand, we found no traces of the above synthetic isoswinholides in our specimen of *T. swinhoei*.

Swinholide K (**6**) was isolated as a white powder with molecular formula C<sub>78</sub>H<sub>132</sub>O<sub>21</sub>, one oxygen atom more than swinholide A, as indicated by HR-ESIMS. Inspection of the <sup>1</sup>H NMR spectrum of **6** (**Table 2.2**), clearly revealed that this compound, similarly to **5**, experienced a loss of symmetry of the two C<sub>39</sub> units, which could be, most likely, ascribed to the presence of the additional oxygen atom in one of the two units. In particular, the <sup>1</sup>H NMR spectrum of **6** showed thirteen resonances in the region 5.43-7.43 ppm in place of the resonances for six pairs of equivalent protons as in **1**. Moreover, in contrast to **1**, the <sup>1</sup>H NMR spectrum of **6** exhibited an additional resonance in the midfield region of the spectrum ( $\delta_{\text{H}}$  4.62, m), while it clearly lacked of one of the two allylic methyl groups attached at positions 4/4'. COSY and TOCSY spectra of **6** allowed us to build up its proton spin systems which, for resonances assigned to positions from 9 to 31, appeared perfectly symmetric and superimposable to values reported for swinholide A.<sup>30</sup> These data clearly suggested that a perturbation in the dienoate region at one half of the molecule had occurred.



(6)

The  $^{13}\text{C}$  NMR spectrum of **6** (Table 2.2), interpreted with the help of HSQC and HMBC experiments, concurred in suggesting a perturbation in one of the C-1 to C-8 moieties and a perfect symmetry in the remaining parts of the molecule. In particular, the  $^{13}\text{C}$  NMR spectrum showed twelve resonances in the double bond region (seven methines, two of which assignable to the two pairs of equivalent carbons C-10/C-10' and C-11/C-11', one methylene and four unprotonated carbons, including the two ester carbonyl resonances) in place of the seven signals showed by the symmetric swinholide A in the same region. Extensive analysis of COSY, HSQC and HMBC spectra allowed us to define the structures of the two C-1 to C-8 moieties, one of which was established to be identical to that of swinholide A. In the other moiety, the trans ( $J_{\text{H-2/H-3}'} = 16.2$  Hz) double bond C-2/C-3 should be conjugated with an unprecedented C-4/4-CH<sub>2</sub> double bond, as indicated by the HMBC correlations of the sp<sup>2</sup> methylene protons with C-3 and C-4 (Figure 5). The additional oxygen atom implied by molecular formula was placed at C-5 on

the basis of the HMBC correlation of 4-CH<sub>2</sub> with an oxymethine resonating at  $\delta_C$  70.0 (**Figure 2.8**), thus defining the structure of swinholide K (**6**).

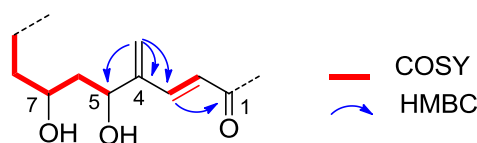


**Figure 2.8** Key COSY and HMBC correlation detected for the C-1/C-8 moiety of swinholide K (**6**)

Swinholide K (**6**) includes an additional stereogenic oxymethine at C-5 and we decided to undertake the elucidation of its configuration. Since the <sup>1</sup>H/<sup>1</sup>H coupling constant pattern exhibited by H-5, H-6a and H-6b (**Table 2.2**) was strongly suggestive of the existence of a predominant staggered rotamer around the C-5/C-6 and C-6/C-7 axes, we deemed possible the application of the Murata's J-based configuration analysis<sup>39</sup> to solve this stereochemical problem.

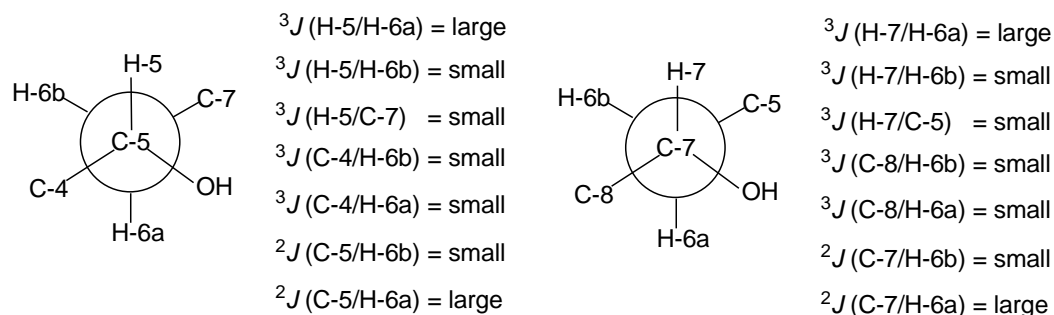


**Figure 2.9** Application of the Murata's method to the C-5/C-6 and C-6/C-7 bonds of swinholide K (**6**)

This NMR-based method allows elucidation of relative configuration in acyclic structures basing on  $^3J_{H,H}$  and  $^{2,3}J_{C,H}$  values. In our case, the required homonuclear coupling constants could be measured from the <sup>1</sup>H NMR spectrum (**Table 2.2**), while the heteronuclear coupling constants were qualitatively evaluated through careful analysis of the phase sensitive (PS)-HMBC spectrum (**Fig. 2.9**).

The obtained pattern of J values appeared perfectly consistent in indicating a C-5/C-7 erythro stereochemical relationship. Thus, on the basis of the known configuration at C-7, we could assign the *R* configuration at C-5, unambiguously defining the stereostructure of swinholide K (**6**). This is a new

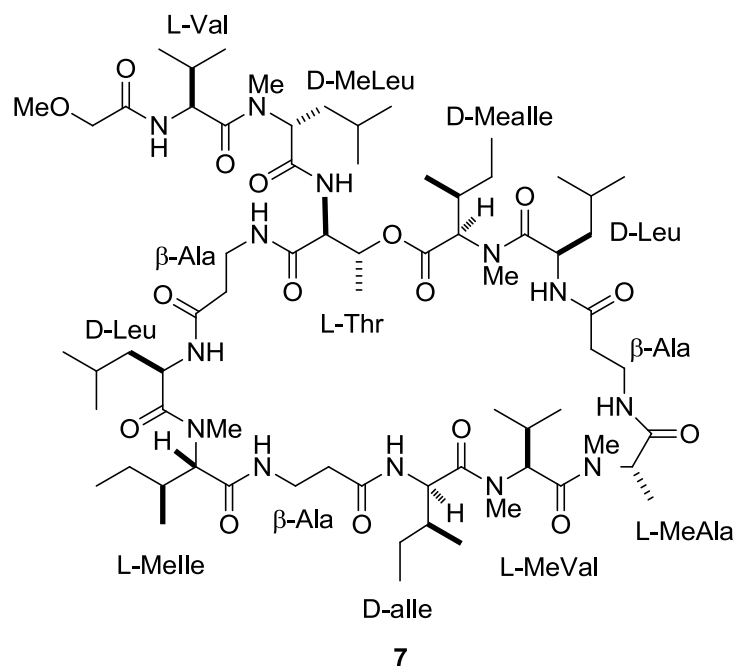
member of the small family of swinholide derivatives showing a structural modification in one or both the dienoate moieties, a family including only bistheonellides (also known as misakinolides),<sup>40</sup> hurghadolide,<sup>33</sup> swinholides F (2Z isomer of swinholide A)<sup>32</sup> and J (4,5-epoxy swinholide A).<sup>26</sup>

**Table 2.2** <sup>1</sup>H (700 MHz) and <sup>13</sup>C (175 MHz) NMR data of swinholide K (**6**) in CD<sub>3</sub>OD.

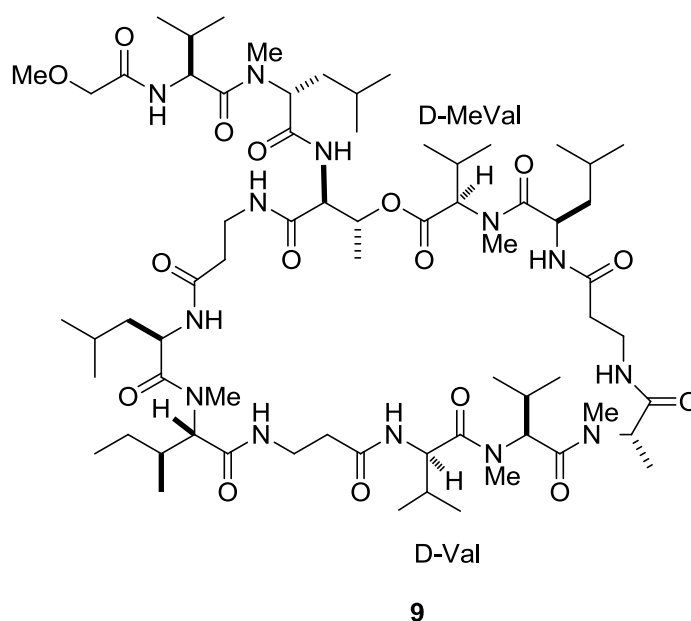
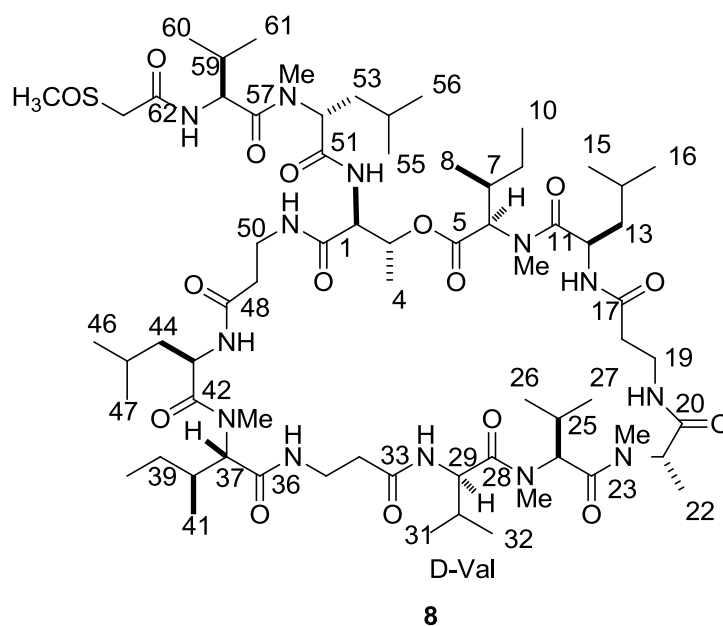
Pos.	$\delta_{\text{H}}$ mult ( <i>J</i> in Hz)	$\delta_{\text{C}}$ (type)	Pos.	$\delta_{\text{H}}$ ( <i>J</i> in Hz)	$\delta_{\text{C}}$ (type)
1	-	169.4 (C)	1'	-	170.3 (C)
2	6.17 d (16.2)	119.3 (CH)	2'	5.89 d (15.7)	115.8 (CH)
3	7.33 d (16.2)	145.5 (CH)	3'	7.43 d (15.7)	150.9 (CH)
4	-	149.5 (C)	4'	-	135.4 (C)
4-CH <sub>2</sub>	5.60 br s, 5.45 br s	121.6 (CH <sub>2</sub> )	4'-Me	1.80, s	11.4 (CH <sub>3</sub> )
5	4.62 dd (8.2, 2.9)	70.5 (CH)	5'	6.14 t (6.8)	139.1 (CH)
6	1.62 dt (11.2, 2.9) 1.82 dt (11.2, 8.2)	36.9 (CH <sub>2</sub> )	6'	2.43 m	37.5 (CH <sub>2</sub> )
7	3.98 ovl	69.9 (CH)	7'	4.03 m	67.7 (CH)
8	1.77 m, 1.36 m	41.0 (CH <sub>2</sub> )	8'	1.76 m, 1.31 m	40.0 (CH <sub>2</sub> )
9	4.49 brd (10.5)	69.1 (CH)	9'	4.49 brd (10.5)	69.1 (CH)
10	5.68 dd (1.8, 10.5)	129.9 (CH)	10'	5.68 dd (1.8, 10.5)	129.8 (CH)
11	5.83 m	123.9 (CH)	11'	5.83 m	123.9 (CH)
12	1.98 m	31.6 (CH <sub>2</sub> )	12'	1.98 m	31.1 (CH <sub>2</sub> )
13	3.57 ovl	63.9 (CH)	13'	3.57 ovl	64.4 (CH)
14	1.58 m, 1.75 m	37.5 (CH <sub>2</sub> )	14'	1.58 m, 1.75 m	35.7 (CH <sub>2</sub> )
15	3.75 m	77.5 (CH)	15'	3.75 m	77.4 (CH)
15-OMe	3.35 s	55.8 (CH <sub>3</sub> )	15'-OMe	3.35 s	55.8 (CH <sub>3</sub> )
16	1.52 m	43.9 (CH)	16'	1.52 m	43.9 (CH)
16-Me	0.85 d (6.7)	8.5 (CH <sub>3</sub> )	16'-Me	0.85 d (6.7)	8.4 (CH <sub>3</sub> )
17	3.61 ovl	73.1 (CH)	17'	3.61 ovl	72.8 (CH)
18	1.65 m, 1.75 m	39.1 (CH <sub>2</sub> )	18'	1.65 m, 1.75 m	39.3 (CH <sub>2</sub> )
19	3.97 ovl	71.9 (CH)	19'	3.97 ovl	71.9 (CH)
20	1.94 m	39.3 (CH)	20'	1.94 m	39.3 (CH)
20-Me	0.91 d (7.0)	9.2 (CH <sub>3</sub> )	20'-Me	0.91 d (7.0)	8.6 (CH <sub>3</sub> )
21	5.43 ovl	74.7 (CH)	21'	5.45 ovl	74.7 (CH)
22	1.98 m	37.7 (CH)	22'	1.98 m	37.9 (CH)
22-Me	0.94 d (7.0)	8.8 (CH <sub>3</sub> )	22'-Me	0.94 d (7.0)	8.8 (CH <sub>3</sub> )
23	3.12 dd (1.8, 9.5)	76.5 (CH)	23'	3.12 dd (1.8, 9.5)	76.5 (CH)
24	1.70 m	34.6 (CH)	24'	1.70 m	34.6 (CH)
24-Me	0.98 d (6.8)	16.7 (CH <sub>3</sub> )	24'-Me	0.98 d (6.8)	16.6 (CH <sub>3</sub> )
25	1.24 ovl, 1.42 m	24.2 (CH <sub>2</sub> )	25'	1.24 ovl, 1.42 m	24.2 (CH <sub>2</sub> )
26	1.28 ovl, 1.95 m	29.0 (CH <sub>2</sub> )	26'	1.28 ovl, 1.95 m	29.0 (CH <sub>2</sub> )
27	3.99 ovl	72.7 (CH)	27'	3.99 ovl	72.4 (CH)
28	1.52 m, 1.88 m	35.7 (CH <sub>2</sub> )	28'	1.52 m, 1.88 m	35.7 (CH <sub>2</sub> )
29	3.62 m	74.3 (CH)	29'	3.62 m	74.1 (CH)
29-OMe	3.35 s	54.2 (CH <sub>3</sub> )	29'-OMe	3.35 s	54.2 (CH <sub>3</sub> )
30	1.10 dd (10.4, 12.8), 2.03 br d (12.8)	39.6 (CH <sub>2</sub> )	30'	1.10 dd (10.4, 12.8), 2.03 br d (12.8)	39.5 (CH <sub>2</sub> )
31	3.74 m	65.7 (CH)	31'	3.74 m	65.7 (CH)
31-Me	1.20 d (6.3)	20.8 (CH <sub>3</sub> )	31'-Me	1.20 d (6.3)	20.8 (CH <sub>3</sub> )

## 2.5 DEPSIPEPTIDES FROM *THEONELLA SWINHOEI*

Pursuing the study of the chloroform extract of *Theonella swinhoei*, two new cyclic tridecadepsipeptide of the theonellapeptolide family were isolated: sulfiniltheonellapeptolide (**8**), characterized by a methylsulfinylacetyl group at the N-terminus, and theonellapeptolide If (**9**), the first member of this class of compounds to show four valine residues. The structures of the compounds, isolated along with the known theonellapeptolide Id (**7**), were determined by extensive 2D NMR and MS/MS analyses followed by application of Marfey's method<sup>41</sup>. The isolated peptides exhibited moderate antiproliferative activity against HepG2 cells, a hepatic carcinoma cell line.



Theonellapeptolides are tridecapeptide lactones characterized by the presence of aliphatic and non-polar amino acids including high ratio of D-amino acids, N-methyl amino acids, and  $\beta$ -amino acids. In particular, the structure of theonellapeptolide Id (**7**) includes three  $\beta$ -Ala, three D-Leu (one N-methylated), two L-Val (one N-methylated), one L-MeAla, one L-Thr, one L-Melle, and two D-allole (one N-methylated) units.



Sulfinyltheonellapeptolide (**8**,  $[\alpha]^D_{-38.1}$ , c 0.1, MeOH) was isolated as a colorless amorphous solid with pseudomolecular ion peaks at  $m/z$  1423  $[M + H]^+$  and 1445  $[M+Na]^+$  in the ESIMS, and high-resolution analysis established the molecular formula  $C_{69}H_{123}N_{13}O_{16}S$ . Inspection of its  $^1H$  NMR spectrum (CD<sub>3</sub>OD, **Table 2.3**) clearly suggested the peptide nature of **8** and placed it into the theonellapeptolide class. Given this characterization of **8** the presence of the sulfur atom in the molecular formula appeared especially remarkable. In particular, the  $^1H$  and  $^{13}C$  NMR data of **8** indicated the presence of six methyl singlets ( $\delta_H$  2.77, 2.79, 3.22, 3.30, 3.31, and 3.35) and

fourteen carbonyl groups (resonating from  $\delta_c$  166.5 to 177.0). Extensive analysis of homonuclear and heteronuclear 2D NMR spectra including  $^1\text{H}/^1\text{H}$  COSY,  $^1\text{H}/^1\text{H}$  TOCSY,  $^1\text{H}/^{13}\text{C}$  HSQC and  $^1\text{H}/^{13}\text{C}$  HMBC allowed to overcome the difficulty posed by the severe signal overlap in the  $^1\text{H}$  NMR spectrum and to establish the presence of three  $\beta$ -Ala, three Leu (one *N*-methylated), two Ile (both *N*-methylated), three Val (one *N*-methylated), one Thr, and one *N*-methylAla, the same amino acid composition as in theonellapeptolide Id (**7**) except for one residue. The above analysis left unassigned a methyl singlet at  $\delta_H$  2.79 ( $\delta_C$  39.2) and a pair of mutually coupled doublets at  $\delta_H$  3.67 and 3.86, with these latter signals showing HMBC correlations both with the methyl carbon at  $\delta_C$  39.2 and an amide carbonyl resonating at  $\delta_C$  166.5. The  $^1\text{H}$  and  $^{13}\text{C}$  NMR chemical shift values of both the methyl and the methylene groups strongly suggested their linkage to a sulfoxide group, and the presence of a methylsulfinylacetyl (MeS(O)Ac) subunit was also in full agreement with the molecular formula. The amino acid sequence of **8** was then disclosed by careful analysis of the pattern of HMBC correlations, whose key cross-peaks are shown in **Figure 2.10**. The cross-peak of the Thr low-field shifted  $\beta$ -CH ( $\delta_H$  5.19) with the Me-Ile carbonyl group revealed the presence of an ester linkage.

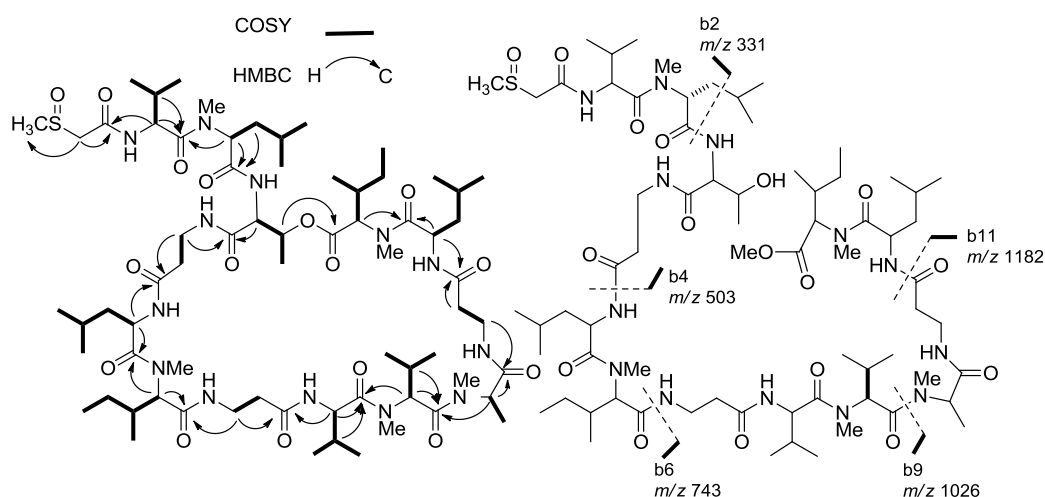


**Figure 2.10** COSY and key HMBC correlations (left) and MS/MS fragmentations of **8** and its ring-opened methanolysis product, respectively.

HMBC analysis also revealed that the amide carbonyl at  $\delta_C$  166.5 assigned to the methylsulfinylacetyl subunit was correlated to the  $\text{H}\alpha$  of Val-1 residue,

thus establishing the acetylation of the *N*-terminus in **8**. Methanolysis of **8**, followed by ESI (positive ion mode) MS/MS analysis of the obtained acyclic methyl ester derivative provided key fragment peaks, shown in **Figure 2.10**, giving definitive confirmation of the sulfinyltheonellapeptolide gross structure. In addition to the pseudomolecular ion at  $m/z$  1454  $[M + H]^+$ , corresponding to the introduction of 32 mass units (MeOH) in the molecule, the ESIMS/MS spectrum provided several fragment ion peaks corresponding to *N*-terminus fragments due to the cleavage of the amide bond, and referred to as the b series in Roepstorff and Fohlman nomenclature<sup>42</sup>. In particular, the presence of the b2 fragmentation peak at  $m/z$  331 supported, once again, the presence of the MeS(O)Ac unit.

Complete acid hydrolysis of **8** and Marfey's analysis<sup>37</sup> on the hydrolysate (derivatization with L-FDAA, 1-fluoro-2,4-dinitrophenyl-5-L-alanine amide, followed by LC-MS comparison with the FDAA derivatives of appropriate standards) enabled us to determine the configuration of the chiral amino acid residues as L-MeAla, D-Leu ( $\times 2$ ), D-MeLeu, L-Thr, L-Me-Val, L-Me-Ile, D-Me-*allo*-Ile, D-Val and L-Val. This result left the ambiguity on the localization of the two methylisoleucine residues and of the two enantiomeric valine residues. Since the  $^1\text{H}$  and  $^{13}\text{C}$  NMR resonances for the amino acids at positions 5–10 and 36–41 of **8** were almost superimposable with the corresponding values reported for theonellapeptolide Id (**7**)<sup>43</sup>, we assumed that the two peptides share the configurations at those positions, thus inferring the configurations of the two isoleucine residues. Similarly, it appeared reasonable to assume that, as in the co-occurring theonellapeptolide Id (and in all the theonellapeptolide found to date), the L-Val could be the *N*-terminal amino acid and thus, the D-Val should be the amino acid at positions 28–32. A D-Val residue at these positions has been found previously in the structure of theonellapeptolide Ia<sup>44</sup>. The configuration at the stereogenic sulfur atom of **8** has been left undetermined.

**Table 2.3**  $^1\text{H}$  (500 MHz) and  $^{13}\text{C}$  (125 MHz) NMR data of sulfinyltheonellapeptolide in  $\text{CD}_3\text{OD}$  (**8**).

AA	Pos.	$\delta_{\text{H}}$ , m, J in Hz	$\delta_{\text{C}}$	AA	Pos.	$\delta_{\text{H}}$ , m, J in Hz	$\delta_{\text{C}}$	
L-Thr	1	-	171.2	$\beta$ -Ala	33	-	173.2	
	2	4.36, m	58.5		34/34'	2.29, m; 2.59, m	36.5	
	3	5.19, m	70.6		35/35'	3.10, m; 4.23, m	36.8	
	4	1.11, d, 6.5	19.1	L-Me-Ile	36	-	172.5	
D-Me-Ile	5	-	173.4		37	3.14, m	71.2	
	6	5.06, m	62.5		38	2.48, m	36.5	
	7	2.14 <sup>a</sup>	34.2		39/39'	1.04, m; 1.92 <sup>a</sup>	30.2	
	8	0.78, d, 7.2	11.5		40	1.00 <sup>a</sup>	13.2	
	9/9'	1.10, m; 1.38, m	26.5		41	0.81, d, 6.4	15.3	
	10	0.98, t, 7.6	17.0		37-NMe	3.35, s	39.9	
D-Leu	6-NMe	3.22, s	32.0	D-Leu	42	-	176.2	
	11	-	177.0		43	5.06, m	50.6	
	12	5.03, m	50.5	44	1.72 <sup>a</sup> ; 1.25 <sup>a</sup>	41.2		
	13/13'	1.74 <sup>a</sup> , 1.25 <sup>a</sup>	40.4	45	1.80 <sup>a</sup>	26.6		
	14	1.81 <sup>a</sup>	26.3	46	1.03 <sup>a</sup>	21.0		
	15	0.89 <sup>a</sup>	11.1	47	1.04 <sup>a</sup>	25.0		
	16	0.94 d, 7.3	17.2	$\beta$ -Ala	48	-	175.0	
	$\beta$ -Ala	17	-	174.3		49/49'	2.28, m; 2.36, m	39.1
18/18'		2.23, m 2.29 m	39.5		50/50'	3.14, m; 3.81, m	37.7	
19/19'		3.24, m 3.69, m	38.2	D-Me-Leu	51	-	175.2	
L-Me-Ala	20	-	172.5		52	5.24, m	57.5	
	21	5.17 <sup>a</sup>	58.5		53/53'	1.41 <sup>a</sup> ; 2.03 m	39.5	
	22	1.45, d, 7.1	16.0		54	1.52 <sup>a</sup>	27.1	
	21-NMe	2.77 s	30.5		55	0.83, d, 6.7	22.1	
L-Me-Val	23	-	173.0		56	0.95 <sup>a</sup>	24.3	
	24	5.02 <sup>a</sup>	59.4		52-NMe	3.30 s	33.0	
	25	2.40, m	30.2	L-Val	57	-	176.0	
	26	0.86 <sup>a</sup>	20.6		58	4.76, m	57.7	
	27	0.92, d, 6.1	20.8		59	2.12, m	32.5	
	24-NMe	3.31 s	31.9		60	0.96 <sup>a</sup>	20.4	
	D-Val	28	-	173.2		61	1.01 <sup>a</sup>	19.2
		29	4.76, m	68.9	Me-SAc	62	-	166.5
30		2.68, m	27.6			63/63'	3.67, d, 11.2; 3.86, d, 11.2	58.9
31		0.86 <sup>a</sup>	18.1		63-SOME	2.79, s	39.2	
32		1.17, d, 6.5	23.3					

<sup>a</sup>Overlapped with other signals.

Theonellapeptolide If (**9**,  $[\alpha]_{\text{D}} -26.7$ ,  $c$  1.0, MeOH) was isolated as a colorless amorphous solid and its molecular formula was established to be  $\text{C}_{68}\text{H}_{121}\text{N}_{13}\text{O}_{16}$  by means of high resolution ESIMS. Inspection of  $^1\text{H}$  and  $^{13}\text{C}$  NMR spectra of **9** ( $\text{CD}_3\text{OD}$ , **Table 2.4**) revealed extensive similarities with parallel data detected for **8**. The most important differences could be recognized in the downfield shift of one methyl singlet (from  $\delta_{\text{H}}$  2.79,  $\delta_{\text{C}}$  39.2 in **8** to  $\delta_{\text{H}}$  3.38,  $\delta_{\text{C}}$  59.1 in **9**) and of a pair of mutually coupled doublets (from

$\delta_{\text{H}}$  3.67 and 3.86,  $\delta_{\text{C}}$  58.9 in **8** to  $\delta_{\text{H}}$  3.88 and 3.97,  $\delta_{\text{C}}$  71.8 in **9**). These data were easily rationalized with the replacement of the terminal methylsulfinylacetyl group with a methoxyacetyl group, a typical *N*-terminus acylating unit, already found in the theonellapeptolide family.

Careful inspection of COSY and TOCSY spectra revealed also that, in agreement with the molecular formula, one isoleucine residue of **8** is replaced by a valine residue in **9**. A subsequent combined analysis of homonuclear and heteronuclear 2D NMR spectra disclosed the presence of the following residues: three  $\beta$ -Ala, three Leu (one *N*-methylated), one *N*-methyl-Ile, four Val (two *N*-methylated), one Thr, and one *N*-methylAla. As detailed for **8**, the amino acid sequence of **9** was deduced by careful analysis of HMBC correlations and supported by the MS/MS spectrum of the methanolysis product mixture. Thus, theonellapeptolide If (**9**) has been identified as a new member of the theonellapeptolide family differing from theonellapeptolide Id (**7**) by the replacement of two isoleucine residues (positions 5–10 and 28–32) with valine residues. Complete acid hydrolysis of **9** and Marfey's analysis on the hydrolysate mixture provided the configuration of the chiral amino acid residues as L-MeAla, D-Leu ( $\times 2$ ), D-MeLeu, L-Thr, L-Me-Ile, D-Me-Val, D-Val, L-Me-Val and L-Val. With these data in hands, it was not possible to unambiguously define the exact localization of the valine residues. However, if we assume that the L-Val and L-Me-Val residues are localized at the same positions as in theonellapeptolide Id, then the positions of their enantiomeric counterparts are consequently deduced. In summary, compound **9** is a valine-rich theonellapeptolide, being the first member of this class to possess four valine residues.<sup>45</sup>

**Table 2.4**  $^1\text{H}$  (500 MHz) and  $^{13}\text{C}$  (125 MHz) NMR data of theonellapeptolide If (**9**) in  $\text{CD}_3\text{OD}$ .

AA	Pos.	$\delta_{\text{H}}$ , m, J in Hz	$\delta_{\text{C}}$	AA	Pos.	$\delta_{\text{H}}$ , m, J in Hz	$\delta_{\text{C}}$
L-Thr	1	-	169.2	$\beta$ -Ala	33	-	173.2
	2	4.38, m	57.5		34/34'	2.29, m; 2.59, m	36.5
	3	5.15, m	69.3		35/35'	3.10, m; 4.17, m	36.8
	4	1.13, d, 6.5	17.5	L-Me-Ile	36	-	172.5
D-Me-Val	5	-	171.5		37	3.14, m	71.2
	6	4.95, m	62.2		38	2.48, m	36.5
	7	2.27 <sup>a</sup>	26.7		39/39'	1.04, m; 1.92 <sup>a</sup>	30.2
	8	0.76, d, 7.2	11.5		40	1.00 <sup>a</sup>	13.2
	9	0.99, d, 7.2	23.5		41	0.81, d, 6.4	15.3
	6-NMe	3.17, s	31.3		37-NMe	3.35, s	39.9
D-Leu	11	-	177.0	D-Leu	42	-	176.2
	12	5.01, m	48.5		43	5.09, m	50.6
	13/13'	1.65 <sup>a</sup> , 1.25 <sup>a</sup>	40.3		44	1.72 <sup>a</sup> ; 1.25 <sup>a</sup>	41.2
	14	1.74 <sup>a</sup>	24.9		45	1.78 <sup>a</sup>	26.6
	15	0.96 <sup>a</sup>	11.1		46	1.03 <sup>a</sup>	21.0
	16	0.98 d, 7.3	17.2		47	1.04 <sup>a</sup>	25.0
	$\beta$ -Ala	17	-	174.3	$\beta$ -Ala	48	-
$\beta$ -Ala	18/18'	2.23, m 2.31 m	39.5		49/49'	2.28, m; 2.36, m	39.1
	19/19'	3.15, m 3.85, m	38.2		50/50'	3.14, m; 3.81, m	37.7
				D-Me-Leu	51	-	175.2
L-Me-Ala	20	-	172.5		52	5.18, m	56.4
	21	5.17 <sup>a</sup>	58.5		53/53'	1.41 <sup>a</sup> ; 2.03 m	39.5
	22	1.45, d, 7.1	16.0		54	1.52 <sup>a</sup>	27.1
	21-NMe	2.77 s	30.5		55	0.83, d, 6.7	22.1
L-Me-Val	23	-	173.0		56	0.95 <sup>a</sup>	24.3
	24	5.02 <sup>a</sup>	59.4		52-NMe	3.30 s	33.0
	25	2.40, m	30.2	L-Val	57	-	176.0
	26	0.86 <sup>a</sup>	20.6		58	4.98, m	54.6
	27	0.92, d, 6.1	20.8		59	2.08, m	31.6
	24-NMe	3.31 s	31.9		60	0.98 <sup>a</sup>	20.4
	D-Val	28	-	173.2		61	1.01 <sup>a</sup>
29		4.76, m	68.9	MeO-Ac	62	-	169.2
30		2.68, m	27.6		63/63'	3.88, d, 11.2;	71.8
31		0.86 <sup>a</sup>	18.1			3.97, d, 11.2	
32		1.17, d, 6.5	23.3		63-OMe	3.38	59.1

<sup>a</sup>Overlapped with other signals.

## 2.6 ANTIPROLIFERATIVE ACTIVITY OF SWINHOLIDES AND THEONELLAPEPTOLIDES.

Swinholide A and many of its analogues have been demonstrated to be potent cell growth inhibitors active against several cancer cell lines, including KB cells (epidermal carcinoma), PC (lung carcinoma), L1210 (mouse leukemia), colon (SW480) and gastric adenocarcinoma (KATO-III).<sup>7-24</sup> It has been shown that swinholides exert their cytotoxic effect by disrupting the actin

cytoskeleton, a ubiquitous protein system essential for cell motility and cytokinesis in all eukariotes.<sup>46</sup> The actin-swinholide complex has been investigated in detail by X-ray diffraction and observed that the macrolide binds simultaneously to two molecules of G-actin (globular form), forming a tertiary complex with the two side chains of the macrolide (from C-21 to the pyran ring) inhibiting polymerization by sequestration of G-actin, thus affecting many crucial cellular processes (**Figure 2.11**). Interestingly, the different size of the macrocyclic dilactone ring shown by isoswinholide A was responsible of a marked decrease of activity against L210 and KB cell lines ( $IC_{50} > 1 \mu M$ )<sup>36</sup>. On the other hand, bistheonellides, lacking one of the conjugated double bonds (C-2/C-3 and C-2'/C-3'), have been shown to link efficiently with actin but they are not able to cause breakage of actin strands.<sup>47</sup>

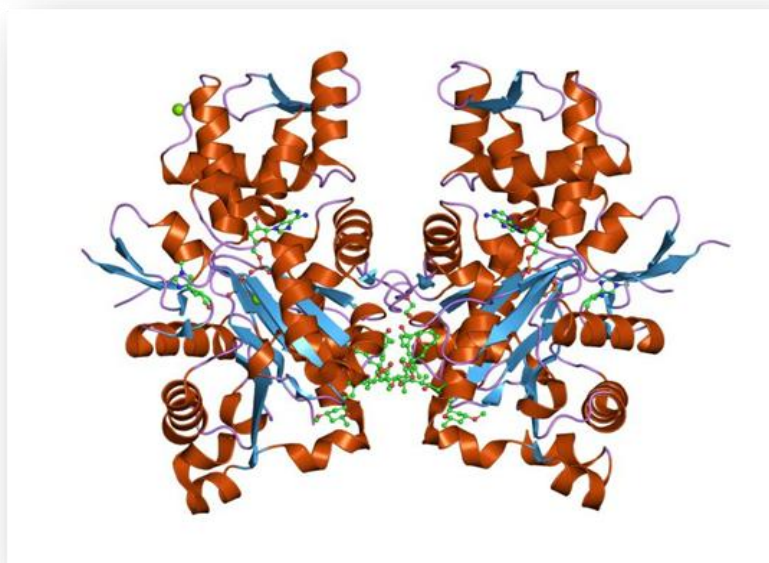


**Figure 2.11** Crystal structure of actin in complex with swinholide A.

Theonellapeptolides are structurally similar to the widely used immunosuppressant drug cyclosporin A, sharing at least three important features: i) the exclusive presence of hydrophobic aliphatic amino acids; ii) the abundance of *N*-methylated residues and iii) the presence of a macrocycle made up by more than ten amino acids. Only a few theonellapeptolides have been tested for immunosuppressive activity and they revealed a moderate potency.<sup>26</sup> In general, the potential bioactivity of this class of unique

cyclopeptides has not been investigated in great detail, and an inhibition of the development of fertilized eggs of sea urchin, an activity on the transport of Na<sup>+</sup> and K<sup>+</sup> ions<sup>45</sup>, and a moderate cytotoxicity have been reported.

Considering all these data, swinholides and theonellapeptolides isolated during the present investigation (**1-9**) have been evaluated for their anti-proliferative activity in HepG2 cells, an hepatic carcinoma cell line.

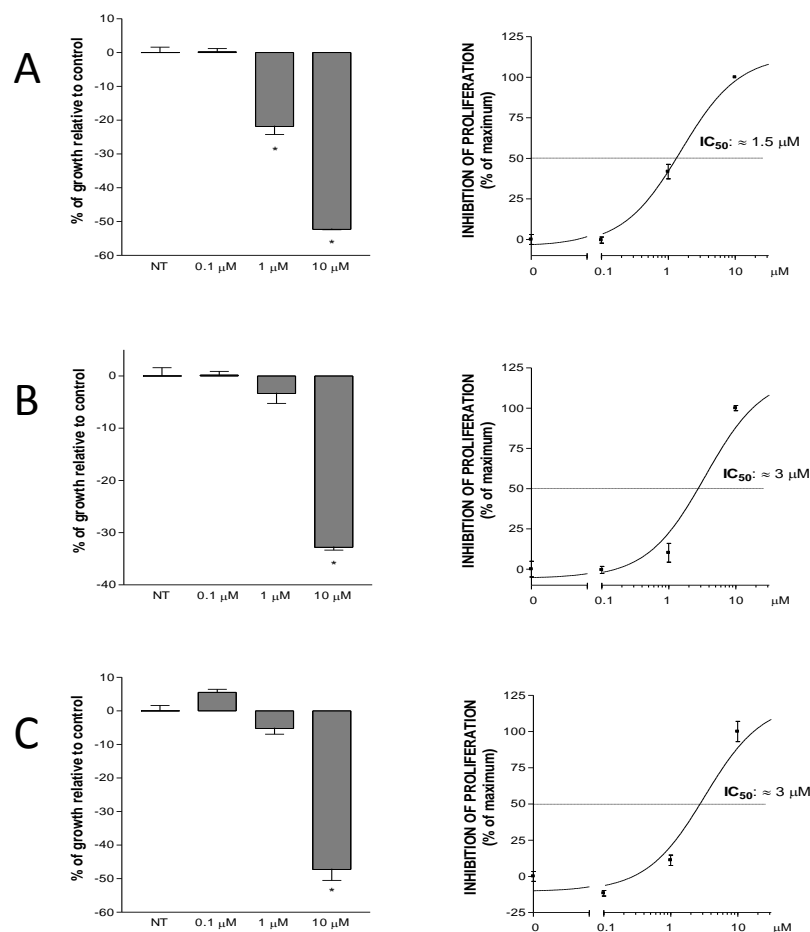


**Figure 2.12** Anti-proliferative activity of theonellapeptolides **7-9** on hepatic carcinoma cell line.\*

\*MTT assay was performed on HepG2 cells treated with increasing doses for 48 hours. Left panel: proliferation rate expressed as Δ% of absorbance compared to untreated cells. The values are expressed as mean ± SE. Right panel: computation of IC<sub>50</sub> values. (A) Theonellapeptolide Id; (B) Sulfinyltheonellapeptolide; (C) Theonellapeptolide If (\*<0.05 compared to not treated cells; N=4).

As reported in **Figure 2.12**, all tested theonellapeptolides showed antiproliferative activity at low micromolar doses, with a similar pattern of potency. At the dose 10 μM, the proliferation rate of HepG2 cells was

significantly reduced by theonallapeptolide Id (**7**), sulfinyltheonellapeptolide (**8**) and theonellapeptolide If (**9**) to about 50%, 30% and 50%, respectively (**Figure 2.12**, panels A, B and C; \*  $p < 0.05$  compared to untreated cells;  $n = 4$ ). Only theonellapeptolide Id was able to significantly reduce the proliferation at 1  $\mu\text{M}$ . At this dose, the proliferation reduction was equal to 20% (**Figure 2.12**, panel A; \*  $p < 0.05$  compared to untreated cells;  $n = 4$ ). Computation of 50% inhibitory drug concentration ( $\text{IC}_{50}$ ) revealed that compounds **7**, **8** and **9** were characterized by very similar  $\text{IC}_{50}$  values of about 1.5  $\mu\text{M}$  for theonellapeptolide Id and 3  $\mu\text{M}$  for sulfinyltheonellapeptolide and theonellapeptolide If.

**Table 2.5**  $\text{IC}_{50}$  and efficiency (as % of growth inhibition relative to Swinholide A 100nM) of swinholides (**1-6**) on HepG2

Compound	$\text{IC}_{50}$ (nM)	Efficiency
Swinholide A ( <b>1</b> )	20	-
Swinholide B ( <b>2</b> )	25	89.38 $\pm$ 4.1 %
Swinholide D ( <b>3</b> )	30	45.35 $\pm$ 1.4 %
Isoswinholide A ( <b>4</b> )	35	16.28 $\pm$ 1.7 %
Isoswinholide B ( <b>5</b> )	1500	7.52 $\pm$ 1.2 %
Swinholide K ( <b>6</b> )	15	42.67 $\pm$ 0.85 %

On the other hand, all tested swinholides showed anti-proliferative activity at nanomolar doses, with the exception of isoswinholide B: with this compound a block of proliferation was observed at 1  $\mu\text{M}$  (**Fig. 2.13 E**; \* $p < 0.05$  vs NT,  $n=4$ ). Swinholides A (**1**) B (**2**) showed very similar anti-proliferative capability: at the dose 100 nM both compounds reduced proliferation rate of HepG2 cells approximately of 50% (**Fig. 2.13 A-B**; \* $p < 0.05$  vs NT,  $n=4$ ). Moreover, swinholide A was able to significantly reduce proliferation at 10 nM (**Fig. 2.13 A**; \* $p < 0.05$  vs NT,  $n=4$ ). Swinholide D and isoswinholide A were less potent compared to swinholide A, with an efficiency of 45% and 7%, respectively (**Fig. 2.13 C-D**; \* $p < 0.05$  vs NT,  $n=4$ . **Table 2.5**). Finally,

swinholide K (**6**) reduced significantly growth rate in HepG2 cells both at 10 nM and 100 nM, showing an IC<sub>50</sub> value of about 15 nM, but its efficiency was about 42% compared to swinholide A (Fig. 7F; \*p<0.05 vs NT,n=4. **Table 2.5**). These data support the observation that the size of the dilactone ring has a crucial impact on the activity and this effect would be worthy of a more detailed investigation. Interestingly, the new swinholide K exhibited a similar (slightly lower) IC<sub>50</sub> value but a halved efficiency compared to that of swinholide A.

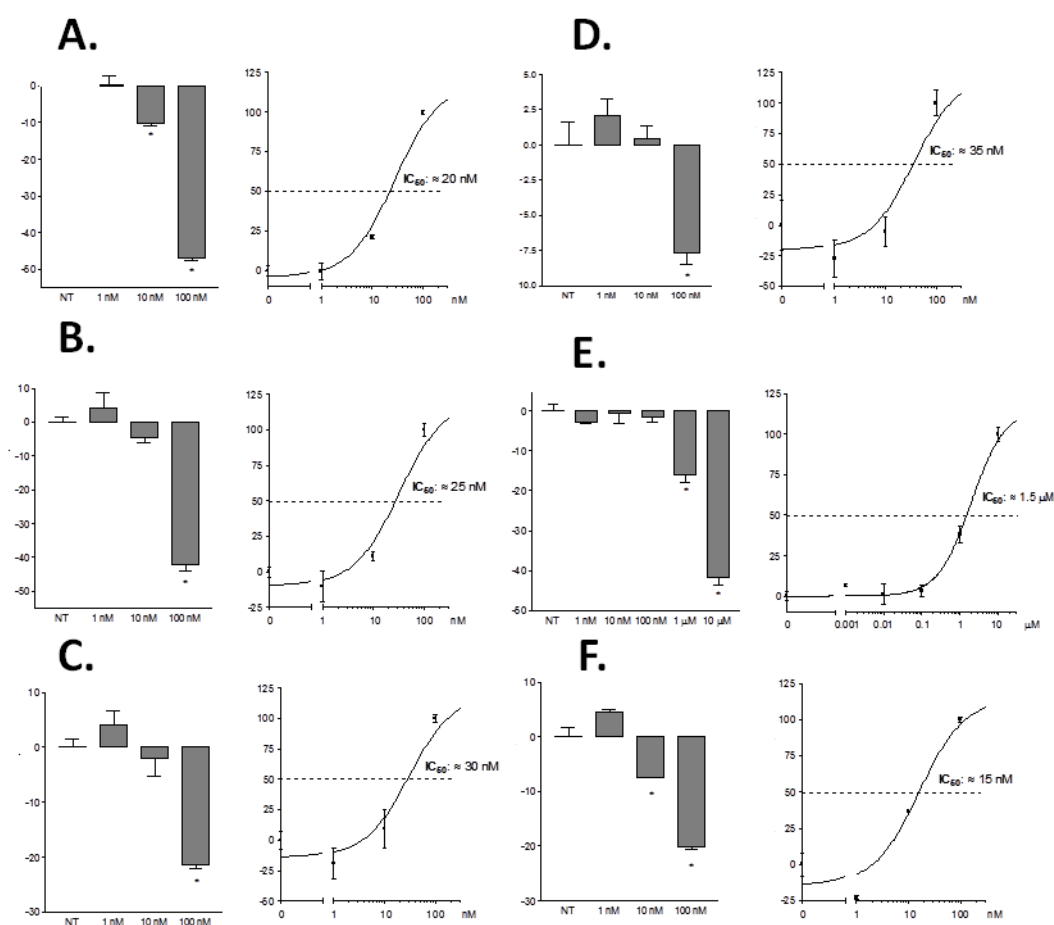
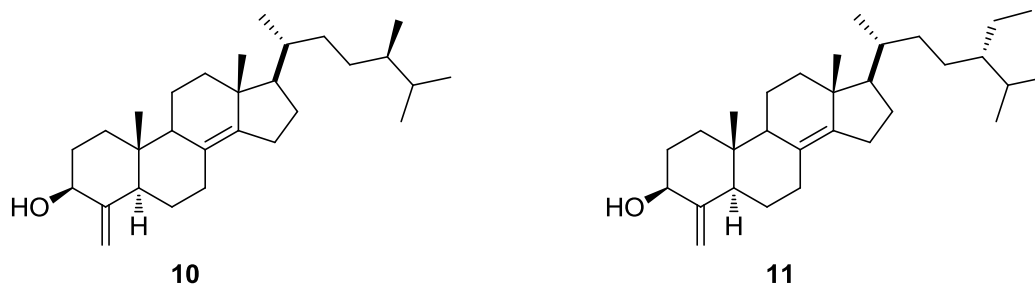


**Figure 2.13** Anti-proliferative activity of swinholides (**1-6**) on hepatic carcinoma cell line.\*

\*MTT assay was performed on HepG2 cells treated with increasing doses of swinholides for 48 hours. Left panel: proliferation rate expressed as  $\Delta\%$  of absorbance compared to untreated cells. The values are expressed as mean  $\pm$  SE. Right panel: computation of IC<sub>50</sub> values. (A) Swinholide A; (B) Swinholide B; (C) Swinholide D; (D) Isoswinholide A; (E) Isoswinholide B; (F) Swinholide K. (\*<0.05 compared to untreated cells; N=4).

## 2.7. 4-METHYLENESTEROLS: TYPICAL *THEONELLA* METABOLITES

The investigation of *Theonella swinhoei* steroidal fraction has resulted in the isolation of several members of the 4-methylenesteroids family. The rare 4-methylenesteroids represent the exclusive elements of the steroid biogenetic class in *Theonella* sponges with conicasterol (**10**) and theonellasterol (**11**) as ideal biomarkers of *Theonella conica* and *Theonella swinhoei*, respectively<sup>48</sup>.



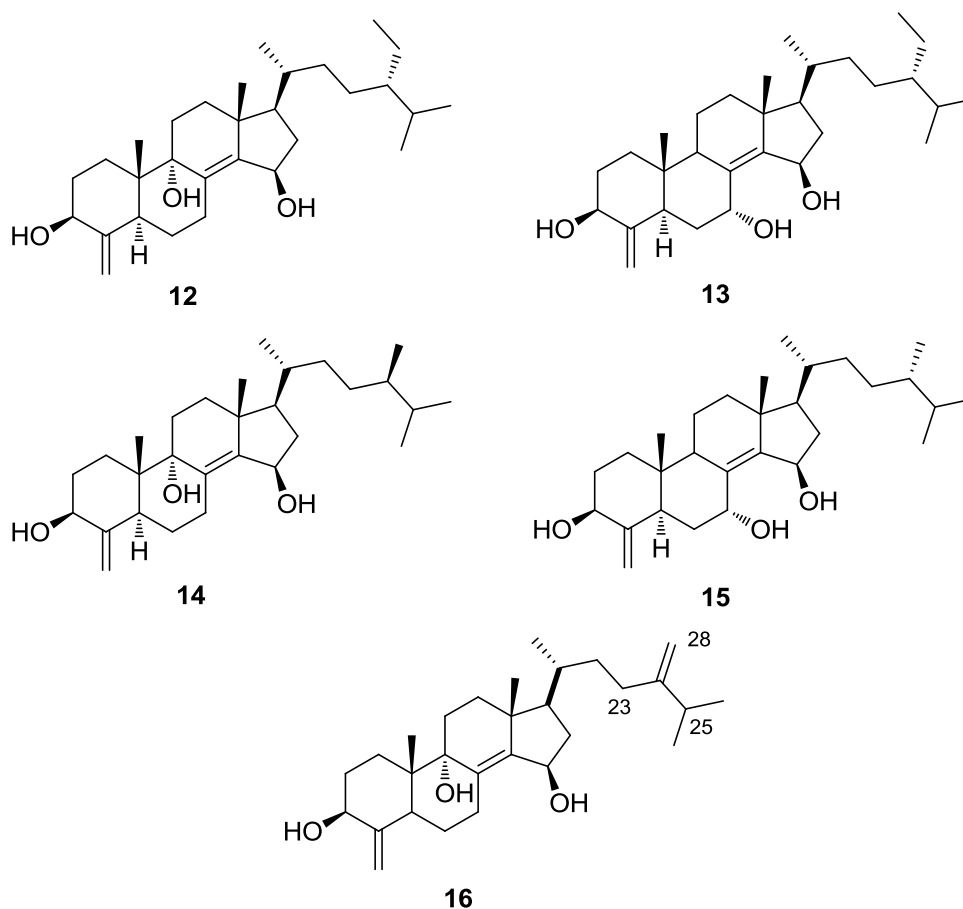
These molecules share substituents and unsaturations on tetracyclic core but differ in the side chain with a 24*S*-ethyl group in theonellasterol and a 24*R*-methyl group in conicasterol. 4-methylenesteroids are endowed with peculiar pharmacological profiles, ranging from selective antagonism on FXR<sup>49</sup> to dual modulation on FXR/PXR; *Theonella* sponges genus is an invaluable source of NRs ligands.<sup>50</sup>

In particular, during my PhD period, two known theonellasterols (E and F) (**12-13**), two known conicasterols (D and E) (**14-15**) and one new side chain modified sterol, 24-dehydroconicasterol D (**16**), with an additional methylene group in position 24, have been isolated.

This new metabolite has been evaluated by the group of Prof. Fiorucci (University of Perugia-Italy) for interaction with the nuclear receptor FXR, together with which some natural and semisynthetic analogues (obtained in the laboratories of Prof. D'Auria, University of Naples), while compounds **12-13-14-15** were already tested for this activity<sup>51-52</sup>.

Structural elucidation of compounds **16** was helped by comparison of spectroscopic data with those of known analogue, indeed it showed NMR

signals of the tetracyclic core superimposable to the one of already published derivative conicasterol D (**14**).<sup>53</sup>



COSY analysis of the <sup>1</sup>H NMR spectrum of 24-dehydroconicasterol D (**16**) (see Experimental Section, paragraph **2.9.2**), C<sub>29</sub>H<sub>46</sub>O<sub>3</sub> by HR-ESIMS, indicated that its side chain should include an *sp*<sup>2</sup> methylene, three methyl groups (all doublets at δ<sub>H</sub> 0.99, 1.09 and 1.10), two *sp*<sup>3</sup> methines and two *sp*<sup>3</sup> methylenes. The HMBC correlations of the *sp*<sup>2</sup> methylene with C-23, C-24 and C-25 indicated its attachment at C-24, thus defining the structure of compound 4 as a new sterol differing from conicasterol D (**14**) for the presence of an additional double bond between C-24 and C-28.

## 2.8 PXR MODULATION ACTIVITY OF *THEONELLA* STEROIDS

24-Dehydroconicasterol D (**16**) together with which some natural and semisynthetic conicasterol analogues were evaluated on PXR in a luciferase

reporter assay on a human hepatocyte cell line (HepG2 cells), in collaboration with Prof. Fiorucci (University of Perugia).

Nuclear receptors (NRs) are a large superfamily of ligand-dependent transcription factors that regulate expression of genes involved in metabolism, homeostasis, growth and differentiation, aging, and reproduction.<sup>54</sup> These regulatory proteins have a common evolutionary history as evidenced by their similar sequences and overlapping cellular functions. In addition, their ligands are often not selective for one particular NR, but rather are partial or full agonists for several receptors.

Despite a complex organization, the NR family has a long history of successful drug discovery and those that have been deorphanized thus far have proved to be druggable; in other words, their activity can be modulated by small molecules.<sup>55</sup> Drugs exploiting NRs represent 10–15% of the global pharmaceutical market are a mainstay of treatment in various human conditions including diabetes, hyperlipidemias, contraception, hormone replacement therapy, osteoporosis and cancers.<sup>56</sup>

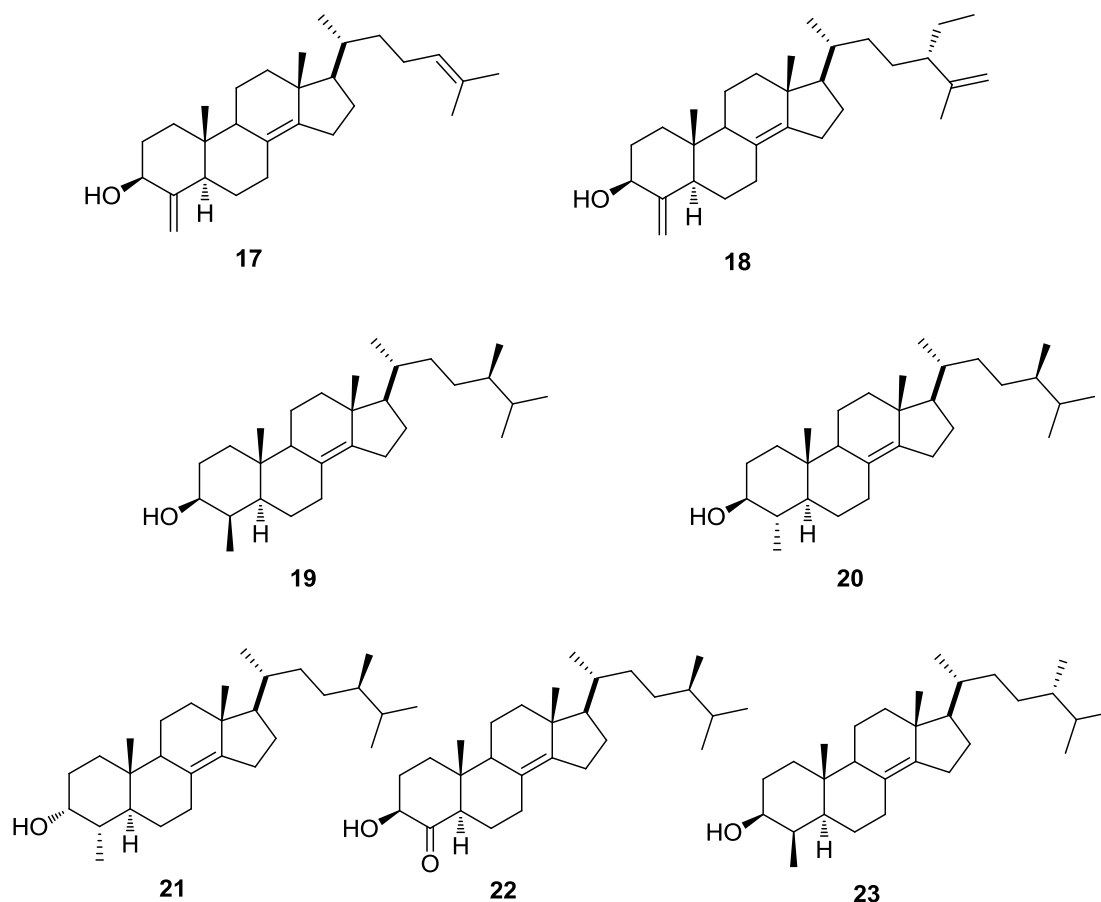
Pregnane-X-receptor (PXR) is a member of nuclear receptors (NRs) superfamily. PXR plays a fundamental role in protecting body tissues from xenobiotics and toxic bile acids.<sup>57</sup> PXR is almost exclusively expressed in the gastrointestinal tract and liver, with lower levels in the kidney and ovary. PXR dysfunction is associated with immune disorders including PBC (primary biliary cirrhosis), PSC (primary sclerosing cholangitis) and inflammatory bowel diseases (IBDs), a family of highly prevalent disorders encompassing two major diseases: ulcerative colitis and Crohn's disease. Apart crucial role in regulating drug detoxification, PXR plays also pleiotropic role of endobiotic metabolism. PXR regulates bile acids homeostasis,<sup>58,59</sup> glucose and lipid metabolism,<sup>60,61</sup> energy homeostasis, immune responses<sup>62</sup> and, notably, drug-drug interactions. As a result, PXR ligands (agonists and antagonists) are recognized opportunity for the pharmacotherapy of several human diseases including diabetes and obesity, dyslipidemia, liver disorders, immune mediate dysfunctions and cancer.

Expectedly, in the last decades a considerable number of chemicals have been show to function as PXR ligands, including several natural compounds

isolated from herbal medicines and marine organisms, which have highlighted the potential of novel chemical scaffolds useful for the development of PXR ligands.

In this context several compounds isolated from marine sponges have been described to be endowed with agonistic activity on PXR, including solomonsterols, side chain truncated steroids,<sup>63</sup> and the large family of 4-methylenesteroids from *Theonella swinhoei*.<sup>64-65</sup>

24-dehydroconicasterol D (**16**), together with other three new side chain modified 4-methylenesteroids named preconicalsterol (**17**) and 24-dehydrotheonellasterol (**18**) and with some semisynthetic compounds (**19-20-21-22-23**), isolated or obtained from conicasterol (**10**), allowed to speculate on the effect of punctual modifications on ring A and on the side chain toward PXR modulation and, notably, to identify a new chemotype of PXR antagonist.



These molecules were evaluated on PXR in a luciferase reporter assay on human hepatocyte (HepG2 cells) transiently transfected with pSG5-PXR, pSG5-RXR, pCMV- $\beta$ galactosidase, and p(CYP3A4)-TK-Luc vectors (**Figure 2.14**). HepG2 cells were stimulated with compounds **16-23** in the presence or in absence of rifaximin, a well characterized PXR agonist (10  $\mu$ M). As shown in **Figure 2.14**, compounds **17** and **21**, when administered alone, partially transactivate PXR whereas **19** at 50  $\mu$ M dose was relatively effective in inhibiting PXR transactivation caused by rifaximin, thus behaving as an antagonist. Even if partial inhibitions of PXR transactivation caused by rifaximin are shown in **Figure 18B**, none compound of this series could be judged an effective antagonist. In details, when cells were co-exposed to compounds **17** and **21** and rifaximin, the two compounds caused a slightly reversion of the pharmacological effect of rifaximin. This finding is common when a full agonist (rifaximin) is mixed with partial (less potent) agonists such as compounds **17** and **21**. As concern compound **19**, even if a slight antagonistic effect was demonstrated at 50 mM, this behavior was not confirmed when **19** was co-administered with rifaximin at different concentration.<sup>66</sup>

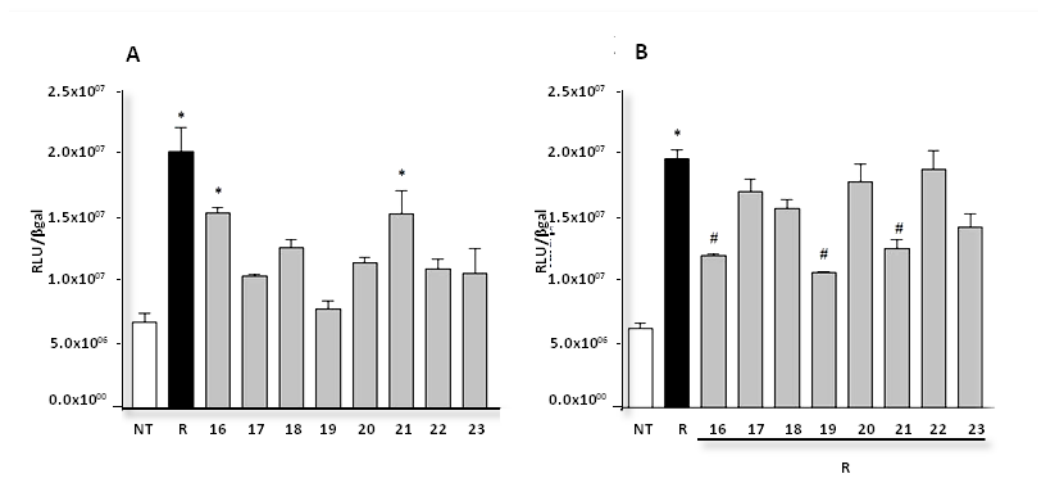


**Figure 2.14** Transactivation assay performed on HepG2 cells transiently transfected with full-length FXR,RXR,  $\beta$ gal and the canonical FXRE containing 3 inverted repeats (IR1). \*

\*At 24 h post-transfection, cells were primed with (A) Rifaximin (R) and compounds 16-23 10 $\mu$ M or with (B) compounds 16-23 50  $\mu$ M plus Rifaximin 10  $\mu$ M for 18 h (\*:  $p < 0.05$  versus not treated cells; #:  $p < 0.05$  versus Rifaximin).

To further investigate the structure-activity, a substitution of the exomethylene at C-4 with a methyl appendage to produce derivatives **19**, **20**, **21**, and **23** has been performed, with only **21** still able to fit in PXR-LBD. Compatible with the large contribution of apolar aminoacids in PXR LBD, the introduction of an additional polar group on ring A in derivative **22** causes a loss of activity in luciferase reporter assay. Second, in the derivatives that still retain the exomethylene functionality, the substitution on the side chain produces a high impact on PXR activity. Similarly to theonellasterol, a potent and selective FXR antagonist devoid of any activity toward PXR and other metabolic NRs,<sup>49</sup> compound **18**, with an ethyl group at C-24, was inactive. Also in vitro data on **16** and **17** are quite interesting. 24-dehydroconicasterol D (**16**) shares the tetracyclic core with the PXR agonists theonellasterol E (**12**) and conicasterol D (**14**) and the side chain with the inactive dehydroconicasterol.<sup>65</sup> The observed loss of activity for **16** points the attention on the negative effect played by the presence of an exomethylene functionality on the side chain of this reach family of marine PXR ligands. On the other hand preconicasterol (**17**), endowed with a cholestan-type side chain, maintains an agonistic behavior toward PXR. Then the concentration-response curve for preconicasterol (**17**) and semi-synthetic derivative **21** was investigated. As shown in **Figure 2.15**, compounds **17** and **21** transactivate PXR with an EC<sub>50</sub> of  $\approx 21$  mM and of  $\approx 18$  mM, thus indicating a dose dependent agonism towards PXR for both conicasterol derivatives.

To further characterize these derivatives, the effect of compounds **17** and **21** on the expression of CyP3A4 (cytochrome P) and on Multidrug Resistance Proteins (MDR1 and MPR3), three canonical PXR target genes, was examined by RT-PCR. As shown in **Figure 2.16**, the exposure of HepG2 cells to **17** and **21** increased the expression of mRNA for the above PXR targeted genes, thereby confirming at molecular level that this compound is a PXR agonists.

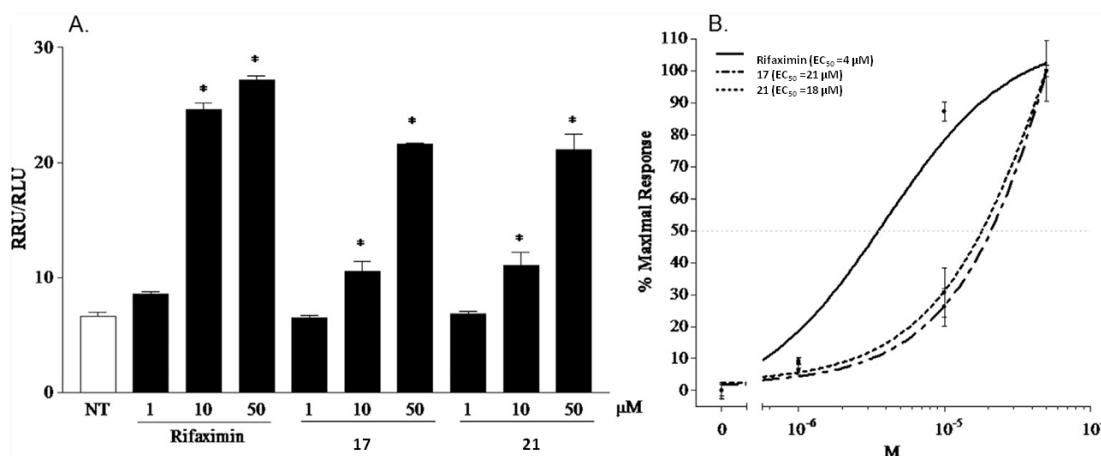


**Figure 2.15** Concentration response-curves for 17 and 21.\*

\*HepG2 cells were transfected for PXR transactivation assay and stimulated with rising concentrations of 17 and 21 (1, 10 and 50 μM). Rifaximin (1, 10 and 50 μM) was used as a positive control to evaluate the PXR transactivation. RLU: Luciferase Relative light Units, RRU: Renilla Relative light Units. Results are expressed as mean ± standard error; \*p < 0.05 vs not treated cells.

To elucidate at the atomic level the interaction between PXR and the 4-methylenesteroids derivatives, docking calculations on the most active compounds of the series have been performed. In particular, three different x-ray structures of the PXR LBD (pdb codes: 3hvl, 1nrl and 1m13) have been used to take into account the conformational plasticity of the binding site. In fact, docking software treats protein as a rigid body, thus the use of multiple conformations of the target, if available, is advisable to increase the chances of success of the calculation. In the present case, the agonist compounds, prenicasterol **17** and derivative **21** were undergone to the docking calculations that predict a very similar binding behavior for both agonists in PXR-LBD. In particular, considering the docking results obtained using the three LBD x-ray structures, the most occurring binding mode of prenicasterol **17** and derivative **21** is that shown in **Figure 2.17**.

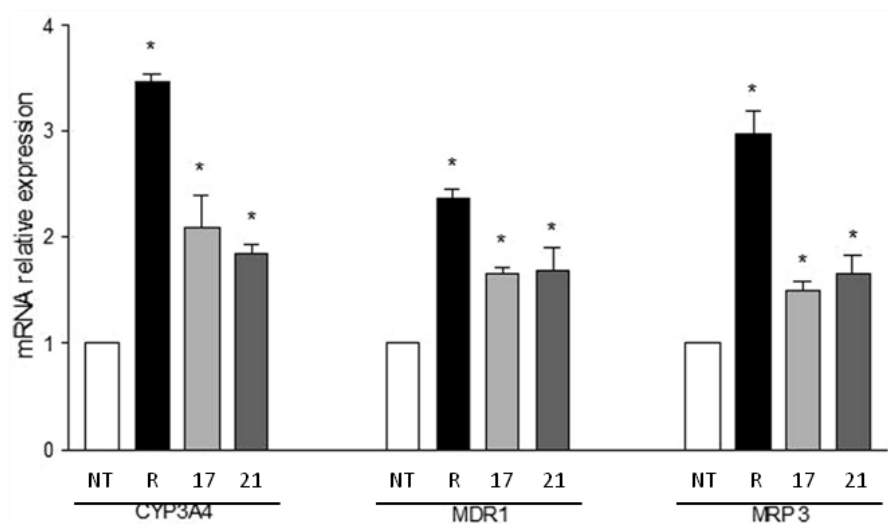


**Figure 2.16** Real-Time PCR analysis of mRNA relative expression of the PXR target genes CYP3A4, MDR1, MRP3 in HepG2 cells treated with Rifaximin (10  $\mu$ M), **17** and **21** (10  $\mu$ M).\*

\*Values are normalized relatively to GAPDH mRNA and are expressed relative to those of not treated cells (NT), which are arbitrarily set to 1. (\*:p< 0.05 vs not treated cells).

In this state, the hydroxyl group on the ring A of preconicasterol **17** and derivative **21** engages H-bond interactions with the backbone carbonyl oxygens of His407 and Thr408. These interactions represent the anchor point of the ligands in the LBD with the rest of the molecule oriented in the binding pocket forming further favorable interactions such as hydrophobic contacts between the Me-19 and the ring A with residues such as Met243, Phe251, Met425 and Phe429. In particular, the last two residues are located in the activation function 2 region (AF-2) on a small flexible alpha helix (AF-2 helix) responsible for the binding of the co-activator and co-repressor peptides. This part of the protein is supposed to undergo conformational motion responsible for the transition of the nuclear receptor from the agonist to the antagonist form. A similar mechanism of action has been very recently suggested by us and other authors for other nuclear receptors.<sup>67-68-69</sup> On this background, it is reasonable to think that the hydrophobic package established at the AF-2 region by agonist compounds such as preconicasterol **17** and derivative **21**, stabilizes PXR in the agonist conformation.

Finally, in the LBD, the steroidal scaffolds of **17** and **21** engage similar interactions with residues such as Leu209, while the flexible aliphatic tails

are settled in a very hydrophobic pocket. Here, prenicasterol **17** and derivative **21** establish a number of favorable contacts with residues such as Phe288, Trp299, Tyr306 and Met246 (**Figure 2.17A and 2.17B**).

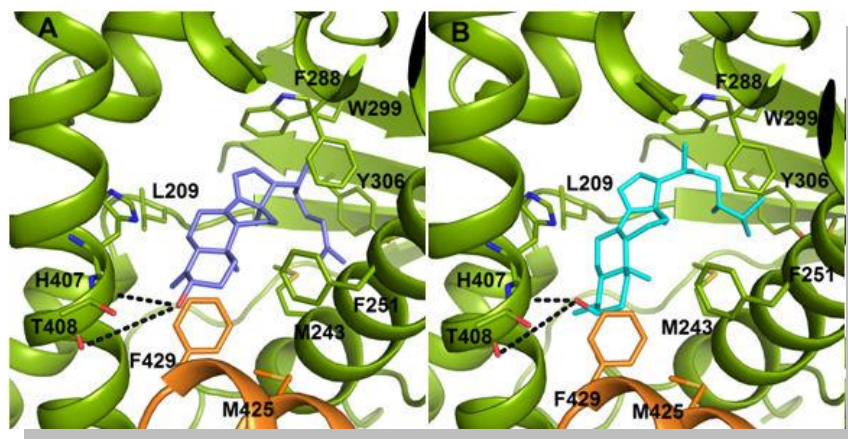


**Figure 2.17** Representation of the binding mode of the agonist prenicasterol **17** (violet sticks in A) and **21** (cyan sticks in B) predicted by docking calculations in the PXR LBD (PDB code 3HVL).\*

\*PXR is shown as green cartoon, while AF-2 helix is colored in orange. Amino acids involved in ligand binding are shown as green and orange sticks. Residues from Pro268 to Arg287, from Ser350 to Arg360, and all hydrogens are omitted for clarity.

Of relevance despite the different stereochemistry at C-3 on ring A and the presence of a methylene group in prenicasterol **17** instead of the methyl one in derivative **21**, the binding pattern of these compounds is very similar, supporting the reproducibility and the reliability of the docking calculations. In conclusion, NRs play a key role in cellular homeostasis, controlling a wide range of reactions through the regulation of the transcription of specific target genes. This receptor family shares common structural features such as the presence of the LBD responsible for the binding of ligands and co-activator peptides necessary to activate the gene transcription. Despite these similarities, each nuclear receptor shows a specific pattern of interaction with its ligands that, together with the conformational plasticity of the LBD, hampers the rational drug design of new active molecules. In this scenario, elucidating the molecular requisites for the binding to a specific nuclear

receptor represents an important advance to understand its functional mechanisms and provide the bases for an exogenous control of its activity.

In this framework, we have developed a series of 4-methylenesteroids derivatives, originally isolated from *Theonella* marine sponges, as novel modulators of the nuclear receptor PXR. We have assessed their activity profiles through a number of pharmacological experiments and, with the aid of computational studies, we have investigated the effects of different modifications on ring A and on the side chain of the 4-methylenesteroids derivatives toward PXR. Our results led to the identification of the first example of PXR antagonist with a steroidal scaffold, also elucidating the molecular requisites for PXR interaction. This study reaffirms the role of natural products as essential chemical probes in the today's research arsenal to shed light on complex biological processes and biochemical pathways.

## **2.9 EXPERIMENTAL SECTION**

### ***2.9.1 Animal material, Extraction and Isolation***

*Theonella swinhoei* (order Lithistida, family Theonellidae) was collected in the Bunaken Marine Park of Manado (North Sualwesi, Indonesia) in January 2010 and frozen immediately after collection. A reference sample of the sponge has been saved at the Department of Pharmacy, University of Naples Federico II, with the code Man-10-06. The frozen material (16.5 g) was extracted with methanol (3 × 1.5 L) at room temperature and the crude methanolic extract was subjected to a modified Kupchan's partitioning procedure as follows. The methanol extract was dissolved in a mixture of MeOH/H<sub>2</sub>O containing 10% H<sub>2</sub>O and partitioned against n-hexane (1.81 g). The water content (% v/v) of the MeOH extract was adjusted to 30% and partitioned against CHCl<sub>3</sub> (4.76 g). The aqueous phase was concentrated to remove MeOH and then extracted with n-BuOH (2.0 g). The CHCl<sub>3</sub> extract was chromatographed by silica gel MPLC using a solvent gradient system from CH<sub>2</sub>Cl<sub>2</sub> to CH<sub>2</sub>Cl<sub>2</sub>:MeOH 8:2. Fractions eluted with CH<sub>2</sub>Cl<sub>2</sub>:MeOH 97:3 (3 mg) were further purified by HPLC on a Luna 5 $\mu$ 100-5 C18 (5 $\mu$ m; 4.5 mm i.d. x 250 mm) with MeOH:H<sub>2</sub>O (95:5) as eluent (flow rate 0.8 mL/min) to give 0.2

mg of 24-dehydroconicasterol D (**16**) ( $t_R=9$  min). Fractions eluted with  $\text{CH}_2\text{Cl}_2:\text{MeOH}$  95:5 (174.5 mg) were further purified by HPLC on a Nucleodur 100-5  $\text{C}_{18}$  (Phenomenex) (5  $\mu\text{m}$ ; 7.8 mm i.d.  $\times$  250 mm) with  $\text{MeOH}:\text{H}_2\text{O}$  (85:15) as eluent (flow rate 0.9 mL/min) to give swinholide A (**1**) (43.3 mg), swinholide B (**2**, 2.4 mg), swinholide D (**3**, 2.2 mg), isoswinholide A (**4**, 2.0 mg), isoswinholide B (**5**, 2.7 mg), swinholide K (**6**, 5.3 mg). Fractions eluted with  $\text{CH}_2\text{Cl}_2:\text{MeOH}$  9:1 (853.3 mg) were further purified by silica column followed by HPLC on a Nucleodur 100-5  $\text{C}_{18}$  (Phenomenex) (5  $\mu\text{m}$ ; 7.8 mm i.d.  $\times$  250 mm) with  $\text{MeOH}:\text{H}_2\text{O}$  (9:1) as eluent (flow rate 0.9 mL/min) to give theonellapeptolide Id (**7**) (68.5 mg), sulfinyltheonellapeptolide (**8**, 4.6 mg) and theonellapeptolide If (**9**, 2.1 mg).

### 2.9.2 Spectroscopic data for the isolated compounds

**Isoswinholide B (5):** white powder;  $[\alpha]_D^{25} - 7.4$  ( $c$  0.02,  $\text{CH}_3\text{OH}$ );  $^1\text{H}$  and  $^{13}\text{C}$  NMR data in  $\text{CD}_3\text{OD}$  given in Table 2.1; ESIMS:  $m/z$  1411.9  $[\text{M}+\text{Na}]^+$ . HRMS (ESI): calcd for  $\text{C}_{78}\text{H}_{132}\text{NaO}_{20}$ : 1411.9210; found 1411.9216  $[\text{M}+\text{Na}]^+$ .

**Swinholide K (6):** white powder;  $[\alpha]_D^{25} - 15.2$  ( $c$  0.04,  $\text{CH}_3\text{OH}$ );  $^1\text{H}$  and  $^{13}\text{C}$  NMR data in  $\text{CD}_3\text{OD}$  given in Table 2.2; ESIMS:  $m/z$  1427.9  $[\text{M}+\text{Na}]^+$ . HRMS (ESI): calcd for  $\text{C}_{78}\text{H}_{132}\text{NaO}_{21}$ : 1427.9159; found 1427.9167  $[\text{M}+\text{Na}]^+$ .

**Sulfinyltheonellapeptolide (8):** colorless amorphous solid;  $[\alpha]_D^{25} - 38.0$  ( $c$  0.1,  $\text{CH}_3\text{OH}$ );  $^1\text{H}$  and  $^{13}\text{C}$  NMR data in  $\text{CD}_3\text{OD}$  given in Table 2.3; ESIMS:  $m/z$  1423  $[\text{M}+\text{H}]^+$  and 1445  $[\text{M}+\text{Na}]^+$ . HRMS (ESI): calcd for  $\text{C}_{69}\text{H}_{123}\text{N}_{13}\text{NaO}_{16}\text{S}$ : 1444.8829; found 1444.8834  $[\text{M}+\text{Na}]^+$ .

**Theonellapeptolide If (9):** colorless amorphous solid;  $[\alpha]_D^{25} - 26.7$  ( $c$  0.1,  $\text{CH}_3\text{OH}$ );  $^1\text{H}$  and  $^{13}\text{C}$  NMR data in  $\text{CD}_3\text{OD}$  given in table 2.4; ESIMS:  $m/z$  1377  $[\text{M}+\text{H}]^+$  and 1399  $[\text{M}+\text{Na}]^+$ . HRMS (ESI): calcd for  $\text{C}_{69}\text{H}_{121}\text{N}_{13}\text{NaO}_{16}$ : 1398.8952; found 1398.8949  $[\text{M}+\text{Na}]^+$ .

**24-dehydroconicasterol D (16):** white amorphous solid;  $[\alpha]_D^{25} - 67.0$  ( $c$  0.02,  $\text{CHCl}_3$ );  $^1\text{H}$ -NMR ( $\text{C}_6\text{D}_6$ ):  $\delta$  5.35 ( $\text{H}_A-29$ , 1H, br s), 4.93 ( $\text{H}_A-28$ , 1H, br s), 4.90 ( $\text{H}_B-28$ , 1H, br s), 4.74 ( $\text{H}_B-29$ , 1H, br s), 4.47 ( $\text{H}-15$ , 1H, br d), 3.88 ( $\text{H}-3$ , 1H, m), 2.70 ( $\text{H}-5$ , 1H, br d,  $J=12.51$  Hz), 2.54 ( $\text{H}_A-7$ , 1H, m), 2.37 ( $\text{H}_B-7$ , 1H, ddd,  $J=1.8, 4.7, 14.6$ ), 2.27 ( $\text{H}-25$ , 1H, hep,  $J=6.8$ ), 2.24 ( $\text{H}_A-23$ , 1H, m), 2.07 ( $\text{H}_A-1$ , 1H, m), 2.01 ( $\text{H}_B-23$ , 1H, m), 1.90 ( $\text{H}_A-2$ , 1H, m), 1.82 ( $\text{H}_A-16$ , 1H, m), 1.81 ( $\text{H}_A-11$ , 1H, m), 1.76 ( $\text{H}_A-12$ , 1H, m), 1.69 ( $\text{H}_A-22$ , 1H, ovl), 1.62 ( $\text{H}-17$ , 1H, m), 1.59 ( $\text{H}_A-$

6, 1H, m), 1.55 (H<sub>B</sub>-11, 1H, m), 1.54 (H<sub>B</sub>-16, 1H, m), 1.50 (H-20, 1H, ovl), 1.41 (H<sub>B</sub>-12, 1H, m), 1.39 (H<sub>B</sub>-6, 1H, m), 1.37 (H<sub>B</sub>-2, 1H, m), 1.35 (H<sub>B</sub>-1, 1H, m), 1.34 (H<sub>B</sub>-22, 1H, ovl), 1.10 (H- 27, 1H, *J*= 6.8), 1.09 (H- 26, 1H, *J*= 6.8), 0.99 (H- 21, 1H, *J*= 6.7), 0.71 (H- 18, 1H, s), 0.68 (H-19, 1H, s) ppm; <sup>13</sup>C-NMR (C<sub>6</sub>D<sub>6</sub>): δ 154.2 (C-4), 150.3 (C-14), 135.3 (C-8), 105.8 (C-28), 103.7 (C-29), 74.9 (C-9), 73.0 (C-3), 69.6 (C-15), 53.7 (C-17), 44.2 (C-13), 43.8 (C-10), 41.7 (C-5), 39.4 (C-16), 39.2 (C-24), 34.9 (C-20), 34.4 (C-12), 33.8 (C-22), 33.4 (C-2), 32.7 (C-25), 30.6 (C-23), 30.1 (C-1), 29.2 (C-11), 27.1 (C-7), 24.8 (C-6), 20.3 (C-27), 19.2 (C-21), 18.4 (C-26), 18.3 (C-18), 17.0 (C-19) ppm. HRMS-ESI *m/z* 443.3527 [M+H<sup>+</sup>], C<sub>29</sub>H<sub>47</sub>O<sub>3</sub> requires 443.3525.

### 2.9.3. Evaluation of antiproliferative activity

HepG2 cells were plated in a 24-wells plate at 3×10<sup>4</sup> cells/well, in Minimum Essential Medium with Earl's salts containing 10% fetal bovine serum (FBS), 1% L-glutamine and 1% penicillin/streptomycin. On day 2, cells were treated with increasing doses of Swinholide A (1, 10 and 100 nM), Swinholide B (1, 10 and 100 nM), Swinholide D (1, 10 and 100 nM), Isoswinholide A (1, 10 and 100 nM), Isoswinholide B (0.001, 0.01, 0.1, 1 and 10 μM), Swinholide K (1, 10 and 100 nM), Theonellapeptolide Id (0.1, 1 and 10 μM), Sulfinyltheonellapeptolide (0.1, 1 and 10 μM) and Theonellapeptolide If (0.1, 1 and 10 μM) for 48 hours. On day 4 MTT assay was assessed; 100 μL of MTT solution (5mg/ml) were added to each well and cells were incubated at 37°C for 4 hours. After incubation, culture medium was removed and 1mL of DMSO was added to each well; absorbance was read using spectrophotometer at 590 nm. Proliferation rate was reported as delta of absorbance compared to untreated cells; values are expressed as mean ± SE. For each compound, IC<sub>50</sub> was evaluated as follow: inhibition of proliferation was expressed as percentage compared to the inhibition of proliferation observed at the highest dose of any experimental setting (which was arbitrarily assigned a value of 100%).

### 2.9.4. Luciferase assay

HepG2 cells were cultured at 37 °C in Minimum Essential Medium with Earl's salts containing 10% fetal bovine serum (FBS), 1% L-glutamine and 1%

penicillin/streptomycin. Cells were plated in a 24-wells plate at  $5 \times 10^4$  cells/well. The transfection experiments were performed using Fugene HD (Promega, Milan, Italy) according to manufacturer specifications. For PXR mediated transactivation, cells were transfected with 75 ng pSG5-hPXRT1, 75 ng pSG5-RXR, 125 ngpCMV- $\beta$ gal and with 250 ng of the reporter vector pGL3(henance)PXRE. At 24 hours post-transfection, cells were primed with rifaximin or compounds **16-23** 1-0 $\mu$ M (agonism) or with compounds **16-23** 50 $\mu$ M plus rifaximin 10 $\mu$ M (antagonism) for 18 hours. 20  $\mu$ L of cellular lysates were read using the Luciferase Substrate (Promega) and luminescence was measured using the Glomax 10/10 luminometer (Promega). Luciferase activities were normalized for transfection efficiencies by dividing the relative light units by  $\beta$ -galactosidase activity expressed from co-transfected pCMV- $\beta$ gal.

### 2.9.5 Real Time PCR

HepG2 cells were stimulated 18 h with rifaximin (10  $\mu$ M), compounds **19** and **21** (10  $\mu$ M) or with the combination of compounds **19** or **21** (50 $\mu$ M) plus rifaximin (10 $\mu$ M). Total RNA was extracted using the TRIzol reagent (Invitrogen), and reverse-transcribed using random hexamer primers and Super Script-II reverse transcriptase (Invitrogen). mRNA was quantified by Real-Time quantitative PCR on iCycler apparatus (Biorad) using specific primers: hGAPDH: *gaaggagaaggcggagt* and *catgggtggaatcatattggaa*; hCYP3A4: *caagacccttgtggaaaa* and *cgaggcgactttctttcatc*. For quantitative RT-PCR, 10 ng of template was dissolved in a 20  $\mu$ l solution containing 200 nM of each primer and 10  $\mu$ l of KAPA SYBR FAST Universal qPCR Kit (KAPA BIOSYSTEMS). All reactions were performed in triplicate, and the thermal cycling conditions were as follows: 3 min at 95  $^{\circ}$ C, followed by 40 cycles of 95  $^{\circ}$ C for 15 s, 58  $^{\circ}$ C for 20 s and 72  $^{\circ}$ C for 30 s. The relative mRNA expression was calculated accordingly with the Ct method. All PCR primers were designed using the software PRIMER3 (<http://frodo.wi.mit.edu/primer3/>) using published sequence data obtained from the NCBI database.

### **2.9.6 Computational Details**

Molecular docking of **17** and **21** in the three-dimensional X-ray structures of the PXR LBD (PDB codes: 3hvl, 1nrl and 1m13) without the co-crystallized inhibitor and waters were carried out using the AutoDock software package (version 4.2). Ligands and receptor structures were converted to AutoDock format files using the ADT software, and the Gasteiger-Marsili partial charges were then assigned. A box around the binding pocket has defined the docking area and grids points of 48×40×38 with 0.375 Å spacing were calculated within the this area for all the ligand atom types using AutoGrid4. For each ligand, 100 separate docking calculations were performed. Each docking run consisted of 25 million energy evaluations using the Lamarckian genetic algorithm local search (GALS) method. Otherwise default docking parameters were applied. The docking conformations were clustered on the basis of the root-mean square deviation values (rmsd tolerance = 1.5 Å) between the cartesian coordinates of the ligand atoms and were ranked based on the AutoDock scoring function.

## References

---

- <sup>1</sup> Bergquist, P.R., The Porifera, in *Invertebrate Zoology*, Anderson, D.T., Ed., Oxford University Press, Melbourne, **1998**, 2.
- <sup>2</sup> Faulkner, D. *Nat. Prod. Rep.*, **2000**, *17*, 1-6.
- <sup>3</sup> Perkel. *The Scientist*, **2003**, *17*, 6.
- <sup>4</sup> Mootz et al. *Chembiochem*, **2002**, *3*, 490-504.
- <sup>5</sup> Von Dohren, Kaufer et al. *Chembiochem*, **2006**, *7*, 612-622
- <sup>6</sup> Wegerski, C. J.; Hammond, J.; Tenney, K.; Matainaho, C.; Crews, P. *J. Nat. Prod.*, **2007**, *70*, 89-94.
- <sup>7</sup> a) Carmely, S.; Kashman, Y. *Tetrahedron Lett.* **1985**, *26*, 511-514. b) Kobayashi, M.; Tanaka, J.; Katori, T.; Matsuura, M.; Kitagawa, I. *Tetrahedron Lett.* **1989**, *22*, 2963-2966.
- <sup>8</sup> Matsunaga, S.; Fusetani, N.; Kato, Y. *J. Am. Chem. Soc.* **1991**, *113*, 9690-9692.
- <sup>9</sup> a) De Marino, S.; Ummarino, R.; D'Auria, M. V.; Chini, M. G.; Bifulco, G.; Renga, B.; D'Amore, C.; Fiorucci, S.; Debitus, C.; Zampella, A. *J. Med. Chem.* **2011**, *54*, 3065-3075; b) De Marino, S.; Sepe, V.; D'Auria, M. V.; Bifulco, G.; Renga, B.; Petek, S.; Fiorucci, S.; Zampella, A. *Org. Biomol. Chem.* **2011**, *9*, 4856-4862.
- <sup>10</sup> Festa, C.; De Marino, S.; D'Auria, M.V.; Bifulco, G.; Renga, B.; Fiorucci, S.; Petek, S.; Zampella, A. *J. Med. Chem.* **2011**, *54*, 401-405.
- <sup>11</sup> Fiorucci, S.; Distrutti, E.; Bifulco, G.; D'Auria, M. V.; Zampella, A. *Trends Pharmacol. Sci.* **2012**, *33*, 591-601.
- <sup>12</sup> Hamada, T.; Matsunaga, S.; Yano, G.; Fusetani, N. *J. Am. Chem. Soc.*, **2005**, *127*, 110-118.
- <sup>13</sup> Nakao, Y.; Matsunaga, S.; Fusetani, N. *Bioorg. Med. Chem.*, **1995**, *3*, 1115-1122.

- 
- <sup>14</sup> Nakao, Y.; Oku, N.; Matsunaga, S.; Fusetani, N. *J. Nat. Prod.*, **1998**, *61*, 667–670.
- <sup>15</sup> Kobayashi, J.; Sato, M.; Murayama, T.; Ishibashi, M.; Walchi, M. R.; Kanai, M.; Shoji, J.; Ohizumi, Y. *J. Chem. Soc. Chem. Commun.*, **1991**, 1050–1052.
- <sup>16</sup> Fusetani, N.; Sugawara, T.; Matsunaga, S.; Hirota, H. *J. Am. Chem. Soc.*, **1991**, *113*, 7811–7812.
- <sup>17</sup> Roy, M. C.; Ohtani, I. I.; Tanaka, J.; Higa, T.; Satari, R. *Tetrahedron Lett.*, **1999**, *40*, 5373–5376.
- <sup>18</sup> Kobayashi, J.; Sato, M.; Ishibashi, M.; Shigemori, H.; Nakamura, T.; Ohizumi, Y. *J. Chem. Soc. Perkin Trans.*, **1991**, *1*, 2609–2611.
- <sup>19</sup> a) Itagaki, F.; Shigemori, H.; Ishibashi, M.; Nakamura, T.; Sasaki, T.; Kobayashi, J. *J. Org. Chem.*, **1992**, *57*, 5540–5542; b) Kobayashi, J.; Itagaki, F.; Shigemori, H.; Takao, T.; Shimonishi, Y. *Tetrahedron*, **1995**, *51*, 2525–2532; c) Uemoto, H.; Yahiro, Y.; Shigemori, H.; Tsuda, M.; Takao, T.; Shimonishi, Y.; Kobayashi, J. *Tetrahedron*, **1998**, *54*, 6719–6724; d) Tsuda, M.; Ishiyama, H.; Masuko, K.; Takao, T.; Shimonishi, Y.; Kobayashi, J. *Tetrahedron*, **1999**, *55*, 12543–12548; e) Bonnington, L. S.; Tanaka, J.; Higa, T.; Kimura, J.; Yoshimura, Y.; Nakao, Y.; Yoshida, W. Y.; Scheuer, P. J. *J. Org. Chem.*, **1997**, *62*, 7765–7767.
- <sup>20</sup> Chill, L.; Kashman, Y.; Schleyer, M. *Tetrahedron*, **1997**, *53*, 16147–16152.
- <sup>21</sup> Matsunaga, S.; Fusetani, N.; Hashimoto, K.; Walchli, M. *J. Am. Chem. Soc.*, **1989**, *111*, 2582–2588.
- <sup>22</sup> Festa, C.; De Marino, S.; Sepe, V.; Monti, M. C.; Luciano, P.; D'Auria, M. V.; Debitus, C.; Bucci, M.; Vellecco, V.; Zampella, A. *Tetrahedron* **2009**, *65*, 10424–10429.
- <sup>23</sup> Festa, C.; De Marino, S.; Sepe, V.; D'Auria, M. V.; Bifulco, G.; Debitus, C.; Bucci, M.; Vellecco, V.; Zampella, A. *Org. Lett.* **2011**, *13*, 1532–1535
- <sup>24</sup> Kobayashi, M.; Kanzaki, K.; Katayama, S.; Ohashi, K.; Okada, H.; Ikegami, S.; Kitagawa, I. *Chem. Pharm. Bull.*, **1994**, *42*, 1410–1415.

- <sup>25</sup> Bewley, C. A.; Faulkner, D. J. *J. Org. Chem.*, **1994**, *59*, 4849–4852.
- <sup>26</sup> Bewley, C.A.; Faulkner, D.J. *Angew. Chem. Int. Ed.*, **1998**, *37*, 2162-2178.
- <sup>27</sup> Andrianasolo, E. H.; Gross, H.; Goeger, D.; Musafija-Girt, M.; McPhail, K.; Leal, R. M.; Mooberry, S. L.; Gerwick, W. H. *Org. Lett.*, **2005**, *7*, 1375-1378.
- <sup>28</sup> Piel, J.; Butzke, D.; Fusetani, N.; Hui, D.; Platzer, M.; Wen, G.; Matsunaga, S. *J. Nat. Prod.*, **2005**, *68*, 472-479.
- <sup>29</sup> Tsukamoto, S.; Matsunaga, S.; Fusetani, N.; Toh-E, A. *Tetrahedron*, **1999**, *55*, 13697-13702.
- <sup>30</sup> Wilson, M. C.; Mori, T.; Ruckert, C.; Uria, A.; Helf, M. J.; Takada, K.; Gernert, C.; Steffens, U.A.; Heycke, N.; Schmitt, S.; Rinke, C.; Helfrich, E. J. N.; Brachmann, A., O.; Gurgui, C.; Wakimoto, T.; Kracht, M.; Crusemann, M.; Hentschel, U.; Abe, I.; Matsunaga, S.; Kalinowski, J.; Takeyama, H.; Piel, J., *Nature*, **2014**, *506*, 58-62.
- <sup>31</sup> Schmidt, E. W.; Obraztsova, A. Y.; Davidson, S. K.; Faulkner, D. J.; Haygood, M. G. *Mar. Biol.*, **2000**, *136*, 969-977.
- <sup>32</sup> Angawi, R. F.; Bavestrello, G.; Calcinai, B.; Dien, H. A.; Donnarumma, G.; Tufano, M. A.; Paoletti, I.; Grimaldi, E.; Chianese, G.; Fattorusso, E.; Tagliatela-Scafati, O. *Mar. Drugs* **2011**, *9*, 2809-2817.
- <sup>33</sup> Angawi, R. F.; Calcinai, B.; Cerrano, C.; Dien, H. A.; Fattorusso, E.; Scala, F.; Tagliatela-Scafati, O. *J. Nat. Prod.* **2009**, *72*, 2195-2198.
- <sup>34</sup> De Marino, S.; Festa, C.; D'Auria, M. V.; Cresteil, T.; Debitus, C.; Zampella, A. *Mar. Drugs* **2011**, *9*, 1133-1141.
- <sup>35</sup> Kobayashi, M.; Tanaka, J.; Katori, T.; Kitagawa, I. *Chem. Pharm. Bull.* **1990**, *38*, 2960–2966.
- <sup>36</sup> Tsukamoto, S.; Ishibashi, M.; Sasaki, T.; Kobayashi, J. *J. Chem. Soc. Perkin Trans. 1* **1991**, 3185–3188.
- <sup>37</sup> Youssef, D.T.A.; Mooberry, L.S. *J. Nat. Prod.* **2006**, *69*, 154–157.

- 
- <sup>38</sup> Kobayashi, M.; Kawazoe, K.; Okamoto, T.; Sasaki, T.; Kitagawa, I. *Chem Pharm Bull*, **1994**, *42*, 19-26.
- <sup>39</sup> Matsumori, N.; Kaneno, D.; Murata, M.; Nakamura, H.; Tachibana, K. *J. Org. Chem.*, **1999**, *64*, 866-876.
- <sup>40</sup> Kato, Y.; Fusetani, N.; Matsunaga, S.; Hashimoto, K.; Sakai, R.; Higa, T.; Kashman, Y. *Tetrahedron Lett.* **1987**, *28*, 6225-6228.
- <sup>41</sup> Marfey, P.; *Carlsberg Res. Commun.* **1984**, *49*, 591-596. DOI: 10.1007/BF02908688
- <sup>42</sup> Roepstorff, P.; Fohlman, J. *Biomed. Mass Spectrom.* **1984**, *11*, 601. DOI:10.1002/bms.1200111109
- <sup>43</sup> Kitagawa, I.; Lee, N K; Kobayashi, M; Shibuya, H. *Tetrahedron* **1991**, *47*, 2169-2180. DOI: 10.1016/S0040-4020(01)96128-9.
- <sup>44</sup> Kobayashi, M.; Lee, N.K.; Shibuya, H.; Momose, T.; Kitagawa, I. *Chem. Pharm. Bull.* **1991**, *39*, 1177-1184. PMID: 1913995.
- <sup>45</sup> In the numbering system of theonellapeptolide If (**9**) we have skipped position 10 in order to allow a better comparison of NMR data with those of sulfinyltheonellapeptolide (**8**).
- <sup>46</sup> Bubb, M. R.; Spector, I.; Bershadsky, A. D.; Korn, E. D. *J. Biol. Chem.* **1995**, *270*, 3463-3466.
- <sup>47</sup> Terry, D. R.; Spector, I.; Higa, T.; Bubb, M. R. *J. Biol. Chem.* **1997**, *272*, 7841-7845.
- <sup>48</sup> E. Kho, D. K. Imagawa, M. Rohmer, Y. Kashman, C. Djerassi, *J. Org. Chem.* **1981**, *46*, 1836-1839.
- <sup>49</sup> B. Renga, A. Mencarelli, C. D'Amore, S. Cipriani, M. V. D'Auria, V. Sepe, M. G. Chini, M. C. Monti, G. Bifulco, A. Zampella, S. Fiorucci, *PLoS One*, **2012**, *7*, e30443.

- 
- <sup>50</sup> S. Fiorucci, E. Distrutti, G. Bifulco, M. V. D'Auria, A. Zampella, *Trends Pharmacol. Sci.*, **2012**, *33*, 591-601.
- <sup>51</sup> S. De Marino, R. Ummarino, M. V. D'Auria, M. G. Chini, G. Bifulco, B. Renga, C. D'Amore, S. Fiorucci, C. Debitus, A. Zampella, *J. Med. Chem.* **2011**, *54*, 3065-3075.
- <sup>52</sup> V. Sepe, R. Ummarino, M. V. D'Auria, M. G. Chini, G. Bifulco, B. Renga, C. D'Amore, C. Debitus, S. Fiorucci, A. Zampella, *J. Med. Chem.* **2012**, *55*, 84-93.
- <sup>53</sup> S. De Marino, R. Ummarino, M. V. D'Auria, M. G. Chini, G. Bifulco, B. Renga, C. D'Amore, S. Fiorucci, C. Debitus, A. Zampella, **2011**, *54*, 3065-3075.
- <sup>54</sup> Pawlak, M. et al., *Curr. Top. Med. Chem.*, **2012**, *12*, 486-504
- <sup>55</sup> De Lera, A.R. et al., *Nat. Rev. Drug Discov.* **2007**, *6*, 811-820
- <sup>56</sup> Schulman, I.G., *Adv. Drug Deliv. Rev.*, **2010**, *62*, 1307-1315
- <sup>57</sup> Stedman, C.A. et al., *Proc. Natl. Acad. Sci. U.S.A.*, **2005**, *102*, 2063-2068
- <sup>58</sup> B. Staudinger, S. A. Goodwin, D. Jones, K. I. Hawkins-Brown, A. MacKenzie, Y. LaTour, C. D. Liu, K. K. Klaassen, J. Brown, T. M. Reinhard, B. H. Willson, S. A. Kliewer, *Proc. Natl. Acad. Sci. USA*, **2001**, *98*, 3369-3374.
- <sup>59</sup> S. Fiorucci, S. Cipriani, F. Baldelli, A. Mencarelli, *Prog. Lipid Res.*, **2010**, *49*, 171-185.
- <sup>60</sup> J. Gao, W. Xie, *Trends Pharmacol. Sci.*, **2012**, *33*, 552-558.
- <sup>61</sup> H. I. Swanson, T. Wada, W. Xie, B. Renga, A. Zampella, E. Distrutti, S. Fiorucci, B. Kong, A. M. Thomas, G. L. Guo, R. Narayanan, M. Yepuru, J. T. Dalton, J. Y. Chiang, *Drug Metab. Dispos.*, **2013**, *41*, 1-11.
- <sup>62</sup> J. Cheng, Y. M. Shah, X. Ma, X. Pang, T. Tanaka, T. Kodama, K. W. Krausz, F. J. Gonzalez, *J. Pharmacol. Exp. Ther.*, **2010**, *335*, 32-41.
- <sup>63</sup> C. Festa, S. De Marino, M. V. D'Auria, G. Bifulco, B. Renga, S. Fiorucci, S. Petek, A. Zampella, *J. Med. Chem.*, **2011**, *54*, 401-405.

<sup>64</sup> S. De Marino, R. Ummarino, M. V. D'Auria, M. G. Chini, G. Bifulco, B. Renga, C. D'Amore, S. Fiorucci, C. Debitus, A. Zampella, *J. Med. Chem.*, **2011**, *54*, 3065-3075.

<sup>65</sup> S. De Marino, R. Ummarino, M. V. D'Auria, M. G. Chini, G. Bifulco, C. D'Amore, B. Renga, A. Mencarelli, S. Petek, S. Fiorucci, A. Zampella, *Steroids*, **2012**, *77*, 484-495.

<sup>66</sup> Compound **19** was tested, in combination with rifaximin (10 mM), in a doseresponsive manner (10, 25, 50 mM) in a luciferase reporter assay. No effect was observed at 10 and 25 mM doses and the slightly antagonistic effect respect to rifaximin at 50 mM resulted not enough significant from a statistic point of view, thus preventing from the chance to calculate a formal IC<sub>50</sub>.

<sup>67</sup> F.S. Di Leva, C. Festa, C. D'Amore, S. De Marino, B. Renga, M.V. D'Auria, E. Novellino, V. Limongelli, A. Zampella, S. Fiorucci, *J. Med. Chem.*, **2013**, *56*, 4701e4717.

<sup>68</sup> S. Ekins, C. Chang, S. Mani, M.D. Krasowski, E.J. Reschly, M. Iyer, V. Kholodovych, N. Ai, W.J. Welsh, M. Sinz, P.W. Swaan, R. Patel, K. Bachmann, *Mol. Pharmacol.*, **2007**, *72*, 592e603.

<sup>69</sup> J.T. Link, B. Sorensen, J. Patel, M. Grynfarb, A. Goos-Nilsson, J. Wang, S. Fung, D. Wilcox, B. Zinker, P. Nguyen, B. Hickman, J.M. Schmidt, S. Swanson, Z. Tian, T.J. Reisch, G. Rotert, J. Du, B. Lane, T.W. von Geldern, P.B. Jacobson, *J. Med. Chem.*, **2005**, *48*, 5295e5304.

## CHAPTER 3 -HALOINDOLES FROM *IOTROCHOTA*

### *PURPUREA*

---

In the frame of Bluegenics European project (From gene to bioactive product: Exploiting marine genomics for an innovative and sustainable European blue biotechnology industry, 311848, 7th Framework programme), a bioguided analysis of a specimen of *Iotrochota purpurea* (order Poecilosclerida, family Myxillidae) (**Figure 3.1**) collected in Indonesian Sea, has been undertaken during a visit period in the Muséum National d'Histoire Naturelle, in the research group of Dr. Marie-Lise Bourguet-Kondracki (CNRS-Paris, France).



**Figure 3.1** *Iotrochota purpurea*

Marine sponges belonging to the genus *Iotrochota* are a promising source of diverse chemical metabolites with a wide range of bioactivity. Previous studies on marine sponges of the genus *Iotrochota* resulted in the isolation of haloindole derivatives, e.g. methyl (E)-3-(6-bromoindol-3-yl)-prop-2-enoate,<sup>1</sup> matemone<sup>2</sup> and 6-bromoindole-3-carbaldehyde;<sup>2</sup> the aromatic halogenated tyrosine derivatives<sup>3</sup>, e.g. itampolins A and B<sup>4</sup>, the pyrrole derivative purpurone,<sup>5</sup> ecdysteroids,<sup>6</sup> 6-hydroxy-4-en-3-one steroids.<sup>7</sup> The cytotoxic glycosphingolipid iotroridoside A,<sup>8</sup> 3-octadecyloxy-1,2-propanediol (batyl alcohol),<sup>9</sup> and ceramides<sup>10</sup> have been isolated from *Iotrochota ridley*. In addition, the sponge *Iotrochota baculifera* was reported to contain sphingolipids and the glycosphingolipid iotroridoside B.<sup>11-12</sup>

The bioassay-guided fractionation of the crude extract of *I. purpurea* resulted in the isolation of a series of bromoindole derivatives, which were subjected to pharmacological assays to evaluate antikinase activity.

### 3.1 HALOGENATED METABOLITES FROM SPONGES

Unlike terrestrial organisms, marine organisms often produce halogenated secondary metabolites: the frequent occurrence of this kind of metabolites is a unique feature of marine natural product chemistry. They are not uniformly distributed among the marine plant and invertebrate taxa, and are most commonly found in red algae and sponges. Even in this latter phylum they are present in a relatively small number of species, and are mainly associated with horny sponges, which are distributed in the three orders Dictyoceratida, Dendroceratida, and Verongida. In particular, Verongida are characterized by their ability to synthesize bromotyrosine derivatives, which seem to be peculiar to these sponges, and have been suggested as chemical markers for taxonomic studies.<sup>13</sup> Sponges belonging to the genus *Iotrochota* are a rare example of sponge that elaborates such metabolites not belonging to the order Verongida.

Many sponges are symbiotic organisms and the content of microbial endosymbionts in them can be very significant and comparable in the mass and volume to the cells of the host: this fact appears to explain, at least partly, the vast variety of secondary halogenated metabolites in sponges.

The most widely represented among the classes of halogenated metabolites are alkaloids. A number of these alkaloids display high biological activities, including antimicrobial and antitumor activities. Among the halogenated alkaloids, bromoalkaloids form the most widely distributed group, which are predominantly found in marine eukaryotes, are significantly rarer in prokaryotic microorganisms, and are almost absent from terrestrial plants and animals.<sup>14-15</sup> Iodoalkaloids compose a rare group of natural compounds that has up until now only been isolated from marine organisms.<sup>14-15-16</sup> Chloro-containing alkaloids are widely distributed in nature and have been isolated until now from microorganisms, plants, terrestrial animals, and marine invertebrates.<sup>17</sup>

Thus, in sponge the following large groups of halogenated alkaloids are represented: indole alkaloids, including diverse tryptamine derivatives, bis- and trisindole compounds, pyrrole-containing alkaloids and, finally, the alkaloids derived from dibromotyrosine. Some other smaller series of compounds are the pyrroloquinoline, and different classes of peptides.

Cytotoxicity towards tumor cells, antimicrobial activity, and antifungal action are typical of the halogenated alkaloids. Other types of biological activities are rarely found.

### **3.1.1 Bromoindole alkaloids**

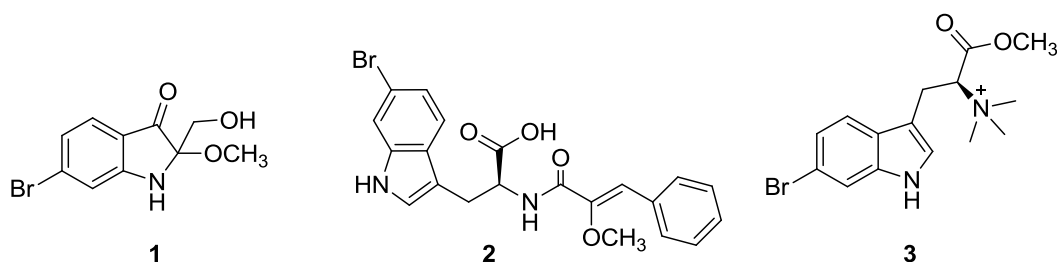
Structural analysis of many halogenated alkaloids from sponges indicates that they derive biogenetically from tryptophan, known to be one of the basic amino acids in eukaryotic organisms, and, hence, it was not surprising that halogenated indoles were found in numerous natural sources, including marine invertebrates.<sup>18-19</sup> Bromoindole alkaloids were isolated from various marine sponge species, for example *Oceanapia bartschi*<sup>20</sup>, *Pleroma menoui*<sup>21</sup>, *Plocamissma igzo*<sup>22</sup>, and *Pseudosyberites hyalinus*.<sup>23</sup>

The oxindole system is an analogue of the indole nucleus found in a large number of naturally occurring products. It is a benzopyrrolidinone, with the pyrrolidinone ring fused to the benzene ring, and the carbonyl group being either in the 2- or the 3-position of the nucleus. In particular, 3-indolinones have been found in terrestrial sources.<sup>24-25</sup> Their derivatives have been identified as antibiotic compounds produced by bacteria isolated from the toxic mucus of the boxfish<sup>26</sup> and by symbiotic bacteria of crustacean embryos.<sup>27</sup> Dimers of 3-indolinone are responsible for the bright colors of mollusks, such as the Tyrian purple of Muricidae and Thaisidae.<sup>28</sup> Indolinone derivatives and bromoindole metabolites are often proposed to be repellent or antifeedant substances. Bromoindoles have also been reported to show antimicrobial, antiproliferative, and antifouling effects.<sup>29</sup>

Recently, matemone (**1**), a bromine-containing 3-oxindole alkaloid, has been isolated from *Iotrochota purpurea*, found off the coast of Mozambican Matemo Islands.<sup>7</sup> Matemone is marginally active against the bacterium

*Staphylococcus aureus* and has significant binding affinity to DNA. It also showed activity against a panel of cancer cell lines.

Other bromine-containing indole alkaloids from *Iotrochota purpurea* are iotrochamide B (**2**), an N-cinnamoyl-amino acid with activity towards *Tripanosoma brucei brucei*, and Purpuroine J (**3**).



Many simple and complex haloindoles and 3-oxindoles have thus been designed, synthesized and screened for activity against diseases targeting specific enzymes. Indeed, the kind of halogenated heterocycles are currently explored for different targets and, among them, inhibition of cyclin dependent kinases (CDKs) appear one of the most promising. CDKs have a vital role of regulating cell cycle events in malaria<sup>30</sup> and a variety of human cancer cells.<sup>31</sup> The activity of CDKs depend on a regulatory subunit called cyclin which binds to and activates the relevant CDKs. Direct inhibitors are preferably low molecular weight compounds that block the enzymatic activity of the CDKs.<sup>32</sup>

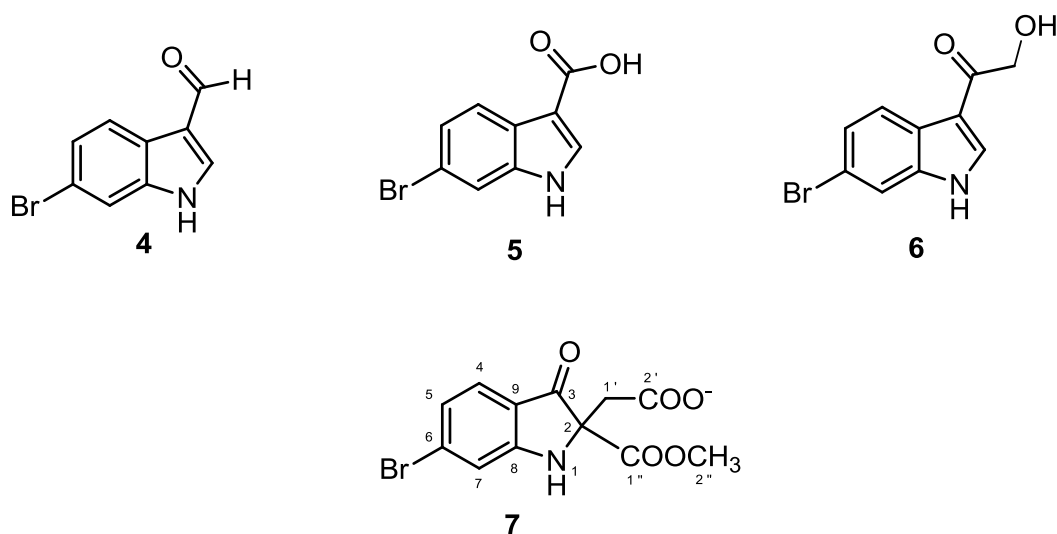
Therefore, the final goal of bioassay-guided fractionation of the crude extract of *I. purpurea* was the isolation of derivatives with anti-kinase activity.

### 3.2 ISOLATION AND STRUCTURAL ELUCIDATION OF BROMOINDOLE DERIVATIVES

*Iotrochota purpurea* (order Poecilosclerida, family Myxillidae) was collected in South Sulawesi (Spermonde Archipelago off Ujung Pandang). The material was sequentially extracted with dichloromethane, ethyl acetate and butanol, to obtain CH<sub>2</sub>Cl<sub>2</sub>, AcOEt and BuOH extract. Each extract was subjected to flash chromatography with a gradient CH<sub>2</sub>Cl<sub>2</sub>/MeOH of increasing polarity to obtain six fractions from each extract. Preliminary pharmacological assays,

performed by Prof. Laurent Meijer in laboratory ManRos Therapeutics (Roscoff-France), showed antikinase activity for each extract and selected some specific fractions obtained from flash chromatography.

These active fractions were further purified by semipreparative and analytic RP-HPLC. The analysis of CH<sub>2</sub>Cl<sub>2</sub> and BuOH extracts afforded the isolation of three known bromoindole derivatives (**4-5-6**) and one new brominated 3-oxindole derivatives (**7**).



The dichloromethane extract of *Iotrochota* sponge yielded three known bromoindole derivatives (**4-5-6**), previously isolated from other sponges *Pseudosuberitis hyalinus*, *Pleroma menoui* and also from *Iotrochota purpurea*. These compounds were identified on the basis of the identity of their spectroscopic data with those published in the literature.<sup>20-22</sup> The BuOH extract contained the new 3-oxindoles brominated derivative **7**, which we named matemone B.

Matemone B (**7**) was obtained as a yellow film. The molecular formula was determined as C<sub>12</sub>H<sub>9</sub>NO<sub>5</sub>BrNa by HRESIMS; the mass spectrum gave a double peak at 349/351 (1:1 ratio), suggesting the presence of one bromine atom in the molecule. The <sup>1</sup>H NMR spectrum of **7** showed the presence of a trisubstituted aromatic ring (ortho, meta, meta) [ $\delta$  7.70 (1H, d,  $J$  = 7.6 Hz), 7.33 (1H, dd,  $J$  = 7.6, 1.6 Hz), 7.32 (1H, d,  $J$  = 7.6 Hz)], a methoxy group at  $\delta$  3.49 (3H, s) and two aliphatic protons at  $\delta$  3.19 (2H, s). The <sup>13</sup>C NMR spectrum of **7** showed signals for seven unprotonated carbons ( $\delta$  192.4,

170.9, 170.7, 142.8, 129.8, 116.8, 73.0), three  $sp^2$  methine ( $\delta$  129.3, 125.6, 118.8), one  $sp^3$  methylene ( $\delta$  39.3) and one methyl group ( $\delta$  51.7).

The NMR data of matemone B (**7**) support the presence of a trisubstituted aromatic ring, a conjugated ketone, one ester, one carboxylic acid, a methylene group, and a methoxy group.

The connectivities observed in the  $^1H$ - $^1H$  COSY and HSQC spectra supported the placement of the bromine atom C-6 of an indole-type skeleton. The oxo-indole subunit was confirmed by the HMBC connectivity between H-4 ( $\delta$  7.70) and the ketone C-3 ( $\delta$  192.4). This HMBC connectivity, together with the ortho- and meta- proton couplings for H-5, confirmed the location of bromine atom at C-6. HSQC and selected HMBC connectivities (shown as arrows in **Fig. 3.2**) allowed the unambiguous assignments of all proton and carbon resonances of **7**. C-2 was assigned as an unprotonated  $sp^3$  carbon resonating at  $\delta$  73.0, on the basis of the HMBC cross-peaks of H<sub>2</sub>-1' with both C-2 and C-3.

Matemone B includes one stereogenic center (C-2). Since  $[\alpha]_D$  of **7** was  $0^\circ$  and its CD spectrum was flat, we assume that matemone B exists as a racemic mixture.

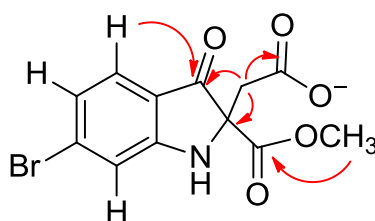


**Figure 3.2** Key HMBC correlation for matemone B (**7**).

Matemone B is related to matemone A since these two metabolites share the 6-bromo-3-oxo-indole nucleus. However, in the case of **7**, a methoxy group is replaced by a ketide unit ( $-CH_2COO^-$ ) raising interesting questions about its biogenetic origin.

### 3.3 ANTIKINASE ACTIVITY

The cyclin-dependent kinases (CDKs) are a group of serine/threonine kinases involved in the regulation of the cell cycle, neuronal functions, transcription and apoptosis.<sup>33</sup> Since in many human cancers hyperactivity of CDKs has been identified as one of the mechanisms underlying the pathological

hyperproliferation,<sup>34</sup> the inhibition of CDKs may offer a therapeutic option for cancer patients.<sup>35-36</sup> Consequently, a number of small molecules with CDK-inhibitory properties have been developed during the past decade.<sup>37-38</sup> At least four CDK inhibitors are currently under clinical trial as anticancer drugs: flavopiridol, the indole dimer UCN-01, roscovitine (CYC202; seliciclib), and the aminothiazole BMS-387032.<sup>39</sup>

Three compounds isolated from *Iotrochota purpurea* extract (**4-5-6**) have been evaluated for their antikinase activity while, unfortunately, matemone B was isolated in too small amounts to be tested. For measurement of protein kinase inhibitory activities, a panel of nine different kinases involved in cell proliferation, diabetes and neurodegenerative disorders (dual-specificity tyrosine-(Y)-phosphorylation-regulated kinase 1A (DYRK1A), CDC-like kinase 1 (CLK-1), casein kinase 1 (CK-1), cyclin-dependent kinase 5 (CDK5), glycogen synthase kinase-3 (GSK-3), cyclin-dependent kinase 1 (CDK1), cyclin-dependent kinase 2 (CDK2/A) and complex of cyclin-dependent kinase 9 and cyclin T (CDK9/cyclin T) and malaria (PfGSK-3) was used.

Only compound **4** revealed antikinase activity with IC<sub>50</sub> of 2, 10 and 6 μm against CDK9/cyclin T, CLK1 and DYRK1A, respectively, while it was inactive on the other five tested kinases. Given the wide structural similarity within these analogues, we should presume that compound **6** is favored by its lower polarity.

This result inspires the search for new potential candidates for development of new therapeutics for treatment of cancer, diabetes, Alzheimer's disease and malaria.<sup>40</sup>

## 3.4 EXPERIMENTAL SECTION

### 3.4.1 Animal material, Extraction and Isolation

*Iotrochota purpurea* (order Poecilosclerida, family Myxillidae) was collected in South Sulawesi (Spermonde Archipelago off Ujung Pandang). The frozen material (500 g) was sequentially extracted with dichloromethane, ethyl acetate and butanol (1 L for each solvent), to obtain CH<sub>2</sub>Cl<sub>2</sub> (3.0 g), AcOEt (0.4 g) and BuOH (1.2 g) extract. CH<sub>2</sub>Cl<sub>2</sub> extract was subjected to flash

chromatography with a gradient CH<sub>2</sub>Cl<sub>2</sub>/MeOH to obtain six fractions. Fraction number 5 (514.0 mg) was further purified by preparative HPLC on a C-18 column (Knauer, 300 x 8 mm, prefilled with C-18 Eurosphere) with a gradient H<sub>2</sub>O/AcCN (from 5% to 80% of AcCN, 0.1% formic acid), flow rate 10 ml/min, to give compounds **4** (9.1 mg), **5** (5.8 mg) and **6** (3.0 mg).

BuOH extract was subjected to flash chromatography with a gradient CH<sub>2</sub>Cl<sub>2</sub>/MeOH to obtain six fractions. Fraction number 5 (445.0 mg) was further purified first by preparative HPLC on a C-18 column (Knauer, 300 x 8 mm, prefilled with C-18 Eurosphere) with a gradient H<sub>2</sub>O/AcCN (from 5% to 60% of AcCN, 0.1% formic acid), flow rate 10 ml/min, and then by semipreparative HPLC on C<sub>6</sub> column (Gemini C<sub>6</sub> phenyl) with a gradient H<sub>2</sub>O/AcCN (from 15% to 60% of AcCN, 0.1% formic acid), flow rate 3 ml/min, to give matemone B (**7**) (1.1 mg).

### 3.4.2 Spectroscopic data for isolated compounds

**Matemone B (7):** yellow film;  $[\alpha]_D^{25}$  (*c* 0.088, CH<sub>3</sub>OH); <sup>1</sup>H-NMR (DMSO): δ 11.0 (NH-1, 1H, bs), 7.70 (H-4, 1H, d, *J* = 7.6 Hz), 7.33 (H-5, 1H, dd, *J* = 7.6, 1.6 Hz), 7.32 (H-7, 1H, d, *J* = 7.6 Hz), 3.49 (H-2'', 3H, s), 3.19 (H-1', 2H, s) ppm; <sup>13</sup>C-NMR (DMSO): δ 192.4 (C-1), 170.9 (C-1''), 170.7 (C-2'), 142.8 (C-8), 129.8 (C-9), 129.3 (C-4), 125.6 (C-5), 118.8 (C-7), 116.8 (C-6), 73.0 (C-2), 51.7 (C-2''), 39.0 (C-1') ppm. HRMS-ESI *m/z* 351.9569 [M+Na<sup>+</sup>], C<sub>29</sub>H<sub>47</sub>O<sub>3</sub> requires 351.9567.

### 3.4.3 Protein kinases assays <sup>41</sup>

Evaluation of the protein kinase activity was performed *in vitro* as previously described.<sup>42</sup> Briefly, homogenization buffer: 60 mM β-glycerophosphate, 15 mM *p*-nitrophenylphosphate, 25 mM Mops (pH 7.2), 15 mM EGTA, 15 mM MgCl<sub>2</sub>, 1 mM dithiothreitol, 1 mM sodium vanadate, 1mM NaF, 1 mM phenylphosphate, 10 μg leupeptin mL<sup>-1</sup>, 10 μg aprotinin mL<sup>-1</sup>, 10 μg soyabean trypsin inhibitor mL<sup>-1</sup>, and 100 μg benzamidine. Buffer A: 10 mM MgCl<sub>2</sub>, 1mM EGTA, 1 mM dithiothreitol, 25 mM Tris-HCl pH 7.5, 50 μg heparin mL<sup>-1</sup>. Buffer C: homogenization buffer but 5 mM EGTA, no NaF and no protease inhibitors. Kinase activities were assayed in duplicates in buffer A or C at 30°C, at a final

ATP concentration of 15  $\mu\text{M}$ . The order of mixing the reagents was: buffers, substrate, enzyme, and inhibitor. Isolated compounds were tested against a panel of eight kinases; namely, dual-specificity tyrosine-(Y)-phosphorylation regulated kinase 1A (DYRK1A), cyclin-dependent kinase 5 (CDK5), glycogen synthase kinase-3 (GSK-3), CDC-like kinase 1 (CLK-1), casein kinase 1 (CK1), cyclin-dependent kinase 1 (CDK1), cyclin-dependent kinase 2 (CDK2), and complex of cyclin-dependent kinase 9 and cyclin T (CDK9/cyclin T).

## References

---

- <sup>1</sup> Dellar G., Djura P., and Sargent M. V., *J. Chem. Soc. Perkin Trans.*, **1981**, *1*, 1679-1680.
- <sup>2</sup> Carletti I., Banaigs B., and Amade P., *J. Nat. Prod.*, **2000**, *63*, 981-983.
- <sup>3</sup> Costantino V., Fattorusso E., and Mangoni A., *J. Nat. Prod.*, **1994**, *57*, 1552-1556.
- <sup>4</sup> Sorek H., Rudi A., Benayahu Y., and Kashmana Y. , *Tetrahedron Lett.*, **2006**, *47*, 7237-7239.
- <sup>5</sup> Chan G. W., Francis T., Thureen D. R., Offen P. H., Pierce N. J., Westley J. W., and Johnson R. K., *J. Org. Chem.*, **1993**, *58*, 2544-2546.
- <sup>6</sup> Costantino V., Aversano C. D., Fattorusso E., and Mangoni A., *Steroids*, **2000**, *65*, 138-142.
- <sup>7</sup> Li L. Y., Deng Z. W., Fu H. Z., Li J., Lin W. H., and Proksch P., *J. Asian Nat. Prod. Res.*, **2005**, *7*, 115-120.
- <sup>8</sup> Deng S. Z., Tian C. L., Xiao D. J., and Wu H. M., *Chin. J. Chem.*, **2001**, *19*, 362-364.
- <sup>9</sup> Tian C. L. and Deng S. Z., *Guangzhou Chem.*, **1998**, *1*, 36-38.
- <sup>10</sup> Liang L. Y., Deng S. Z., Zhang Q., Xiao D. J., and Wu H. M., *Chin. J. Mar. Drugs*, **2000**, *19*, 1-3.
- <sup>11</sup> Muralidhar P., Krishna N., Kumar M. M., Rao C. B., and Rao D. V., *Chem. Pharm. Bull.*, **2003**, *51*, 1193-1195.
- <sup>12</sup> Muralidhar P. and Rao D. V., *Asian J. Chem.*, **2006**, *18*, 33-36.
- <sup>13</sup> P.R. Bergquist and R.J. Wells, in: "Marine Natural Products: Chemical and Biological Perspectives." Ed. by P.J. Scheuer, Academic Press, New York, **1983**, Vol. V, pp. 17-22.

- 
- <sup>14</sup> Gribble, G.W., *Environ. Sci. Pollut. Res. Intern.*, **2000**, *7*, 37–49.
- <sup>15</sup> Southon, I.W., Buckingham, J., *Dictionary of Alkaloids*, New York: Chapman and Hall, Ltd., **1989**, 1–1161.
- <sup>16</sup> Faulkner, D.J., *Nat. Prod. Rep.*, **1995**, *12*, 223–269.
- <sup>17</sup> Dembitsky V.M., Tolstikov G.A., *Khim. Interes. Ust. Razv. (Novosibirsk)*, **2001**, *9*, 169–181.
- <sup>18</sup> Urban, S., Hickford, S.J.H., Blunt, J.W., Munro, M.H.G., *Curr. Org. Chem.*, **2000**, *4*, 765–807.
- <sup>19</sup> Borrelli, F., Campagnuolo C., Capasso, R., Fattorusso, E., Taglialatela- Scafati, O., *Eur. J. Org. Chem.*, **2004**, 3227-3232.
- <sup>20</sup> Cafieri, F., Fattorusso, E., Mahajnah, Y., and Mangoni, A., *Z. Naturforsch.*, **1993**, *48*, 1408–1410.
- <sup>21</sup> Guella, G.I., Mancini, D., Duhet, D., Richer de Forges, B., Pietra, E., *Z. Naturforsch.*, **1998**, *44*, 914– 919.
- <sup>22</sup> Dumdei, E., Andersen, R.J., *J. Nat. Prod.*, **1993**, *56*, 792–794.
- <sup>23</sup> Rasmussen, T., Jensen, J., Anthoni, U., Christophersen, C., and Nielsen, P.H., *J. Nat. Prod.*, **1993**, *56*, 1553–1558.
- <sup>24</sup> Pang, Z.; Sterner, O. *J. Nat. Prod.*, **1994**, *57*, 852-857.
- <sup>25</sup> Wenkert, E.; Gottlieb, H. E. *Heterocycles*, **1977**, *7*, 753-758.
- <sup>26</sup> Bell, R.; Carmell, S. *J. Nat. Prod.*, **1994**, *57*, 1587-1590.
- <sup>27</sup> Gil-Turnes, M. S.; Hay, M. E.; Fenical, W. *Science*, **1989**, *246*, 116-118.
- <sup>28</sup> Christophersen, C.; Waˆtjen, F.; Buchardt, O.; Anthoni, U. *Tetrahedron*, **1978**, *34*, 2779-2781.

- 
- <sup>29</sup> Olguin-Urbe, G.; Abou-Mansour, E.; Boulanger, A.; Debard, H.; Francisco, C.; Combaut, G. *J. Chem. Ecol.*, **1997**, *23*, 2507-2521.
- <sup>30</sup> Woodard, L. C.; Li, Z.; Terrell, J.; Gerena, L.; Sanchez, L. M.; Kyle, E. D.; Bhattacharjee, K. A.; Nichols, A. D.; Ellis, W.; Prigge, T. S.; Geyer, A. J.; Waters N. C. *J. Am. Chem. Soc.*, **2003**, *125*, 3877.
- <sup>31</sup> Moon, J. M.; Lee, K. S.; Lee, W. J.; Song, K. W.; Kim, W. S.; Kim, I. J.; Cho, C.; Choi, J. S.; Kim, C. Y. *Bioorg. Med. Chem.*, **2006**, *14*, 237.
- <sup>32</sup> Huwe, A.; Mazitschek, R.; Giannis, A.; *Angew. Chem. Int. Ed.*, **2003**, *42*, 2122.
- <sup>33</sup> J. Harper, P. Adams, *Chem. Rev.* **2001**, *101*, 2511–2526.
- <sup>34</sup> M. Malumbres, M. Barbacid, *Nat. Rev. Cancer*, **2001**, *1*, 222–231.
- <sup>35</sup> E. Sausville, *Curr. Med. Chem., Anti-Cancer Agents*, **2003**, *3*, 47–56.
- <sup>36</sup> M. Knockaert, P. Greengard, L. Meijer, *Trends Pharmacol. Sci.*, **2002**, *23*, 417–425.
- <sup>37</sup> L. Fischer, J. Endicott, L. Meijer, *Progress in Cell Cycle Research*, vol. 5, Editions “Life in Progress”, Station Biologique, Roscoff, France, **2003**, pp. 235–248.
- <sup>38</sup> A. Huwe, R. Mazitschek, A. Giannis, *Angew. Chem. Int. Ed. Engl.*, **2003**, *42*, 2122–2138.
- <sup>39</sup> P.M. Fischer, A. Gianella-Borradori, *Expert Opin. Investig. Drugs*, **2003**, *12*, 955–970.
- <sup>40</sup> Bharate SB, Yadav RR, Battula S, Vishwakarma RV., *Med Chem.*, **2012**, *12*, 618–631.
- <sup>41</sup> Tahtouh, T.; Elkins, J. M.; Filippakopoulos, P.; Soundararajan, M.; Burgy, G.; Durieu, E.; Cochet, C.; Schmid, R. S.; Lo, D. C.; Delhommel, F.; Oberholzer, A. E.; Pearl, L. H.; Carreaux, F.; Bazureau, J.-P.; Knapp, S.; Meijer, L., *J. Med. Chem.*, **2012**, *55*, 9312–9330.

---

<sup>42</sup> Xie, X.; Lemcke, T.; Gussio, R.; Zaharevitz, D. W.; Leost, M.; Meijer, L.; Kunick, C., *Eur. J. Med. Chem.*, **2005**, *40*, 655–661.

## CHAPTER 4 -ANTIMALARIAL AND ANTI- INFLAMMATORY SESQUITERPENE LACTONES FROM *VERNONIA AMYGDALINA*

---

The genus *Vernonia Del.* (family Asteraceae, tribe Vernoniae) includes over 1000 species growing mostly, but not exclusively, in tropical regions and in a wide range of habitats, going from deserts to frosty areas.<sup>1</sup> One of the most common members of this genus is *V. amygdalina*, a shrub of savannah and forests of tropical Africa, known with the name *bitter leaf*.

People in the tropics use different parts of *Vernonia amygdalina* for its medicinal value for example, leaves for fever and malaria (East Africa,<sup>2-3</sup> Northeast Nigeria,<sup>4</sup> Ghana<sup>5</sup>) and for tick control in West Ethiopia;<sup>6</sup> roots for sexual transmitted disease in Guruve district, Zimbabwe.<sup>7</sup> In Tanzania, chimpanzees have been observed to ingest the leaves instinctively when suffering from parasitic infections.<sup>8</sup> Beyond *Vernonia's* medicinal value, it is widely grown for edible soup in Cameroon and Nigeria.<sup>9</sup> In Cameroon, leaves are sometimes eaten unprocessed and raw mixed with palm oil and salt.<sup>10</sup> *V. amygdalina* is traditionally used also in the management and prevention of malaria.



*Vernonia amygdalina*

Not surprisingly, the thorough chemical investigation on *V. amygdalina* leaves have resulted in the characterization of a number of secondary metabolites, spanning from sesquiterpene lactones<sup>11-12-13</sup> to stigmastane-type

saponins (vernoniosides),<sup>14</sup> flavonoids,<sup>15</sup> and peptides (edotides).<sup>16</sup> Sesquiterpene lactones have been recognized as the responsible of the marked activity on the blood stages of the *Plasmodium* parasite showed by *V. amygdalina* extracts.<sup>17</sup> On the other hand, the anti-inflammatory and anticancer activities of *Vernonia* extracts have not been unambiguously correlated with a specific component since stigmastane steroids,<sup>18</sup> sesquiterpene lactones,<sup>19</sup> polyacetylenes,<sup>20</sup> and terpene glycosides<sup>21</sup> have all been indicated as likely responsible for these activities. A recent study has demonstrated that the growth inhibition on human breast cancer cell lines exhibited by *V. amygdalina* extracts involved the stimulation of cell-type specific G1/S phase cell cycle arrest through a p53-independent pathway, with apoptosis occurring through both extrinsic and intrinsic pathways.<sup>22</sup>

In the frame of my Ph.D. research, the bioguided analysis of a specimen of *V. amygdalina* has been undertaken as part of a project directed to the phytochemical analysis and pharmacological evaluation of plants from Africa, in collaboration with University of Camerino (Italy) and University of Cordoba (Spain). The study aimed at:

- characterizing plant extracts for stage specific effects on gametocytes and sporogonic stages of *Plasmodium falciparum* and identifying the responsible compounds of antimalarial activity through a bioassay-guided fractionation approach;
- isolation and structural elucidation of compounds with Michael related bioactivity, capable of shedding light on the molecular mechanisms underlying the anti-inflammatory and anticancer activities detected for the extract.

## 4.1 TRANSMISSION BLOCKING ACTIVITY

### 4.1.1 The burden of malaria

It has been estimated that 300-500 million cases of malaria occur annually with 1.75 to 2.5 million deaths. Malaria is a particularly important disease in sub-Saharan Africa, where about 90% of cases and deaths occur, but is also a serious public health problem in certain regions of Southeast Asia and South America.<sup>23</sup>

Human malaria is caused by four species of *Plasmodium*, namely *P. falciparum*, *P. vivax*, *P. ovale* and *P. malariae*, which are transmitted by female *Anopheles* mosquitoes. *P. falciparum* is the parasite that causes most severe diseases and most fatal cases.

The life cycle, immunological defence mechanisms, and clinical development of malaria in humans is complex. The sporozoites that develop in the salivary glands of the female mosquito are inoculated into the human when then the insect bites to acquire a blood meal. The protozoans in the sporozoite form invade selectively the parenchymal cells of the human liver. In this stage, the patient remains asymptomatic and, after an average incubation period of 5-7 days (in the case of *P. falciparum*), protozoa reach the merozoite stage and are released from the liver. The merozoites invade the erythrocytes and start feeding on the haemoglobin. After proliferation, the rupture of the erythrocyte membrane and the consequent liberation of other merozoites, that invade other erythrocytes, cause the massive infection and the symptoms. A small portion of merozoites develops into the sexual stage of gametocytes, a form that is able to re-start the life cycle of the malaria parasite when a mosquito takes a blood meal from an infected person<sup>2</sup> (**Figure 4.1**).

The clinical symptoms of malaria infections are exclusively attributable to parasites in the erythrocytic stage. The rupture of infected erythrocytes is associated with the release into the blood stream of cell debris responsible for the characteristic fever spike patterns. In the lethal cases, a specific protein produced by the protozoan is embedded into the cell membrane of

the infected erythrocyte and, as a consequence of this modification, the erythrocyte sticks to the walls of capillaries causing obstruction of vessels. When this mechanism operates at the level of brain vessels, the loss of consciousness is the first symptom, but, if this form of cerebral malaria is not treated immediately, it is soon followed by death.

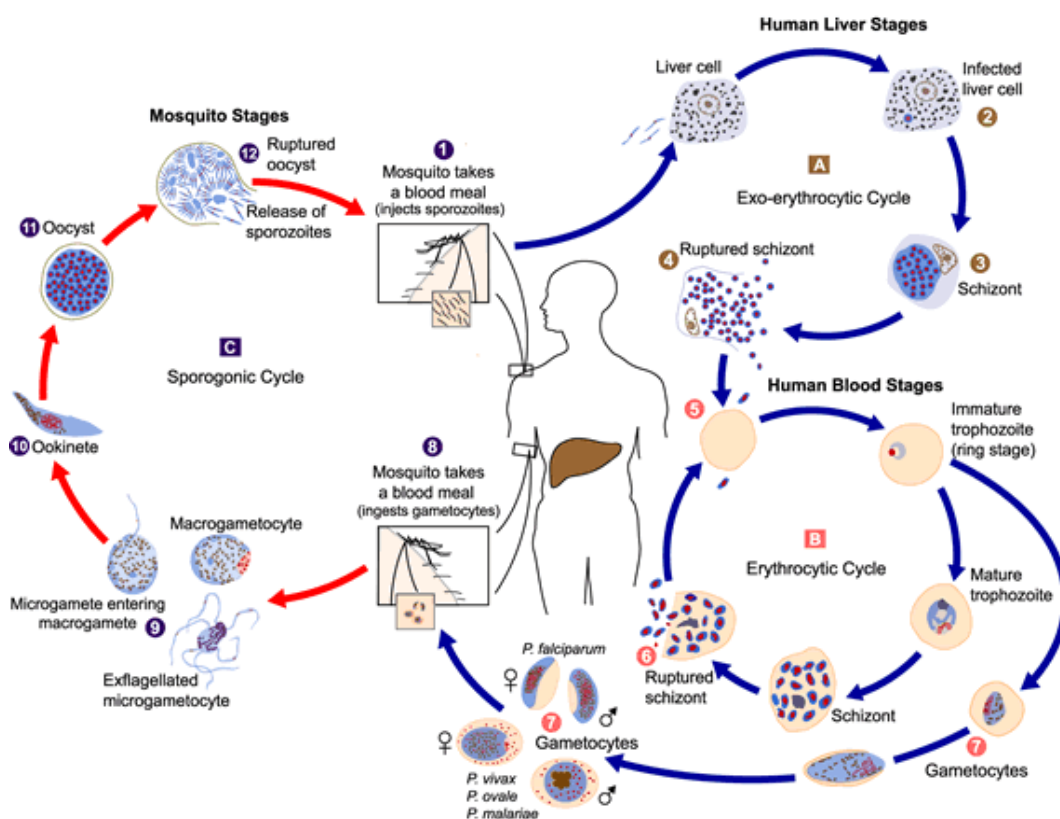
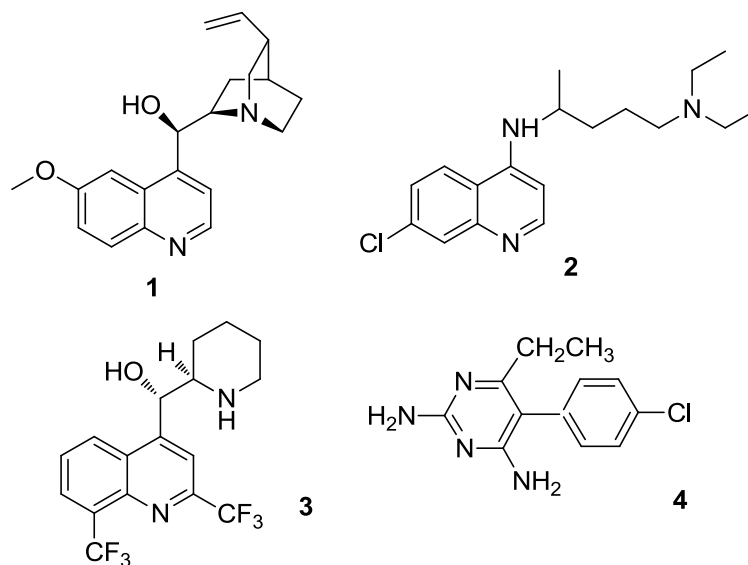


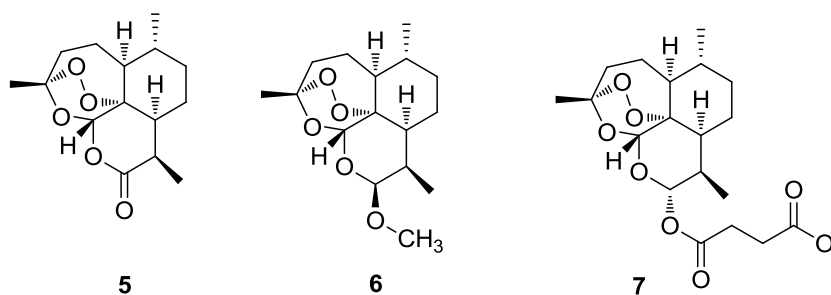
**Figure 4.1** The malaria cell cycle

The treatment of malaria infections holds a important place in the history of natural product chemistry. In the 17<sup>th</sup> century the bark of *Cinchona* trees was used as the best tool to face infections of malaria, that was endemic in Africa, Asia but also in several parts of Europe and North America: this was the first specific treatment for malaria. Later, quinine (1), isolated from the *Cinchona* bark in 1820, was the first active principle isolated from a natural source employed to treat malaria disease; and, later again, malaria was the first human disease to be treated with a synthetic drug (methylene blue in 1891). In the course of 20<sup>th</sup> century, a series of effective synthetic antimalarial drugs have been developed: chloroquine (2), mefloquine (3), and pyrimethamine

(4) became the drugs of choice and contributed to the almost complete eradication of malaria from Europe and North America.



The development of worldwide resistance of *P. falciparum* to the 4-aminoquinoline chloroquine (first observed in the 1960s) as well as resistance to the antifolates pyrimethamine and cycloguanil, undermined the chemotherapy and prophylaxis of malaria. Two major breakthroughs of the past few decades have renewed the attack of scientists to this disease. The first is the complete sequencing of the genome of *Plasmodium falciparum* that is expected to provide useful information for the identification of new drug targets. The second is the discovery of artemisinin (5, qinghaosu): it is an endoperoxide sesquiterpene lactone, active principle of the sweet wormwood, *Artemisia annua*, an herbal remedy used in folk Chinese medicine. This molecule and its oil soluble (e.g. artemether, 6, and arteether) and water soluble (e.g. artesunate, 7, and artelinate) semi-synthetic derivatives (**Figure 4.3**) have shown excellent efficacy against chloroquine-resistant *Plasmodium* strains and are becoming increasingly used, especially in combination with traditional antimalarials (e.g. mefloquine, 3).



Despite intensive efforts to control malaria, the disease continues to be one of the greatest health problems faced by Asian, African and South American countries.<sup>24</sup> According to WHO estimates, about 207 million clinical cases of malaria occurred in 2012, maintaining its deplorable ranking as one of the top killer diseases.<sup>25</sup> The failure to control malaria in these areas is explained by the emergence and spread of resistance to first-line antimalarial drugs and recently to artemisinin (**5**) too, cross-resistance between the members of the limited number of drug families available, and in some areas, multi-drug resistance.<sup>26</sup> In addition, the prevalent spreading of the disease to poor countries has suggested to many pharmaceutical companies to categorize malaria as a low priority.

Among the drugs currently used for malaria case management, artemisinin based combination therapies (ACTs)<sup>27</sup> and primaquine<sup>28</sup> have impact on malaria transmission, by reducing the infectiousness of individuals to mosquitoes.<sup>29</sup> Clinical evidence indicate that artemisinin derivatives' activity is restricted to developing gametocytes whereas primaquine is able to hit also the circulating mature gametocytes.<sup>30</sup> On the basis of the drugs' respective activity profiles, WHO recommends the addition of a single dose of primaquine to the ACT treatment course for the management of uncomplicated *Plasmodium falciparum* malaria in areas threatened by artemisinin resistance and/or in pre-elimination phase.<sup>31</sup> However, a viable alternative to primaquine is urgently needed, considering that this compound can provoke hemolytic anemia in patients with glucose-6-phosphate dehydrogenase deficiency.<sup>32</sup> Among the various available approaches, the exploration of empirically effective and chemically characterized antimalarial plants represents a valid strategy for the discovery of new druggable

compounds active against gametocytes and/or sporogonic stages for the development of multi-stage combination medicines.

#### **4.1.2 The antimalarial potential of plants**

In many African countries where malaria is endemic and in particular in rural areas where access to modern health care facilities is often hindered, traditional practices to cure or prevent malaria and other diseases still play an important role. People give preference to the use of herbal remedies for several reasons including: easier access, lower cost, lack of awareness about modern drugs and belief that the use of traditional medicine is more safe and effective. Currently, there are several standardized anti-malarial phytomedicines which have obtained official approval for commercialization in various malaria endemic countries over the world, namely China, Ghana, India, Mali and Burkina Faso. Among few such products for which clinical research has been conducted, encouraging results were obtained with Qing hao (*Artemisia annua*, Democratic Republic of Congo trials), Totaquina (*Cinchona spp*, Multicountry trials) and Phyto-laria (*Cryptolepis sanguinolenta*, Ghana trial) showing a parasite clearance at day 5 to 7 after treatment of 70–100%, 92–100% and 100%, respectively, hence supporting their use as complementary tools to the conventional anti-malarial interventions or as alternative treatments in the absence of antimalarial drugs.<sup>33</sup>

The multistage activity of artemisinin derivatives on asexual blood stages and early gametocytes,<sup>34</sup> has encouraged researchers to explore molecules of plant origin seeking not only activity on parasite stages developing in the vertebrate host but also transmission blocking effects against the sporogonic stages developing in the mosquito vector. Recently, Lucantoni *et al.* demonstrated the *in vivo* transmission blocking property of azadirachtin A enriched formulation (NeemAzal<sup>®</sup>) on *P. berghei* sporogonic development in *Anopheles stephensi* mosquitoes.<sup>35</sup> The commercial *Azadirachta indica* seed extract<sup>36</sup> was found to completely block parasite development in the vector. Azadirachtin A has been shown to inhibit the formation of flagellate microgametes from microgametocytes with an IC<sub>50</sub> of 3.5 μM,<sup>37</sup> suggesting

that microgametogenesis is a main target process of NeemAzal® transmission blocking action. The transmission blocking activity of this Azadirachtin A rich neem product was recently confirmed in the human parasite *P. falciparum* by studies conducted in Burkina Faso on field isolates.<sup>38</sup>

In sub-Saharan countries, including Ethiopia, the leaf of *Vernonia amygdalina* Del. is used for the treatment and prevention of malaria.<sup>39</sup> The anti-plasmodial activity of this small shrub of the Asteraceae family has been confirmed by several *in vitro*<sup>40</sup> and *in vivo* studies.

Several secondary metabolites have been isolated and characterized from *V. amygdalina* leaves such as sesquiterpene lactones, steroidal saponins (vernoniosides) and flavonoids (luteolin and its glycosides). The class of sesquiterpene lactones is probably the most peculiar of this plant and it includes the highly oxygenated derivatives vernolide,<sup>41</sup> vernodalol,<sup>41</sup> vernodalinol,<sup>42</sup> epivernodalol,<sup>43</sup> vernodalin and vernomygdalin.<sup>44</sup> Vernolepin, belonging to the same chemical class, has been isolated from the dried fruit of the plant.<sup>45</sup> Vernolide and vernodalin exhibited IC<sub>50</sub> of 1.87 and 0.52 µg/ml, respectively, against *P. falciparum* blood stages *in vitro*.<sup>46</sup> In another study, IC<sub>50</sub> values of 8.4, 4.0, 4.2 and 11.4 µg/ml were obtained for vernolide, vernodalin, vernodalol and hydroxyvernolide, respectively.<sup>47</sup>

On the basis of the above illustrated broad knowledge available on *V. amygdalina* as an antimalarial plant -from its evidenced appreciable clinical efficacy to the partially characterized activity profile of some secondary metabolite- we selected this plant as a valid candidate for investigation on potential inhibitors of *Plasmodium* transmission stages.

#### **4.1.3 Antimalarial activity of *Vernonia amygdalina* extracts**

Exploratory *in vivo* studies conducted with *P. berghei* ANKA strain and *An. stephensi* mosquitoes, revealed transmission blocking activity of *V. amygdalina* aqueous (Ver-H<sub>2</sub>O) and ethanolic (Ver-EtOH) leaf extracts. *An. stephensi* females, fed on gametocytemic mice treated with Ver- H<sub>2</sub>O at 500 mg/kg and Ver-EtOH at 100 mg/kg, developed respectively 55 and 90% fewer oocysts compared to controls.

Methanol extract of *V. amygdalina* leaves was partitioned between water and EtOAc and this latter phase revealed interesting activity against the early stages of sporogonic development. Chromatographic fractionation of this extract yielded 14 fractions, three of which proved to be active. (Table 4.1).

**Table 4.1** Inhibitory activity of ethylacetate phase fractions from *V. amygdalina* leaves against early sporogonic stages.

Test agents	Experiment <sup>‡</sup>	Mean ESS counts (95% CI)*	Percentage inhibition of ESS (95% CI)
Fraction-11	1	1 (0– 2)	96.3 (92.2– 100)
	2	0	100
	3	0 (0– 1)	99.7 (99– 100)
	4	1 (0– 1)	99.7 (99.4– 100)
	5	0	100
Fraction-12	1	0	100
	2	1 (0– 2)	95.1 (85.6– 100)
	3	0 (0– 1)	99.7 (99– 100)
	4	1 (0– 2)	99.7 (99.1– 100)
	5	0 (0– 1)	99.8 (99.3– 100)
Fraction-13	1	0	100
	2	0 (0– 1)	97.6 (92.8– 100)
	3	0	100
	4	0 (0– 1)	99.8 (99.5– 100)
	5	1 (0– 2)	99.5 (98.5– 100)
Solvent control (0.2% DMSO)	1	27 (22– 33)	
	2	14 (9– 19)	
	3	96 (85– 106)	
	4	219 (198– 240)	
	5	135 (111– 158)	

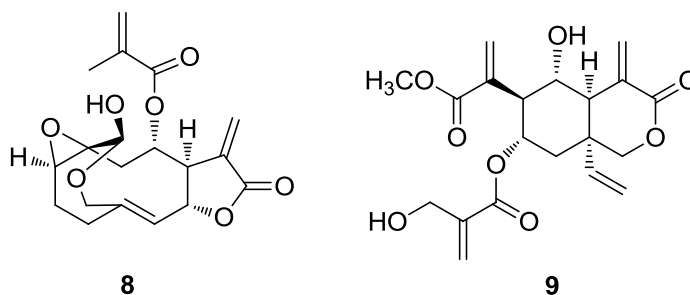
Fractions from ethylacetate phase were tested at 50 µg/mL concentration.

Data are presented as mean early sporogonic stages (ESS) counts calculated from triplicate wells and percentages of ESS inhibition referred to solvent control. Both parameters are presented with 95% confidence intervals (95% CI).

<sup>‡</sup>Each number represents one experiment conducted with gametocyaemic blood from a different mouse.

\*Mean ESS counts are rounded to the nearest whole number.

Chemical analysis of these fractions allowed isolation and identification of the two compounds most likely responsible for the transmission blocking activity observed, namely vernodalol and vernolide, whose structures were identified by comparison with spectroscopic data in the literature.<sup>41</sup> These two molecules are sesquiterpene lactones belonging to the structural classes of germacranolides (vernolide) and elemanolides (vernodalol).



Tested as pure compounds, vernodalol and vernolide exhibited moderate to low activity in the *in vitro* ookinete development assay (ODA) (**Table 4.2**). At a concentration of 50  $\mu\text{M}$  (19.6  $\mu\text{g}/\text{mL}$ ) vernodalol inhibited early sporogonic development (ESS) by 70-90%, while vernolide at the same concentration (50  $\mu\text{M}$ , 18.1  $\mu\text{g}/\text{mL}$ ) reduced ESS by 9–33%.

**Table 4.2** Impact of vernolide and vernodalol on the development of early sporogonic stages *in vitro*

Test compounds	Experiment <sup>‡</sup>	Mean ESS counts (95% CI)*	Percentage inhibition of ESS (95% CI)
Vernodalol	1	24 (21– 26)	79.3 (77.3– 81.4)
	2	12 (8–16)	89.7 (86.4– 92.9)
	3	92 (77–107)	69.3 (64.3– 74.3)
Vernolide	1	103 (90–115)	9.4 (0– 20.5)
	2	79 (63– 95)	30.6 (16.7– 44.5)
	3	201 (182– 220)	33 (26.6– 39.3)
Solvent control (0.2% DMSO)	1	113 (93– 134)	
	2	114 (97–132)	
	3	300 (284– 317)	

Compounds were tested at a concentration of 50  $\mu\text{M}$ .

<sup>‡</sup>Each number represents one experiment conducted with gametocyaemic blood from a different mouse; ESS counts are means from sextuplicate wells.

\*Mean ESS counts are rounded to the nearest whole numbers

In line with these data, *V. amygdalina* AcOEt fractions composed of almost only vernodalol and vernolide showed evident inhibitory activity in the ODA. Fraction 11 (about 91% vernolide), fraction 12 (about 50% vernolide + 50% vernodalol) and fraction 13 (about 85% vernodalol) suppressed ESS by 95 – 100% when tested at 50  $\mu\text{g}/\text{mL}$  (corresponding to amounts of 42 – 50  $\mu\text{g}/\text{mL}$  of vernolide, vernodalol or vernolide + vernodalol).

A relatively stronger activity than expected for its vernodalol and vernolide content, was observed with the AcOEt phase preparation. This finding may indicate the presence of other bioactive constituents in the EtOAc phase, having a direct effect on ESS or influencing the activity of vernolide and vernodalol.

Differential counting of zygotes and ookinetes indicated that Ver-EtOH interfered with processes preceding zygote formation (**Figure 4.2**). At the highest tested concentration (50  $\mu\text{g}/\text{mL}$ ), however, an impact on subsequent ookinete maturation was also observed. Interestingly, this was not the case with pure vernolide and vernodalol or with fractions 11 to 13, consisting almost entirely of these two compounds, an observation suggesting that the two sesquiterpene lactones may interfere with the first processes of sporogonic development, namely gametogenesis and/or macrogamete fertilization.

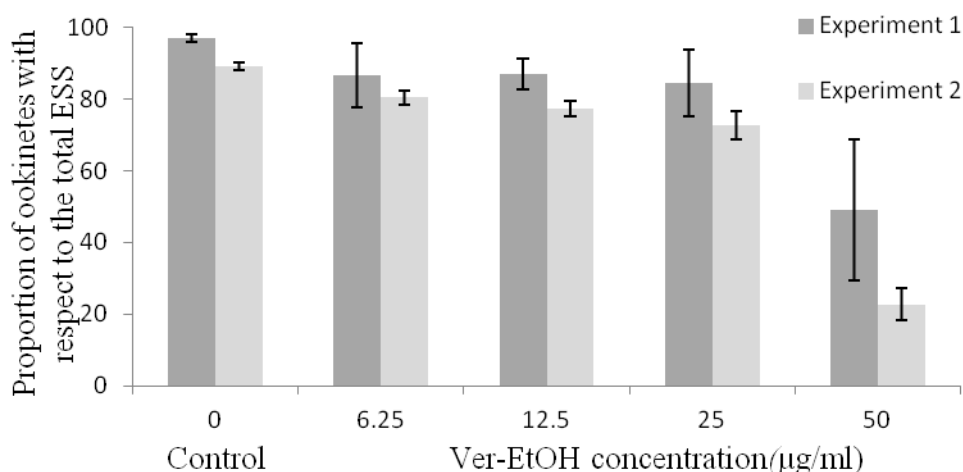


**Figure 4.2** Proportion of mature ookinetes with respect to total early sporogonic stage.\*

\*The test was conducted using ethanolic *V. amygdalina* leaf extract (Ver-EtOH) at different concentration and solvent control (dimethyl sulfoxide). Each bar in the graph refers to readings from 3 and 6 microplate wells in experiment 1 and 2, respectively.

Exflagellation tests performed with vernodalol and Ver-EtOH allowed to further narrow down the possible target stages. Both the compound and the extract, tested at 50  $\mu\text{M}$  and 50  $\mu\text{g}/\text{mL}$  respectively, did not interfere with microgamete formation *in vitro*, suggesting that the processes targeted by

*V. amygdalina* transmission blocking components are mainly macrogametogenesis and/or macrogamete fertilization.

Vernolide and vernodalol have been reported to exhibit moderate activity also on asexual blood stages<sup>46-47</sup> inhibiting *P. falciparum* asexual forms by 50% at a concentration of 1.87–8.4  $\mu\text{M}$  and 4.2  $\mu\text{M}$ , respectively. This multi-stage activity of vernodalol and vernolide raises exciting questions on modes and mechanisms of action of the two sesquiterpene lactones and research focused into this aspect may lead to the discovery of novel multistage drug targets.

The experiments conducted in Burkina Faso with *P. falciparum* field isolates allowed us to evidence the transmission blocking activity of *V. amygdalina* also against the human malaria parasite. *An. coluzzii* mosquitoes that had membrane-fed on gametocytic blood treated with the vernolide and vernodalol-rich EtOAc fractions (fraction 11 and 13 respectively) were less infected and oocyst numbers in positive mosquitoes were reduced by about half. The membrane feeds were supplemented with the fractions at a dosage of 100  $\mu\text{g}/\text{mL}$  corresponding to vernolide and vernodalol equivalents of 91.2  $\mu\text{g}/\text{mL}$  and 85  $\mu\text{g}/\text{mL}$ , respectively. The relatively high dosage needed to achieve a substantial reduction in sporogonic development of *P. falciparum*, taken together with the moderate activity by the pure compounds observed *in vitro* on *P. berghei*, suggest that neither vernodalol nor vernolide possess the potency required for a drug candidate molecule. On the other hand, our *in vivo* experiments evidenced significant transmission blocking activity by the Ver-EtOH extract and the bio-guided fractionation studies revealed a relatively higher *in vitro* activity of extracts compared to that of the pure compounds, suggesting that the development of a phytomedicine based on vernodalol and vernolide enriched standardized extract may be a more appropriate strategy to pursue.

Artemisinin derivatives have been demonstrated to possess activity against *P. falciparum* gametocytes *in vitro*<sup>48</sup> and in clinical trials<sup>27</sup>, shortening the period of gametocytes circulation in patients treated with ACTs<sup>49</sup> and thus decreasing the infection rates of blood seeking mosquitoes. In the current *in vivo* study, Ver-H<sub>2</sub>O administered to mice at 500 mg/kg was found to reduce

macrogametocyte densities by about 50%. A decrease in microgametocyte numbers was also noticed, reaching significance in one of the two replicates carried out. Since Ver-H<sub>2</sub>O did not exhibit *in vitro* activity on early sporogonic stages, but still reduced oocyst densities in mosquitoes when administered to females *in vivo* through an infectious blood meal, the observed transmission blocking effect might be attributed to the gametocytocidal activity of Ver-H<sub>2</sub>O.

Considering the diverging gametocyte biology of *P. falciparum* and *P. berghei*<sup>50</sup>, a validation of the activity of extracts on *P. falciparum* gametocytes is the next step to be undertaken. If confirmed, subsequent bio-guided fractionation studies may allow the identification of new gametocytocidal compounds.

The cytotoxic properties of *V. amygdalina* extracts and compounds have been assessed on various cell lines: IC<sub>50</sub> values vary widely with the compounds and type of cell lines used (**Table 4.3**).

**Table 4.3** Activity of *V. amygdalina* extracts, fractions and pure compounds on cell viability of a human colon cancer and endothelial cell line.

Test agents	IC <sub>50</sub> (95% CI)	
	HCT116	EA.hy 926
Leaf extracts (µg/mL)		
Ver-EtOH	3.66 (3.41– 3.96)	9.46 (8.64– 10.36)
Ver-MeOH	8.09 (7.54– 8.67)	16.94 (15.55– 18.46)
Ver-H <sub>2</sub> O	64.34 (58.75– 70.53)	76.21 (58.09– 100.00)
Fractions from MeOH extract (µg/mL)		
Fraction 11	0.17 (0.15– 0.18)	0.42 (0.39– 0.45)
Fraction 12	0.33 (0.3– 0.37)	1.13 (0.97– 1.31)
Fraction 13	2.41 (2.29– 2.53)	4.52 (4.23– 4.82)
Fraction 14	3.86 (3.62– 4.12)	7.69 (7.10– 8.32)
Molecules from fractions (µM)		
Vernolide	1.49 (1.38– 1.61)	3.18 (2.97– 3.4)
Vernodalol	4.97 (4.78– 5.17)	7.1 (6.51– 7.74)

Each value represents the mean of two experiments carried out in quadruplet wells. HCT 116=Human colon carcinoma cell line, EA.hy 926= Human (non-tumor) endothelial cell line.

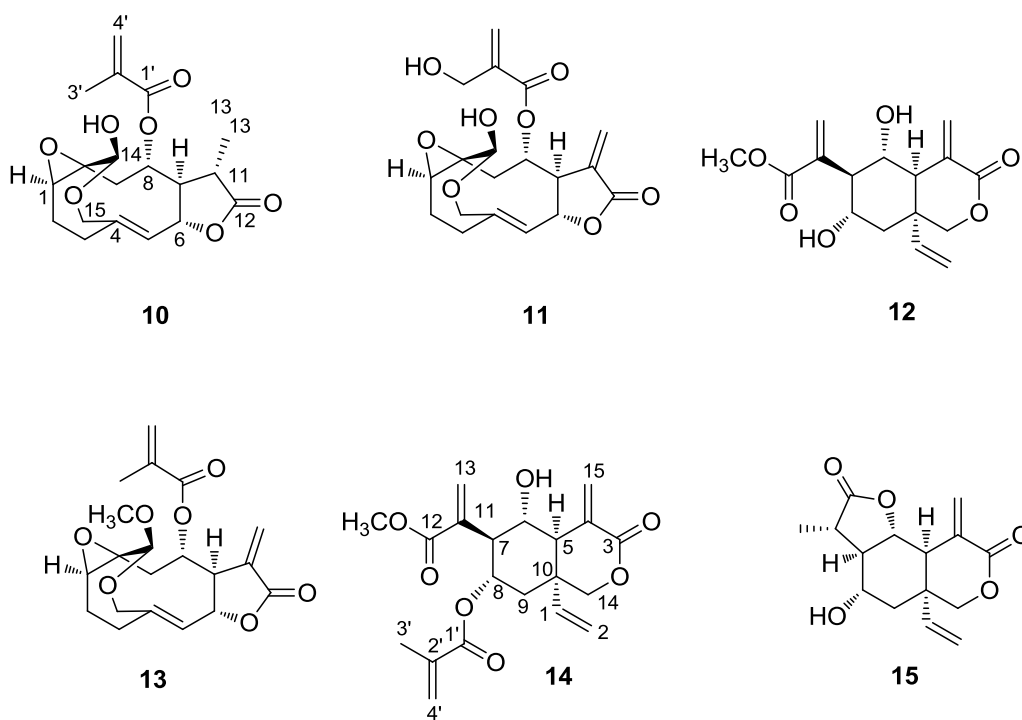
Ver-EtOH, Ver-MeOH, and Ver-H<sub>2</sub>O stands for ethanolic, methanolic and aqueous extract of *V. amygdalina* leaves.

95% CI = 95% confidence interval

However, given the interesting multi-stage activity of vernodalol and vernolide, the molecules still are worth to be considered for structure-activity relationship studies aimed at designing compounds with reduced toxicity and enhanced activity against ESS and asexual blood stage parasites. Also, the compounds might be utilized as tools to investigate potential drug targets expressed in multiple life cycle stages.

## 4.2 MICHAEL-RELATED BIOACTIVITY OF SESQUITERPENES LACTONES

The organic extract obtained from the leaves of an Ethiopian specimen of *V. amygdalina* proved to be a rich source of sesquiterpene lactones. From the detailed chemical analysis of the EtOAc phase, we isolated five known (**8-12**) molecules and three new members of this family, namely methylvernolide (**13**), deoxyvernodalol (**14**) and vernomygdalin (**15**). The availability of these compounds provided the opportunity to shed light on the molecular mechanisms underlying the anti-inflammatory and anticancer activities of the extract of *Vernonia amygdalina*.



There is growing awareness that electrophilic natural products interact with their biological targets according to a “dock and lock” mechanism, where

shape complementarity is important to position the reactive site(s) of a covalent ligand in an optimal orientation for thiol trapping. Given the poly-electrophilic nature of the major sesquiterpene lactones we had isolated, it was important to identify the most reactive thiophilic site within each compound and to rank them in order of reactivity using the cysteamine assay, a straightforward method to identify Michael acceptors, recently published by my research group.<sup>51</sup> By comparing these data with those of bioassays on targets sensitive to thiol trapping and involved in inflammation like the transcription factors NF- $\kappa$ B, STAT3 and Nrf2, the relative contribution of shape and reactivity to the bioactivity of these compounds could be dissected.

#### **4.2.1 Structure elucidation of new sesquiterpenes lactones**

Repeated chromatographic purification of the organic phase of *V. amygdalina* methanol extract, yielded the known compounds vernolide (**8**),<sup>44</sup> dihydroveranolide (**10**),<sup>52</sup> hydroxyveranolide (**11**),<sup>53</sup> vernodalol (**9**),<sup>54</sup> and methoxyvernolepin (**12**),<sup>54</sup> identified on the basis of the comparison of their spectral data with those reported in the literature, and the new methylveranolide (**13**), deoxyvernodalol (**14**), and vernomygdalin (**15**).

Methylveranolide (**13**), C<sub>20</sub>H<sub>24</sub>O<sub>7</sub> by HRMS, was easily identified as the 14-*O*-methyl derivative of the highly oxygenated germacranolide vernolide (**8**). The <sup>1</sup>H NMR spectrum of **13** (CDCl<sub>3</sub>) was practically superimposable to that of **8**, with the single exception of the replacement of the OH-14 signal at  $\delta_{\text{H}}$  4.95 with a methyl singlet resonating at  $\delta_{\text{H}}$  3.91. The location of this group was supported by the HMBC cross-peak of the methyl singlet with C-14 ( $\delta_{\text{C}}$  99.2).

Analogously, the relationship between deoxyvernodalol (**14**), C<sub>20</sub>H<sub>24</sub>NaO<sub>7</sub> by HRMS, and the acylated elemanolide vernodalol (**9**) was suggested by the close similarity between their <sup>1</sup>H NMR spectra. Since the proton resonances attributable to the sesquiterpene core were practically coincident for the two compounds, the differences must be located in the *O*-8 acyl group. A methyl singlet ( $\delta_{\text{H}}$  1.86) and a sp<sup>2</sup> methylene ( $\delta_{\text{H}}$  5.73 and 5.53, both bs,  $\delta_{\text{C}}$  126.4, associated by HSQC) accounted for the five proton signals of this acylating

moiety and its 2-methyl-propenoyl structure was supported by the HMBC cross-peaks of all these proton signals with both C-2' ( $\delta_C$  144.4) and C-1' ( $\delta_C$  167.4). Similarly, the attachment of the acyl group at C-8 was secured by the HMBC cross-peak H-8/C-1'. Thus, in agreement with its molecular formula, the new compound **14** must differ from vernodalol for a deoxygenation at C-3'.

Vernomygdalin (**15**) was isolated in minute amounts as a colorless amorphous solid with molecular formula  $C_{15}H_{18}O_5$  by HRMS.  $^1H$  and  $^{13}C$  NMR spectra of **15** ( $CDCl_3$ ) were suggestive of an elemanolide sesquiterpene of the vernodalol family. The COSY spectrum arranged most of the proton signals within a large spin system (**Figure 4.3**) encompassing five methines (including two oxymethines), a diastereotopic methylene and a methyl doublet ( $\delta_H$  1.46). The remaining proton resonances belonged to a monosubstituted double bond, an uncoupled conjugated  $sp^2$  methylene ( $\delta_H$  6.75, bs; 5.76, bs) and an isolated oxymethylene ( $\delta_H$  4.42 and 4.24, both d). Having associated all the proton resonances to those of the directly attached carbon atoms through the 2D HSQC spectrum, we used the HMBC experiment to join the above different moieties. HMBC cross-peaks of H<sub>2</sub>-14, H<sub>2</sub>-15 and H-1 (red arrows in Figure 4.3) built up a vernodalol-type bicyclic system. The two remaining unsaturation degrees implied by molecular formula were accounted by a  $\gamma$ -lactone ring, as clearly indicated by the HMBC cross-peaks of both H<sub>3</sub>-13 and H-6 with C-12 (violet arrows in Figure 4.3). The network of ROESY correlations of vernomygdalin (**15**) (Figure 4.3) indicated a relative configuration identical to that of vernodalol for parallel stereogenic centers and suggested the  $\alpha$  orientation of the methyl group at C-11.

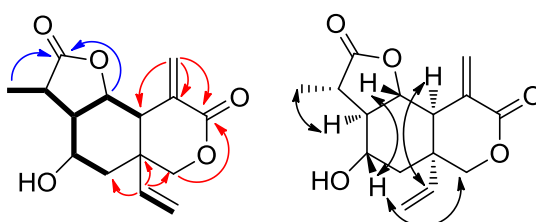


**Figure 4.3** Selected 2D NMR correlations of vernomygdalin (**15**). *left*: COSY (boldened lines) and HMBC correlations (arrows); *right*: ROESY correlations.

#### **4.2.2. Michael related bioactivity: NF- $\kappa$ B and STAT3 inhibition.**

Although the eight sesquiterpene lactones isolated during this study belong to two different structural families, germacranolides of the vernolide-type (**8-10-11-13**) and elemanolides of the vernodalol-type (**9-12-14-15**), they share the common feature of a single (as in **10** and **15**) or multiple (three in **9** and **14**) potential Michael acceptor sites in their structures.

Michael acceptors are generally discarded during drug discovery processes on the basis of their tendency to form off-target covalent linkages, a reactivity considered potentially toxic. However, this bias underestimates the incredible biological potential of selective thiol-reactive Michael acceptors, which have been demonstrated to target a number of important and druggable pathways. For example, protein kinase inhibition,<sup>55</sup> TRPA1 activation,<sup>51-56</sup> PPAR $\gamma$  modulation,<sup>57</sup> and NF- $\kappa$ B inhibition<sup>58</sup> have all been related to thia-Michael acceptor structural motifs. The multi-faceted anti-inflammatory and anticancer bioactivity of the food plant compound curcumin well exemplifies the pharmaceutical relevance of these compounds.<sup>57</sup>

The availability of *Vernonia* poly-electrophilic sesquiterpene lactones made it possible to evaluate the ability of the NMR-based cysteamine assay<sup>51</sup> to discriminate their reactivity as thiol trapping agents. In this assay, the substrate is dissolved in DMSO- $d_6$  and cysteamine (1.2 equivalents) is added directly in the NMR tube: a positive assay is evidenced by the immediate marked reduction or disappearance of the carbonyl conjugated double bond signals. The use of only 1.2 equiv of cysteamine allows to get information on the reactivity order in molecules containing multiple acceptor sites, while competition experiments with different substrate and sub-stoichiometric amounts of cysteamine make it possible to rank them in terms of reactivity.

Vernolide (**8**) and vernodalol (**9**) exemplify the poly-electrophilic nature of the *Vernonia* exomethylene lactones, and were chosen for these experiments. The <sup>1</sup>H NMR spectra of these compounds were first registered in DMSO- $d_6$ , fully assigned by 2D NMR experiments, and then re-analyzed 15 min after addition of 1.2 equiv of cysteamine. Both vernolide and vernodalol gave a

single major product of addition (**Figure 4.4**), but the regiochemistry of addition was surprisingly different.

Thus, vernolide (**8**) underwent exclusive addition of cysteamine to the exomethylene  $\gamma$ -lactone group, with no evidence of reaction at the  $\alpha,\beta$ -unsaturated ester moiety, the epoxide group or the semiacetalized aldehyde function. Conversely, vernodalol (**9**) reacted selectively at the *O*-8 acyl group, with the other electrophilic sites (the exomethylene  $\delta$ -lactone and the acryloyl moiety) remaining unscathed.

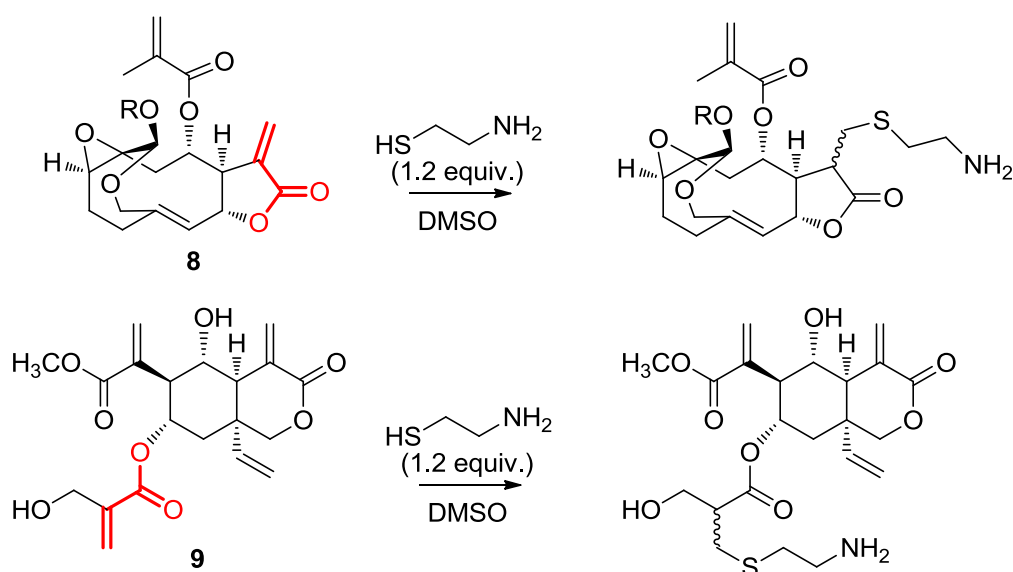


**Figure 4.4** Results of the cysteamine assay for vernolide (**8**) and vernodalol (**9**). The reactive Michael acceptor moiety is marked in red.

These results, while validating the ability of the cysteamine assay to identify the most reactive site in polyfunctional thiol trapping agents, provide solid evidence that electrophilic sesquiterpene lactones are an heterogeneous group of compounds in terms of reactivity sites, that goes substantially beyond the presence of a common 11,13-exomethylene group.

In a comparative experiment, an equimolar mixture of vernolide (**1**) and vernodalol (**5**) was treated with an amount of cysteamine corresponding to the trapping of a single electrophilic group. The <sup>1</sup>H NMR spectrum recorded after 15 min showed the preferential reaction of vernolide, as clearly evidenced by the selective decrease of the signals of its exomethylene- $\gamma$ -lactone protons (H-13a,b  $\delta$  6.06 and 5.58) over the signals of the reactive acyl group of vernodalol (H-4'a,b  $\delta$  6.00 and 5.78) (**Figure 4.5**). This comparative

experiment clearly establishes a ranking in the reactivity, identifying vernolide as the most reactive compound.

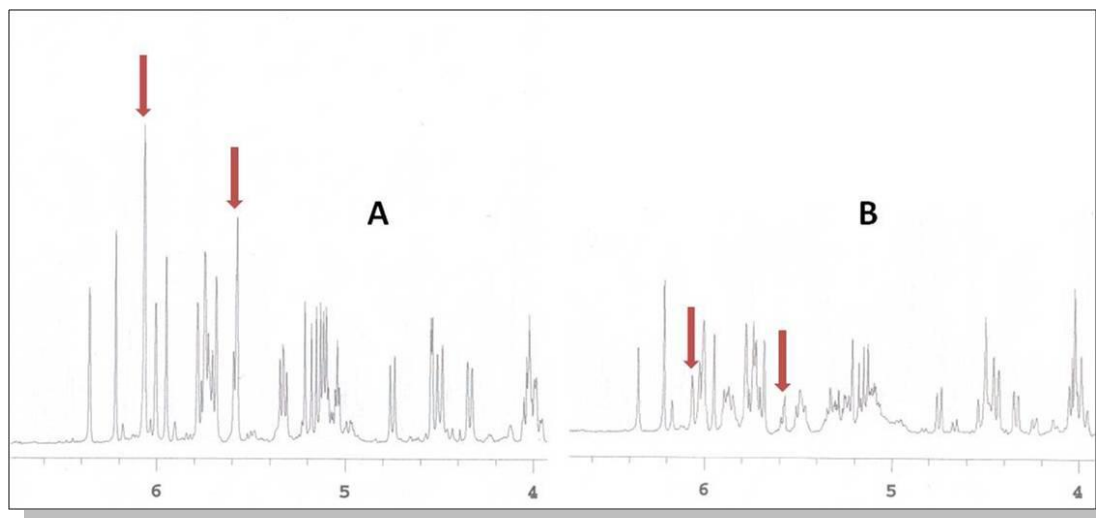


**Figure 4.5** Comparative cysteamine assay of a ca. equimolecular mixture of vernolide (**8**) and vernodalol (**9**). A) reference mixture B) spectrum obtained after the addition of a stoichiometric amount (1.0 equivalent) of cysteamine. The red arrows indicate the signals of the exomethylene- $\gamma$ -lactone protons of vernolide.

Thia-Michael acceptor reactivity has been related to the modulation of a number of important biological targets.<sup>57-59</sup> Among the thiol-trapping sensitive end points, the transcription factors NF- $\kappa$ B, STAT3, and Nrf2 have been described to play a significant role in regulating the expression of genes coding pro-inflammatory cytokines and in the pathogenesis of human disorders characterized by a chronic inflammatory component, including cancer.<sup>60</sup> Thus, we evaluated the sesquiterpene lactones of *V. amygdalina* for inhibition of the pro-inflammatory transcription factors NF- $\kappa$ B and STAT3 and activation of the anti-inflammatory transcription factor Nrf2, which is considered the “master regulator” of the antioxidant response (**Table 4.8**). The anti-NF- $\kappa$ B activity was measured in 5.1 cell line activated with TNF $\alpha$ ; the anti-STAT3 activity was measured in LNCaP cells activated with IFN- $\gamma$ , and Nrf2 activation was investigated in the HaCaT-ARE-Luc cell line. The cytotoxic activity was measured in the prostate cancer cell line DU145.

**Table 4.4** Activity of *V. amygdalina* sesquiterpenoids on inhibition of NF- $\kappa$ B and STAT3, activation of Nrf2 and cytotoxicity in DU145 cells.

Compound	NF- $\kappa$ B	STAT3	Nrf2	Cytotoxicity
	IC <sub>50</sub> ( $\mu$ M)	IC <sub>50</sub> ( $\mu$ M)	EC <sub>50</sub> ( $\mu$ M)	IC <sub>50</sub> ( $\mu$ M)
Vernolide ( <b>8</b> )	6.3 $\pm$ 2.1	6.1 $\pm$ 3.1	0.7 $\pm$ 0.3	40.1 $\pm$ 4.3
Dihydrovernalide ( <b>10</b> )	> 50	> 50	> 50	> 50
Vernodalol ( <b>9</b> )	18.2 $\pm$ 2.6	20.4 $\pm$ 3.8	3.2 $\pm$ 1.8	46.8 $\pm$ 5.8
Deoxyvernodalol ( <b>14</b> )	9.0 $\pm$ 3.2	12.3 $\pm$ 4.1	5.2 $\pm$ 2.3	> 50
Methoxyvernolepin ( <b>12</b> )	> 50	> 50	> 25	> 50

Vernolide (**8**) and deoxyvernodalol (**14**), and to a lesser extent vernodalol (**9**), showed a marked inhibitory activity on STAT3/NF- $\kappa$ B; deoxyvernodalol (**14**) and vernodalol (**9**) showed a good Nrf2 activation evidencing also a good correlation between this activity and cytotoxicity. It is possible that STAT3/NF- $\kappa$ B inhibitory activity of vernolide (**8**) results in an increase in oxidative stress that induces cytotoxicity. In this sense, the ability of deoxyvernodalol (**14**) and vernodalol (**9**) to induce the expression of Nrf2-dependent antioxidant genes may counteract this oxidative stress and prevent the cytotoxicity associated to vernolide (**8**). The structurally related analogues dihydrovernalide (**10**) and methoxyvernolepin (**12**) were practically inactive on the same pharmacological endpoints.

These pharmacological results are in striking agreement with the outcomes of the NMR-based cysteamine assay. Indeed, the inactive dihydrovernalide (**10**) differs from the active vernolide (**8**) only for the lack of the conjugated exomethylene, selected as preferential thia-Michael acceptor by the cysteamine assay. Similarly, the inactive methoxyvernolepin (**12**) differs from the active vernodalol (**9**) only for the lack of the *O*-8 acyl group, the moiety positive in the cysteamine assay, although two other potentially reactive  $\alpha,\beta$ -unsaturated esters are still present in its structure.

In addition to the pro-inflammatory activity, NF- $\kappa$ B and STAT3 are also involved in the aberrant cell cycle progression of cancer cells. Since vernolide (**8**) qualified as the most active NF- $\kappa$ B and STAT3 inhibitor in our assays, we studied its effect on cell cycle progression in the DU145 cell line that

expresses constitutive activation of both transcription factors. In this cell line we found that vernolide is cytotoxic and arrested the cell cycle at the S phase, a clear example of antitumor activity related to NF- $\kappa$ B and STAT3 inhibition (**Figure 4.6**).

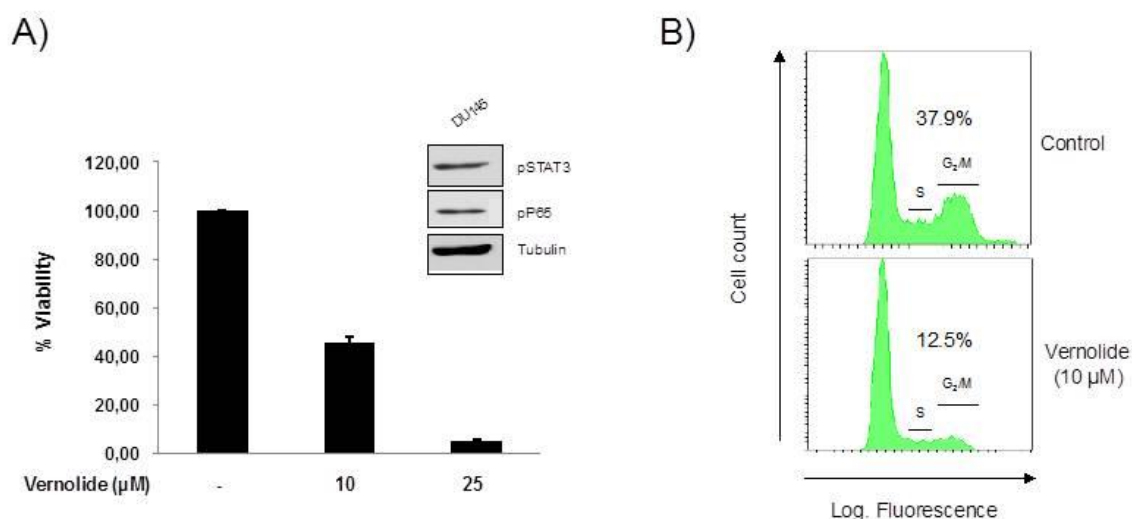


**Figure 4.6** Vernolide induces cell cycle arrest\*.

\* A) DU145 cells were incubated with vernolide (**1**) for 48 h at the indicated concentrations and the cell viability was measured by the MMT assay; insert shows that DU145 cells express STAT3 and NF- $\kappa$ B/p65 constitutively phosphorylated. B) DU145 cells were treated with vernolide (**8**) for 24 h and the cell cycle analyzed by flow cytometry. The percentage of cells in the phases S and G<sub>2</sub>M are indicated.

Taken together, these data show that, due to its high concentration and superior activity, vernolide should be considered the major anti-inflammatory constituent of extracts from *V. amygdalina*.<sup>22</sup> Given the role of the investigated transcription factors in many steps of cancer initiation and progression, their inhibition can be also related to prevention and treatment of cancer, thus providing a molecular rationale for the anticancer activity reported for *V. amygdalina* extracts.<sup>22</sup> Moreover we evidenced the differential bioactivities of deoxyvernodalol (**14**) on STAT3/NF- $\kappa$ B and Nrf2 signaling pathways, and this compound qualifies as an interesting anti-inflammatory and antioxidant agent that could be used for the treatment of chronic inflammatory disorders.

### 4.3 CONCLUSIONS

Previously published works and the present study demonstrate that *V. amygdalina* leaves contain molecules affecting multiple stages of *Plasmodium*, evidencing its potential for drug discovery and for the development of standardized *V. amygdalina* based phytomedicines. On the identified hit molecules, primarily vernodalol, chemical or functional group modification is recommended to generate a druggable sesquiterpene lactone compound with enhanced activity against the blood and sporogonic stages of the malaria parasite and reduced off-target activities. In addition, the development of a multistage phytomedicine, exhibiting both anti-blood stage as well as transmission blocking properties and designed as a preventive treatment to complement existing malaria control tools appears a challenging but feasible goal.

The sesquiterpene lactones *V. amygdalina* provided also the opportunity to validate the cysteamine assay as a tool to investigate thiophilicity and to build a sort of Michael-oma profile of a certain class of compounds, identifying the most reactive site in polyfunctional compounds and ranking them in terms of reactivity. In the pair of compounds investigated (vernolide and vernodalol), a correlation between reactivity and bioactivity was found in all three inflammatory-related end-points investigated. This should, however, be validated using larger databases of sesquiterpene lactones, since in other classes of Michael acceptors like curcuminoids no direct correlation between reactivity and bioactivity was found.<sup>57</sup>

### 4.4 EXPERIMENTAL SECTION

#### 4.4.1 Plant material, extraction and isolation

*V. amygdalina* Del. (Asteraceae) leaves were collected in the area of Karat town, located in Konso district, i.e., 600 km south of Addis Ababa, Ethiopia, after the rainy season (October 2011). A leaf specimen was used for taxonomic identification, and authenticated by Mr. Melaku Wondafrash, a plant taxonomist. A voucher specimen was deposited (Solomon-01) at the National Herbarium, Addis Ababa University, Ethiopia.

*V. amygdalina* leaves were air-dried at room temperature in the shade and ground using a blender. Ground material (50 g) was macerated in ethanol (EtOH) for 24 h and filtered with filter paper (Whatman® no.1). Ethanol was removed using a rotary evaporator at 40 °C under reduced pressure. The extract was further concentrated by freeze drying and stored at -20 °C until use. To prepare the aqueous extract (Ver-H<sub>2</sub>O), 50 g of ground *V. amygdalina* leaves were macerated in distilled water for 24 h, then filtered and freeze dried. The percent yields of the aqueous and ethanol extractions were 14% and 8%, respectively.

To identify secondary metabolites responsible for transmission blocking activity, bio-guided fractionation was employed on a methanol (MeOH) extract of *V. amygdalina* leaves. Briefly, 450 g of leaf powder was macerated in MeOH for 24 h, to obtain a dried MeOH extract (34.5 g, yield 7.6%). A portion of this extract (27.9 g) was then partitioned, first between water and ethyl acetate (EtOAc), and then between water and butanol (BuOH), to get the following phases: EtOAc (14.3 g), BuOH (4.9 g) and H<sub>2</sub>O (7.9 g). The EtOAc phase was selected for bioassay guided fractionation. It was subjected to medium pressure liquid chromatography (MPLC) over a column packed with silica gel (230-400 mesh) and eluted with the following solvent gradient of increasing polarity: *n*-hexane, to *n*-hexane:EtOAc (9:1), *n*-hexane: EtOAc (4:1), *n*-hexane: EtOAc (7:3), *n*-hexane: EtOAc (3:2), *n*-hexane: EtOAc (1:1), *n*-hexane: EtOAc (7:11), *n*-hexane: EtOAc (1:4), EtOAc, EtOAc:MeOH (1:1) and finally MeOH. A total of 40 eluates of 250 mL each were collected and combined on the basis of thin layer chromatography behavior, to get 14 fractions which were then tested for anti-plasmodial activities *in vitro*.

The active fractions (fr. 11– 14) were further purified by high performance liquid chromatography (HPLC) on a Knauer apparatus equipped with a refractive index detector and LUNA (5 $\mu$ , 250  $\times$  4 mm Phenomenex) SI60 or Kinetex (2.6 $\mu$ , 100  $\times$  4.60 mm Phenomenex) C18 columns. Fraction 11 was separated by HPLC (*n*-hexane/EtOAc 75:25, flow 0.8 mL/min) to get pure vernolide (**8**, 225.3 mg), methylvernolide (**13**, 1.5 mg), dihydrovernolide (**10**, 5.5 mg) and deoxyvernodalol (**14**, 3.4 mg). Fraction 12 was separated by HPLC (*n*-hexane/EtOAc 6:4, flow 0.7 mL/min) to get pure hydroxyvernolide

(**11**, 1.2 mg) and vernomygdalin (**15**, 0.8 mg). Fraction 13 was separated by HPLC (*n*-hexane/EtOAc 1:1, flow 0.8 mL/min) to obtain pure methoxyvernolepin (**12**, 6.5 mg) and vernodalol (**9**, 165.5 mg).

#### 4.4.2 Spectroscopic data for isolated compounds.

**Methylvernolide (13)**: colorless amorphous solid;  $[\alpha]_D + 150.0$  (c 0.10, CHCl<sub>3</sub>); <sup>1</sup>H NMR (CDCl<sub>3</sub>, 700 MHz):  $\delta$  6.38 (1H, d,  $J = 2.6$  Hz, H-13a), 6.16 (1H, bd, H-4'a), 5.99 (1H, d,  $J = 2.6$  Hz, H-13b), 5.73 (1H, bd, H-4'b), 5.73 (1H, overlapped, H-8), 5.59 (1H, d,  $J = 7.7$  Hz, H-5), 5.25 (1H, t,  $J = 10.0$  Hz, H-6), 4.62 (1H, d,  $J = 14.2$  Hz, H-15a), 4.56 (1H, s, H-14), 3.91 (3H, s, OCH<sub>3</sub>-14), 3.69 (1H, d,  $J = 14.2$  Hz, H-15b), 3.09 (1H, m, H-7), 2.72 (1H, dd,  $J = 11.3, 3.99$  Hz, H-1), 2.67 (1H, d,  $J = 14.5$  Hz, H-9a), 2.42 (2H, m, H<sub>2</sub>-3), 2.32 (1H, m, H-2a), 1.98 (3H, s, H-3'), 1.69 (1H, m, H-2b), 1.42 (1H, dd,  $J = 14.5, 10.7$  Hz, H-9b); <sup>13</sup>C NMR (CDCl<sub>3</sub>, 175 MHz):  $\delta$  169.4 (C-12), 167.2 (C-1'), 143.7 (C-4), 135.7 (C-2'), 134.9 (C-11), 128.8 (C-5), 127.2 (C-4'), 126.1 (C-13), 99.2 (C-14), 77.4 (C-6), 70.7 (C-8), 66.4 (C-1), 64.3 (C-15), 58.8 (C-10), 55.2 (OCH<sub>3</sub>-14) 51.9 (C-7), 41.3 (C-9), 33.4 (C-3), 22.7 (C-2), 18.3 (C-3'). (+) ESI-MS  $m/z$  399 [M + Na]<sup>+</sup>. HR-ESIMS:  $m/z$  399.1428, calcd. for C<sub>20</sub>H<sub>24</sub>NaO<sub>7</sub> 399.1420.

**Deoxyvernodalol (14)**: colorless amorphous solid;  $[\alpha]_D + 102.7$  (c 0.10, CHCl<sub>3</sub>); <sup>1</sup>H NMR (CDCl<sub>3</sub>, 700 MHz):  $\delta$  6.65 (1H, bs, H-15a), 6.34 (1H, bs, H-13a), 6.01 (1H, bs, H-15b), 5.76 (1H, bs, H-13b), 5.73 (1H, bs, H-4'a), 5.69 (1H, dd,  $J = 18.1, 11.6$  Hz, H-1), 5.53 (1H, bs, H-4'b), 5.31 (1H, ddd,  $J = 11.63, 4.8, 4.8$  Hz, H-8), 5.25 (1H, dd,  $J = 18.1, 1.0$  Hz, H-2a), 5.23 (1H, dd,  $J = 11.6, 1.0$  Hz, H-2b), 4.69 (1H, d,  $J = 12.2$  Hz, H-14a), 4.35 (1H, d,  $J = 12.2$  Hz, H-14b), 4.11 (1H, dd,  $J = 11.3, 10.4$  Hz, H-6), 3.77 (3H, s, OCH<sub>3</sub>-12), 2.74 (1H, t,  $J = 11.3$  Hz, H-7), 2.50 (1H, bd,  $J = 10.4$  Hz, H-5), 1.86 (3H, s, H-3'), 1.50 (1H, m, H-9a), 1.30 (1H, m, H-9b); <sup>13</sup>C NMR (CDCl<sub>3</sub>, 175 MHz):  $\delta$  169.6 (C-12), 167.4 (C-1'), 166.6 (C-3), 144.6 (C-1), 144.4 (C-2'), 141.5 (C-11), 136.4 (C-15), 135.3 (C-4), 130.7 (C-13), 126.4 (C-4'), 117.7 (C-2), 73.5 (C-14), 72.6 (C-8), 71.5 (C-6), 57.0 (C-7), 54.1 (OCH<sub>3</sub>-12), 54.0 (C-5), 42.5 (C-10), 40.7 (C-9), 18.2 (C-3'). (+) ESI-MS  $m/z$  399 [M + Na]<sup>+</sup>. HR-ESIMS:  $m/z$  399.1413, calcd. for C<sub>20</sub>H<sub>24</sub>NaO<sub>7</sub> 399.1420.

**Vernomygdalin (15)**: Colorless amorphous solid;  $[\alpha]_D + 6.5$  (c 0.10, CHCl<sub>3</sub>); <sup>1</sup>H NMR (CDCl<sub>3</sub>, 700 MHz):  $\delta$  6.75 (1H, bs, H-15a), 5.96 (1H, bs, H-15b), 5.72

(1H, m, H-1), 5.29 (1H, overlapped, H-2a), 5.26 (1H, overlapped, H-2b), 4.42 (1H, d,  $J = 11.6$  Hz, H-14a), 4.24 (1H, d,  $J = 11.6$  Hz, H-14b), 3.95 (1H, overlapped, H-8), 3.93 (1H, overlapped, H-6), 2.87 (1H, d,  $J = 12.1$  Hz, H-5), 2.61 (1H, m, H-11), 1.97 (1H, dd,  $J = 14.0, 4.8$  Hz, H-9a), 1.86 (1H, m, H-7), 1.64 (1H, dd,  $J = 14.0, 4.8$  Hz, H-9b), 1.46 (3H, d,  $J = 5.3$  Hz, H-13) ppm;  $^{13}\text{C}$  NMR ( $\text{CDCl}_3$ , 175 MHz):  $\delta$   $^{13}\text{C}$  NMR ( $\text{CDCl}_3$ , 175 MHz):  $\delta$  177.7 (C-12), 163.4 (C-3), 140.2 (C-1), 136.0 (C-15), 130.5 (C-4), 116.6 (C-2), 81.7 (C-6), 71.4 (C-14), 68.8 (C-8), 56.9 (C-7), 46.6 (C-5), 43.2 (C-9), 42.1 (C-10), 41.6 (C-11), 14.1 (C-13) ppm. (+) ESI-MS  $m/z$  301  $[\text{M} + \text{Na}]^+$ . HR-ESIMS:  $m/z$  301.1060, calcd. for  $\text{C}_{15}\text{H}_{18}\text{NaO}_5$  301.1052.

#### 4.4.3 Cysteamine assay

In a standard 5 mm NMR tube (Armar Chemicals), vernolide (**8**) or vernodalol (**9**) (ca. 5 mg) was dissolved in 500  $\mu\text{L}$  DMSO- $d_6$ , and the spectrum was registered. Cysteamine (1.2 mol. equivalents) was next added, and the spectrum was re-registered ten minutes after the addition. A positive assay was evidenced by the disappearance of the carbonyl conjugated double bond signals of the substrate. Comparative experiments of reactivity were carried out by treating roughly equimolar amounts of vernolide (**8**) and vernodalol (**9**) with a stoichiometric amount of cysteamine (1.0 equivalent) calculated on a single reactive site in only one of the two substrates.

$^1\text{H}$  NMR assignment of vernolide (DMSO- $d_6$ ):  $\delta$  6.06 (2H, bs,  $\text{H}_a$ -13,  $\text{H}_a$ -19), 5.75 (1H, bs,  $\text{H}_b$ -19), 5.72 (1H, ovl, H-8), 5.59 (1H, ovl, H-5), 5.58 (1H, bs,  $\text{H}_b$ -13), 5.33 (1H, t,  $J=9.00$  Hz, H-6), 4.54 (1H, bs, H-14), 4.50 (1H, d,  $J=13.67$  Hz,  $\text{H}_a$ -15), 3.66 (1H, d,  $J=13.67$  Hz,  $\text{H}_b$ -15), 3.22 (1H, m, H-7), 2.89 (1H, dd,  $J=11.30-4.00$  Hz, H-1), 2.57 (1H, d,  $J=13.68$  Hz,  $\text{H}_a$ -9), 2.34 (1H, m ovl,  $\text{H}_a$ -3), 2.30 (1H, m ovl,  $\text{H}_b$ -3), 2.18 (1H, m,  $\text{H}_a$ -2), 1.88 (3H, s, H-18), 1.73 (1H, m,  $\text{H}_b$ -2), 1.34 (1H, dd,  $J=13.68-10.00$  Hz,  $\text{H}_b$ -9) ppm.

$^1\text{H}$  NMR assignment of vernodalol (DMSO- $d_6$ ):  $\delta$  6.36 (1H, s,  $\text{H}_a$ -15), 6.22 (1H, s,  $\text{H}_a$ -13), 6.00 (1H, s,  $\text{H}_a$ -4'), 5.95 (1H, s,  $\text{H}_b$ -13), 5.78 (1H, s,  $\text{H}_b$ -4'), 5.73 (1H, ovl, H-1), 5.68 (1H, s,  $\text{H}_b$ -15), 5.18 (1H, ovl,  $\text{H}_a$ -2), 5.12 (1H, ovl,  $\text{H}_b$ -2), 5.04 (1H, m, H-8), 4.75 (1H, d,  $J=12.06$  Hz,  $\text{H}_a$ -14), 4.34 (1H, d,  $J=12.06$  Hz,  $\text{H}_b$ -14), 4.03 (2H, ovl, H-3'), 3.80 (1H, dd,  $J=11.00-10.38$  Hz, H-6), 3.67 (3H, s, H-20),

2.81 (1H, dd,  $J=11.00-10.38$  Hz, H-7), 2.54 (1H, d,  $J=10.38$ , H-5), 1.87 (1H, bd,  $J=14.06$  Hz, H<sub>a</sub>-9), 1.55 (1H, dd,  $J=14.06-12.35$  Hz, H<sub>b</sub>-9) ppm.

#### **4.4.4 Cytotoxicity assays**

DU145 cells were seeded at a density of  $10^4$  cells/well in 96-well plates (200  $\mu$ L) and incubated with increasing concentrations of the compounds for 48 hours. After that, 100  $\mu$ L of MTT (5 mg/ml) from a mixture solution of MTT: DMEM (1:2) was added to each well, and cells were incubated for 4 h at 37 °C in darkness. Then the reaction was stopped, supernatant removed and 100  $\mu$ L of DMSO added to each well and incubated for 10 min in gentle shaking. Finally, the absorbance was measured at 550 nm using a TriStar LB 941 (Berthold Technologies, GmbH & Co. KG). The absorbance of untreated cells was taken as 100% viability and the percentage of cellular viability calculated.

#### **4.4.5 Transcriptional assays**

Anti-NF- $\kappa$ B activity was investigated in 5.1 cells, a validated “in vitro” model to study TNF $\alpha$ -induced NF- $\kappa$ B activation.<sup>29</sup> 5.1 cells were stimulated with TNF $\alpha$  (20 ng/mL) in the presence or absence of the compounds for 6 h. To study the activity of the compounds on the Nrf2 pathway we used the HaCaT-ARE-Luc cell line.<sup>30</sup> Cells were stimulated with the compounds for 6 h. To study STAT3 signaling, LNCaP cells were transiently transfected with the pTATA-TK-Luc plasmid that contains four copies of the STAT-binding site. Transient transfections were performed with Rotifect (Carl Roth GmbH, Karlsruhe, Germany) according to the manufacturer’s instructions, and 24 h after transfection, cells were pre-incubated with increasing concentrations of the compounds and then treated with INF $\gamma$  (10 ng/mL) for another 12 h. After stimulation, cells were washed twice with PBS and lysed in 25 mM Tris-phosphate pH 7.8, 8 mM MgCl<sub>2</sub>, 1 mM DTT, 1% Triton X-100 and 7% glycerol for 15 min at room temperature in a horizontal shaker. Following centrifugation, the supernatant was used to measure luciferase activity using an Autolumat LB 9510 (Berthold) following the instructions of the luciferase assay kit (Promega, Madison, WI, USA).

#### 4.4.6 Cell cycle analysis

The percentage of cells in each phase of the cell cycle was determined by flow cytometry. Briefly DU145 cells were collected after treatments, washed twice with PBS, and fixed with ethanol (70%, for 24 h at 4 °C). Then the cells were washed trice with PBS containing 4% glucose, subjected to RNA digestion (RNase A, 50 units/ml) and propidium iodide (20 µg/mL) staining in PBS for 1 h at room temperature, and analyzed by flow cytometry in a FACSCanto II flow cytometer. Ten thousand gated events were collected per sample, and the percentage of cells in each phase of the cell cycle was analyzed by using BD FACSDiva™ software.

#### 4.4.7 Assessment of transmission blocking activity in vivo

The *in vivo* transmission blocking effect of *V. amygdalina* was estimated by determining oocyst prevalence and density in mosquitoes fed on extract-treated gametocytaemic mice.<sup>35</sup> Briefly, mice were inoculated with  $10^7$  *P. berghei* GFPcon-infected red blood cells (RBCs) through the intraperitoneal (i.p.) route. On day three post-infection, animals allocated to the treatment groups were treated i.p. with 500 mg/kg and 100 mg/kg (maximum tolerable dose) of Ver-H<sub>2</sub>O and Ver-EtOH., respectively, while control animals received 200 µL of the solvents used to dissolve the extracts. On day four post-infection, the treatment was repeated 1 h before the exposure of the mice to mosquitoes (day 4 gametocytes yield consistently high mosquito infections in this model). Mice were anaesthetized and kept on top of mosquito cages containing 150 to 200 *An. stephensi* females for 1 h. Unfed females were removed the following day. On day 10/11 after the blood meal, 17–34 mosquitoes from each cage were dissected. Oocyst prevalence and density were assessed by counting the number of green fluorescent oocysts on mosquito mid-guts under a fluorescence microscope (ZEISS Axio Observer Z1, FITC filter 9). Oocyst density was determined by calculating the geometric mean of the number of oocysts recorded on oocyst positive mosquitoes.<sup>61</sup>

$$\text{Geometric mean} = \text{antilog} \left[ \left( \sum_{i=1}^n \log x \right) / n \right],$$

where n= Number of oocyst positive mosquitoes, x= Oocyst number per mosquito.

The percent reduction of oocyst density in treatment groups was calculated as follows:

$$\text{Percent reduction of oocyst density} = \left( 1 - \frac{\text{average oocyst density in treated group}}{\text{average oocyst density in a control group}} \right) \times 100$$

The experiment was conducted in triplicate, using for each treatment group three mice and for each mouse one cage of mosquitoes.

## References

- <sup>1</sup> Tojang, N. J.; Verpoorte, R. J. *Ethnopharmacol.* **2013**, *146*, 681-723.
- <sup>2</sup> Stangeland *et al.* . *J Ethnopharmacol.*, **2011**, *137*, 154-166
- <sup>3</sup> Namukobe J, *et al.*. *J Ethnopharmacol*, **2011**, *136*(1), 236-45
- <sup>4</sup> Ene AC, *et al.*, *IJTK*, **2010**, *9*, 486-90
- <sup>5</sup> Asase A, *et al.*, *Journal of Ethnopharmacol*, **2005**, *99*, 273–279
- <sup>6</sup> Regassa A , *J S Afr Vet Assoc.*, **2007**, *1*(4), 240-3.
- <sup>7</sup> Kambizi L, *et al.* , *J Ethnopharmacol*, **2001**, *77*, 5-9
- <sup>8</sup> Huffman MA., *Proc Nutr Soc.*, **2003**, *62*, 371-81
- <sup>9</sup> Ebenezer O, *et al.*, *Int J Environ Res Public Health* **2011**, *8*, 2533-55
- <sup>10</sup> Grubben GJH, *et al.*, *Plant resources of tropical Africa*, **2004**. pp: 543
- <sup>11</sup> Erasto, P.; Grierson, D. S.; Afolayan, A. J. *J Ethnopharmacol.*, **2006**, *106*, 117–120.
- <sup>12</sup> Luo, X.; Jiang, Y.; Fronczek, F.; Lin, C.; Izevbigie, E.; Lee, K.; Ernest, B.; Ken, S. *Pharm Biol.*, **2011**, *49*, 464–470.
- <sup>13</sup> Kupchan, S.; Hemmnigway, R.; Karim, A.; Werner, D. *J Org Chem* **1969**, *34*, 3908–11.
- <sup>14</sup> Jisaka, M.; Ohigashi, H.; Takagaki, T.; Nozaki, H.; Tada, T.; Hirota, M.; Irie, R.; Huffman, M. A.; Nishida, T.; Kaji, M.; Koshimizu, K. *Tetrahedron* **1992**, *48*, 625–632.
- <sup>15</sup> Igile, G.O.; Oleszek, W.; Burda, S.; Jurzysta, M. *J Agric Food Chem* **1994**, *42*, 2445–8.
- <sup>16</sup> Izevbigie, E. B. *Exp. Biol. Med.* **2003**, *228*, 293-298.

- <sup>17</sup> Tojang, N. J.; Krause, M. A.; Fairhurst, R. M.; Tane, P.; Bryant, J.; Verpoorte, R. *J. Ethnopharmacol.* **2013**, *147*, 618-621.
- <sup>18</sup> Vassallo, A.; De Tommasi, N.; Merfort, I.; Sanogo, R.; Severino, L.; Pelin, M.; Della Loggia, R.; Tubaro, A.; Sosa, S. *Phytochemistry*, **2013**, *96*, 288-298.
- <sup>19</sup> Youn, U. J.; Park, E.-J.; Kondratyuk, T. P.; Simmons, C. J.; Borris, R. P.; Tanamatayarat, P.; Wongwiwatthananut, S.; Toyama, O.; Songsak, T.; Pezzuto, J. M.; Chang, L. C. *Bioorg. Med. Chem. Lett.* **2012**, *22*, 5559-5562.
- <sup>20</sup> Klein, J. B.; Nowill, A. E.; Franchi, G. C.; Biavatti, M. W.; Quintao, N. L. M.; de Freitas, R. M. *Basic Clin. Pharmacol. Toxicol.*, **2013**, *113*, 307-315.
- <sup>21</sup> Luo, X.; Oyugi, D. A.; Lin, C.; Izevbigie, E. B.; Lee, K. S. *Exper. Biol. Med.*, **2010**, *235*, 1472-1478.
- <sup>22</sup> Wong, F. C.; Woo, C. C.; Hsu, A.; Tan, B. K. H., *Plos One*, **2013**, *8*, e78021.
- <sup>23</sup> Kayser, O.; Kiderlen, A. F.; Croft, S. L.; *Parasitology research*, Vol. 90, Supplement 2, S55-S62.
- <sup>24</sup> World Health Organization: *World Malaria Report 2011*. **2011**.
- <sup>25</sup> World Health Organization: *Fact Sheet No. 94*. **2014**.
- <sup>26</sup> Arav-Boger, R.; Shapiro, T. A.; *Annu Rev Pharmacol Toxicol.*, **2005**, *45*, 565-585.
- <sup>27</sup> Okell LC, Drakeley CJ, Ghani AC, Bousema T, Sutherland C, *Malar J*, **2008**, *7*,125.
- <sup>28</sup> White NJ, *Lancet Infect Dis* **2013**, *13*,175–81.
- <sup>29</sup> Abay S, *Parasit Vectors* **2013**, *6*, 278.
- <sup>30</sup> Wilairatana P, Krudsood S, Tangpukdee N, *Korean J Parasitol*, **2010**, *48*,179-82.

- <sup>31</sup> World Health Organization: *Updated WHO Policy Recommendation (October 2012 ) Single Dose Primaquine as a Gametocytocide in Plasmodium Falciparum Malaria*. **2012** (October).
- <sup>32</sup> Eziefula A, Gosling R, Hwang J, Hsiang M, Bousema T, von Seidlein L, Drakeley C, Primaquine in Africa Discussion Group, *Malar J*, **2012**, *11*,360.
- <sup>33</sup> Willcox M, *Planta Med*, **2011**, *77*,662–671.
- <sup>34</sup> Ukrittayakamee S, Chotivanich K, Clemens R, Looareesuwan S, White NJ, Chantra A, *Antimicrob Agents Chemother*, **2004**, *48*, 1329–1334.
- <sup>35</sup> Lucantoni L, Yerbanga RS, Lupidi G, Pasqualini L, Esposito F, Habluetzel A, *Malar J*, **2010**, *9*, 66.
- <sup>36</sup> Kleeberg H., *Neem Today millenium*. Edited by Koul O, Wahab S. New York: Kluwater Academic Publishers; **2004**,114.
- <sup>37</sup> Jones IW, Denholm a a, Ley S V, Lovell H, Wood A, Sinden RE, *FEMS microbiol Lett Lett*, **1994**, *120*, 267–73.
- <sup>38</sup> Yerbanga R, Lucantoni L, Ouédraogo R, DF D, Yaméogo K, Churcher T, Lupidi G, Gouagna L, Cohuet A, Christophidus G, Ouédraogo J, Habluetzel A, *Parasit Vectors*, **2014**, *7*, 185.
- <sup>39</sup> Toyang N, Verpoorte R., *J Ethnopharmacol*, **2013**, *146*, 681–723.
- <sup>40</sup> a) Masaba SC., *Trans R Soc Trop Med Hyg*, **2000**, *94*, 694–5; b) Omoregie ES, Pal A, Darokar MP, Chanda D, Sisodia B, *Malar J* , **2010**, *9*(Suppl 2), P30.
- <sup>41</sup> Erasto P, Grierson DS, Afolayan AJ., *J Ethnopharmacol*, **2006**, *106*, 117–120.
- <sup>42</sup> Luo X, Jiang Y, Fronczek F, Lin C, Izevbigie E, Lee K, Ernest B, Ken S., *Pharm Biol*, **2011**, *49*, 464–470.
- <sup>43</sup> Owoeye O, Yousuf S, Akhtar M, Qamar K, Dar A, Farombi E, Onwuka S, Choudhary M., *Int J Biol Chem Sci*, **2010**, *4*, 226–34.
- <sup>44</sup> Kupchan S, Hemmnigway R, Karim A, Werner D., *J Org Chem*, **1969**, *34*, 3908–11.

- 
- <sup>45</sup> Laekeman GM, Mertens J, Totté J, Bult H, Vlietinck a J, Herman a G., *J Nat Prod*, **1983**, *46*, 161–9.
- <sup>46</sup> Chukwujekwu JC, Lategan C a., Smith PJ, Van Heerden FR, Van Staden J., *S Afr J Bot*, **2009**, *75*, 176–179.
- <sup>47</sup> Ohigashi H, Huffman AM, Izutsu D, Koshimizu K, Kawanaka M, Sugiyama H, Kirby CG, Warhurst CD, Allen D, Wright WC, J. David Phillipson, Timon-David P, Delmas F, Elias R, Balansard YG., *J Chem Ecol*, **1994**, *20*, 541– 553.
- <sup>48</sup> Mehra N, Bhasin V., *Jpn J Med Sci Biol*, **1993**, *46*, 37 – 43.
- <sup>49</sup> Bousema T, Okell L, Shekalaghe S, Griffin JT, Omar S, Sawa P, Sutherland C, Sauerwein R, Ghani AC, Drakeley C., *Malar J*, **2010**, *9*, 136.
- <sup>50</sup> Baker D., *Mol Biochem parasitol*, **2010**, *172*, 57–65.
- <sup>51</sup> Avonto, C.; Tagliatela-Scafati, O.; Pollastro, F.; Minassi, A.; Di Marzo, V.; De Petrocellis, L.; Appendino, G. *Angew. Chem. Intl. Edit.*, **2011**, *50*, 467-471.
- <sup>52</sup> Rabe, T.; Mullholland, D.; Van Staden, J. *J. Ethnopharmacol.*, **2002**, *80*, 91-94.
- <sup>53</sup> Ho, C. M.; Toubiana, R. *Tetrahedron* **1970**, *26*, 941-948.
- <sup>54</sup> Jakupovic, J.; Baruah, R. N.; Chau Thi, T. V.; Bohlmann, F.; Msonthi, J. D.; Schmeda-Hirschmann, G. *Planta Med.* **1985**, *51*, 378-380.
- <sup>55</sup> Tagliatela-Scafati, O.; Pollastro, F.; Minassi, A.; Chianese, G.; De Petrocellis, L.; Di Marzo, V.; Appendino, G. *Eur. J. Org. Chem.* **2012**, 5162-5170.
- <sup>56</sup> Itoh, T.; Fairall, L.; Amin, K.; Inaba, Y.; Szanto, A.; Balint, B. L.; Nagy, L.; Yamamoto, K.; Schwabe, J. W. R. *Nat. Struct. Mol. Biol.* **2008**, *15*, 924-931.
- <sup>57</sup> Minassi, A.; Sanchez-Duffhues, G.; Collado, J. A.; Munoz, E.; Appendino, G. *J. Nat. Prod.* **2013**, *76*, 1105-1112.
- <sup>58</sup> Kundu, J. K.; Surh, Y.-J. *Free Rad. Biol. Med.* **2012**, *52*, 2013-2037.
- <sup>59</sup> Carmi, C.; Mor, M.; Petronini, P. G.; Alfieri, R. R.; *Biochem. Pharmacol.* **2012**, *84*, 1388-1399.

<sup>60</sup> Muñoz, E.; Blázquez, M.V.; Ortiz, C.; Gomez-Díaz, C.; Navas, P. *Biochem J.* **1997**, *325*, 23-28.

<sup>61</sup> Jarvis B., *Statistical Aspects of the Microbiological Examinations of Foods*. 2nd edition. Amsterdam: Elsevier; **2008**, 8.

## CHAPTER 5 -CONCLUSIONS

---

With over 60% of drugs on the market of natural origin or inspired by natural compounds, the investigation of natural products can be considered as the foundation of the pharmaceutical industry. This PhD thesis was focused on the investigation of bioactive secondary metabolites from different natural sources (terrestrial plants and marine sponges) and the research activity described led to the discovery of new chemistry with potential pharmaceutical and biochemical applications.

Results obtained from my research work show that natural sources (plants and marine organisms) represent, once again, a very important way to obtain molecules with important pharmacological activities.

A demonstration of the impact of natural products chemistry in the discovery of important scaffolds for the design of new drugs, is the high antiproliferative activity showed by swinholides from the sponge *Theonella swinhoei*. Similarly, complex peptide structure in theonellapeptolides is worth considering and deserves additional chemical and pharmacological investigation. To examine these aspects, a project aimed to the synthesis of these molecules is underway.

In the case of research on *Vernonia amygdalina*, the transition from traditional use of a plant as food and as remedy, to the step of phytochemical analysis, then to the isolation of pharmacologically active metabolites, to the step of drug manufacturing on industrial scale, is going to be completed. Based on the results obtained during my PhD, a project of production of a multi-stage antimalarial phytomedicine based on standardized extracts enriched in vernodalol is currently in development by University of Camerino industrial spin-off, named Pro Herbal Care.

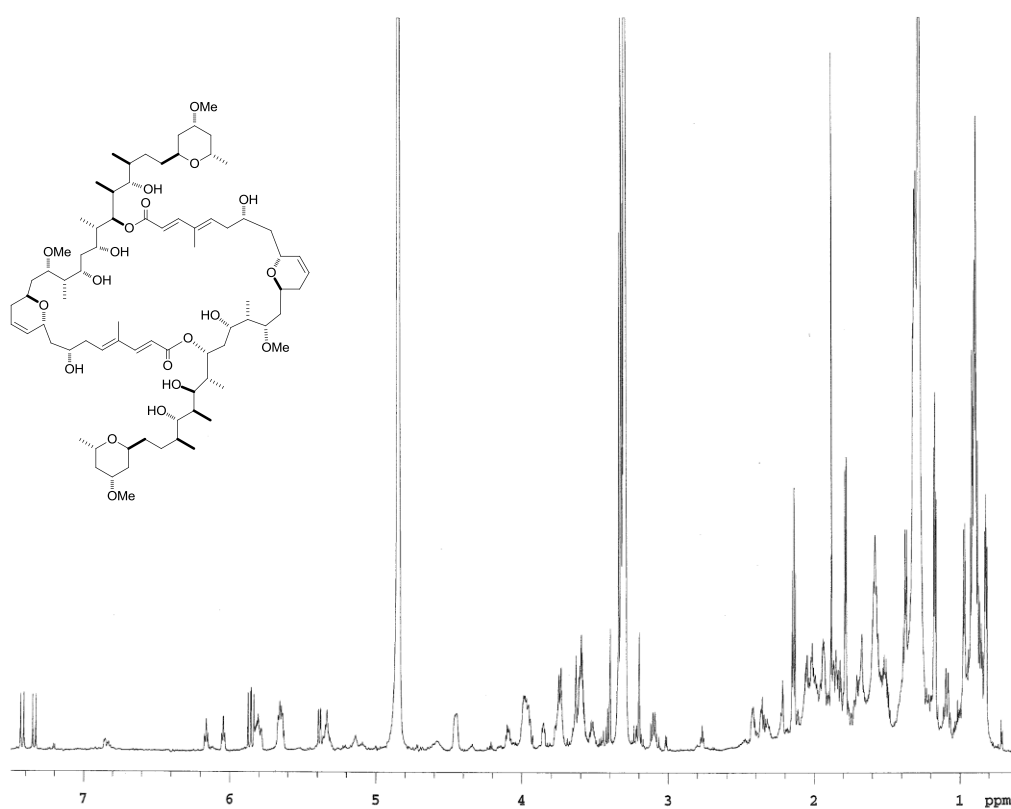
In conclusion, natural product chemistry are an old research field but they can still be considered as an expanding field of research, that holds a lot in store for the future.

## CHAPTER 6 -SPECTRAL DATA

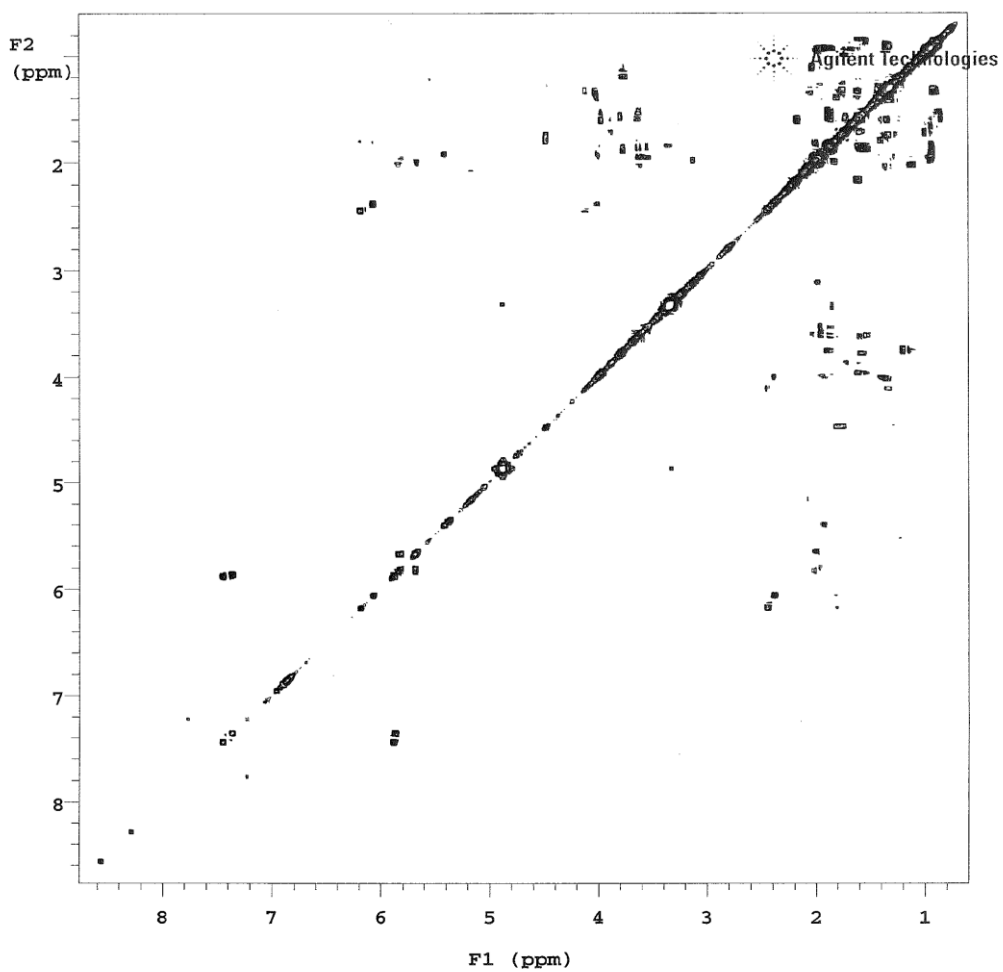
---

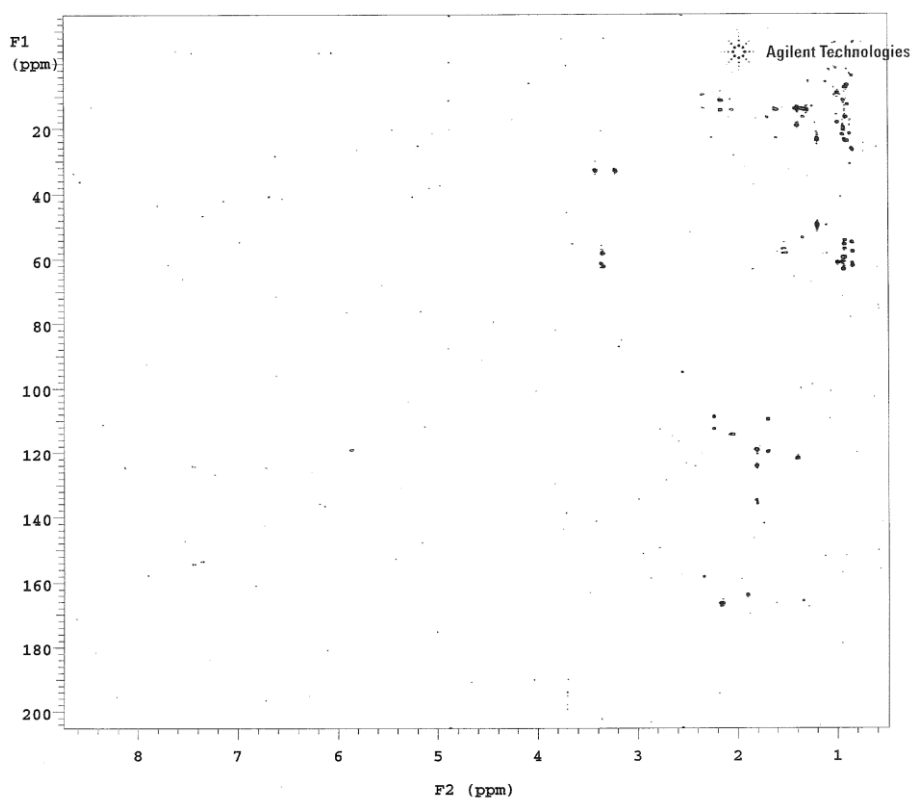
### Spectral data for CHAPTER 2

$^1\text{H}$  spectrum (700 MHz) of isoswinholide B (**5**) in  $\text{CD}_3\text{OD}$

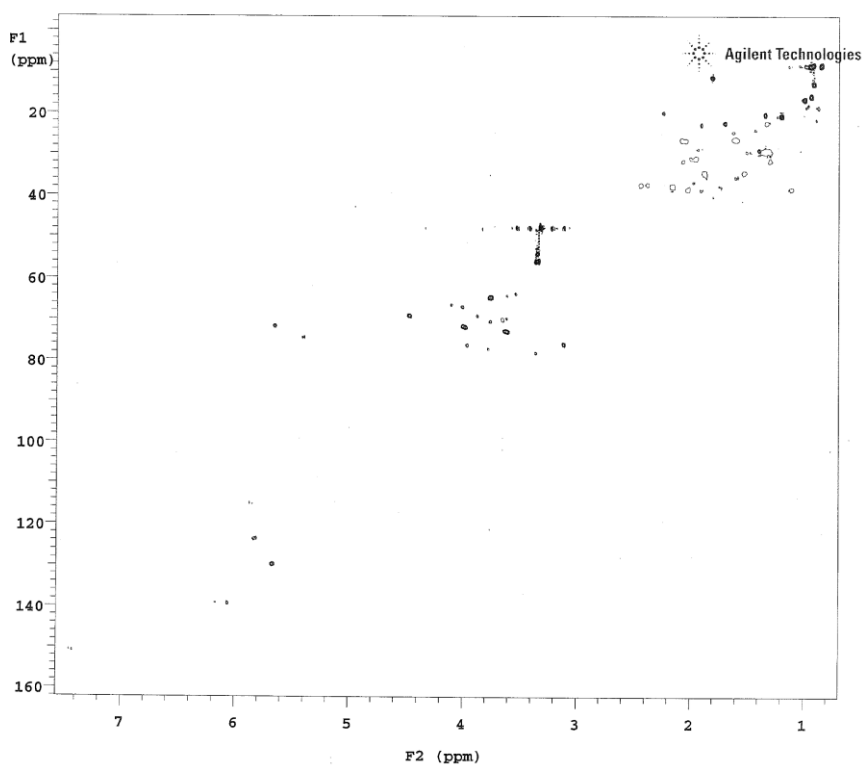


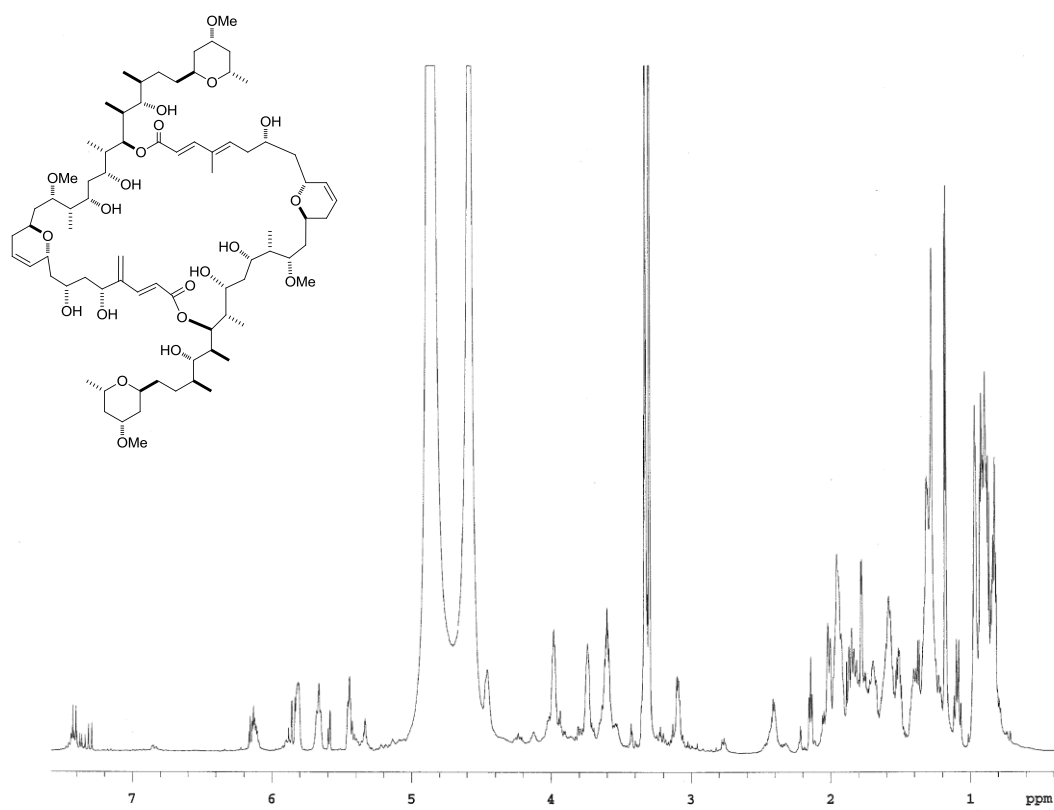
COSY spectrum (700 MHz) of isoswinholide B (5) in CD<sub>3</sub>OD

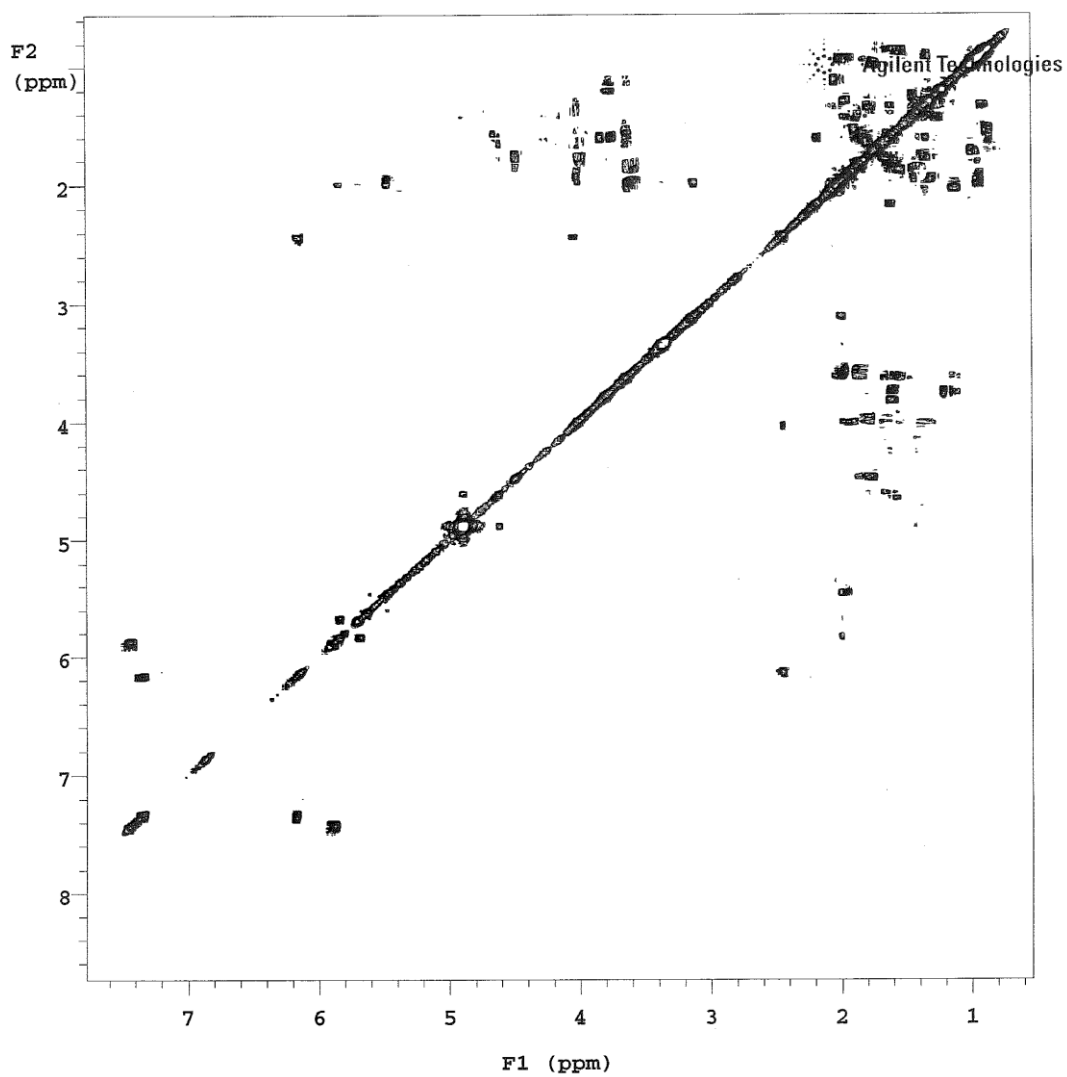


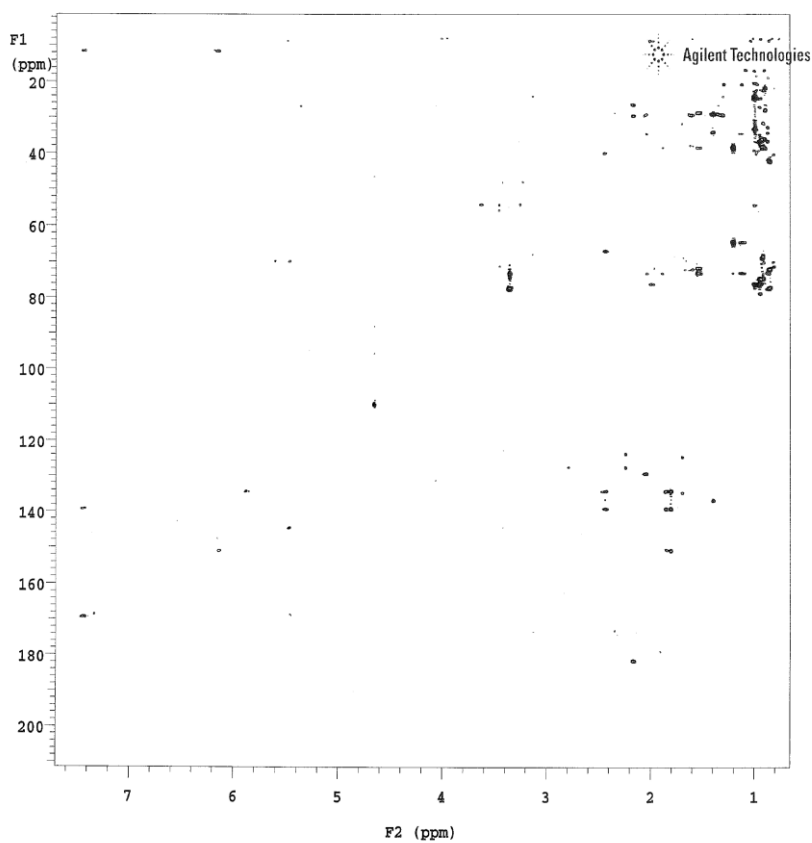
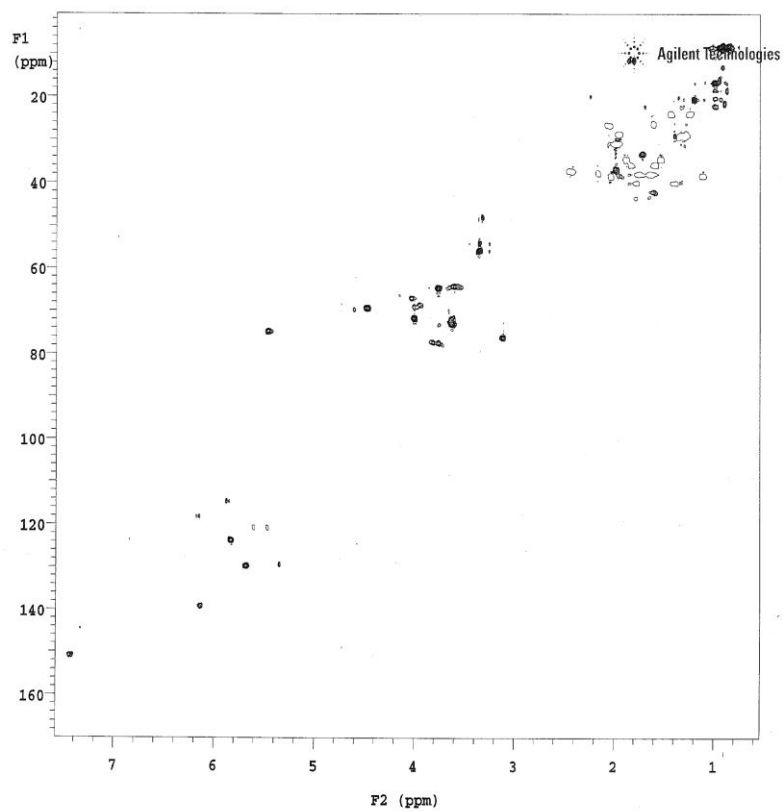
HMBC spectrum (700 MHz) of isoswinholide B (5) in CD<sub>3</sub>OD

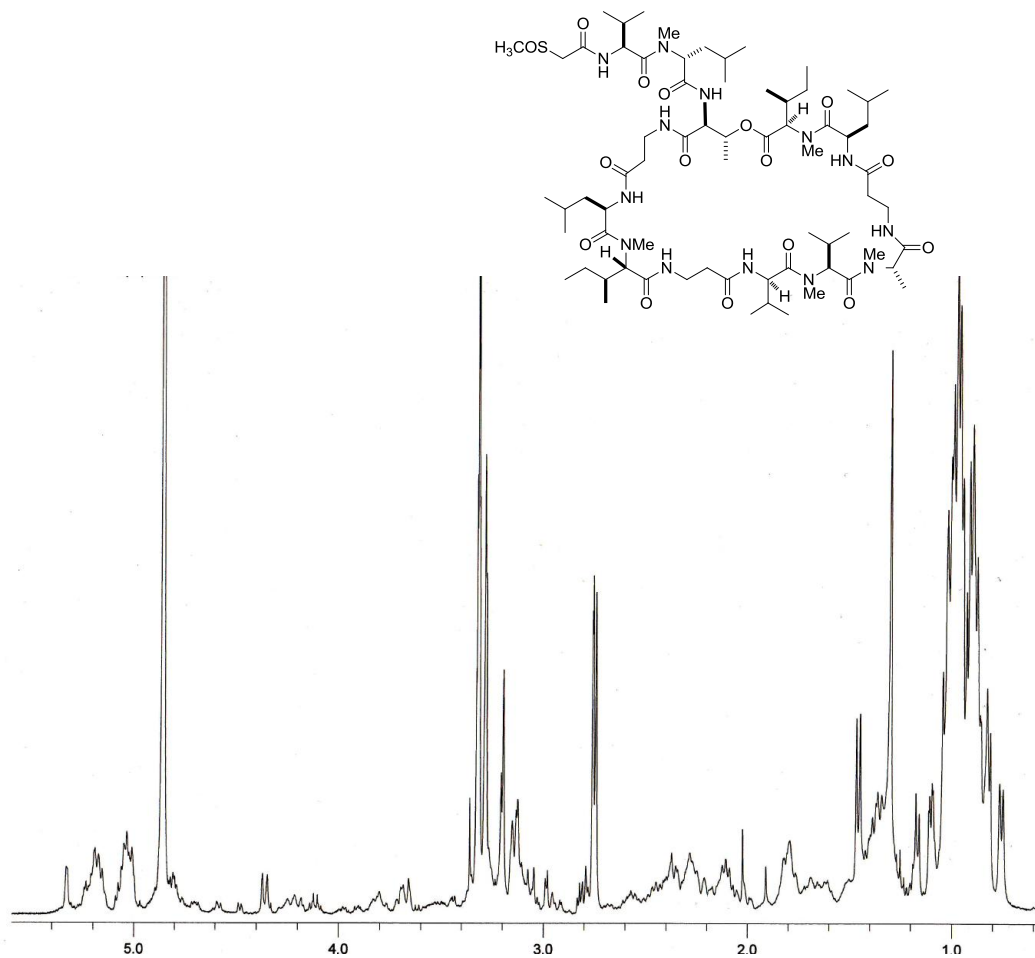
## HSQC spectrum (700 MHz) of isoswinholide B (5)

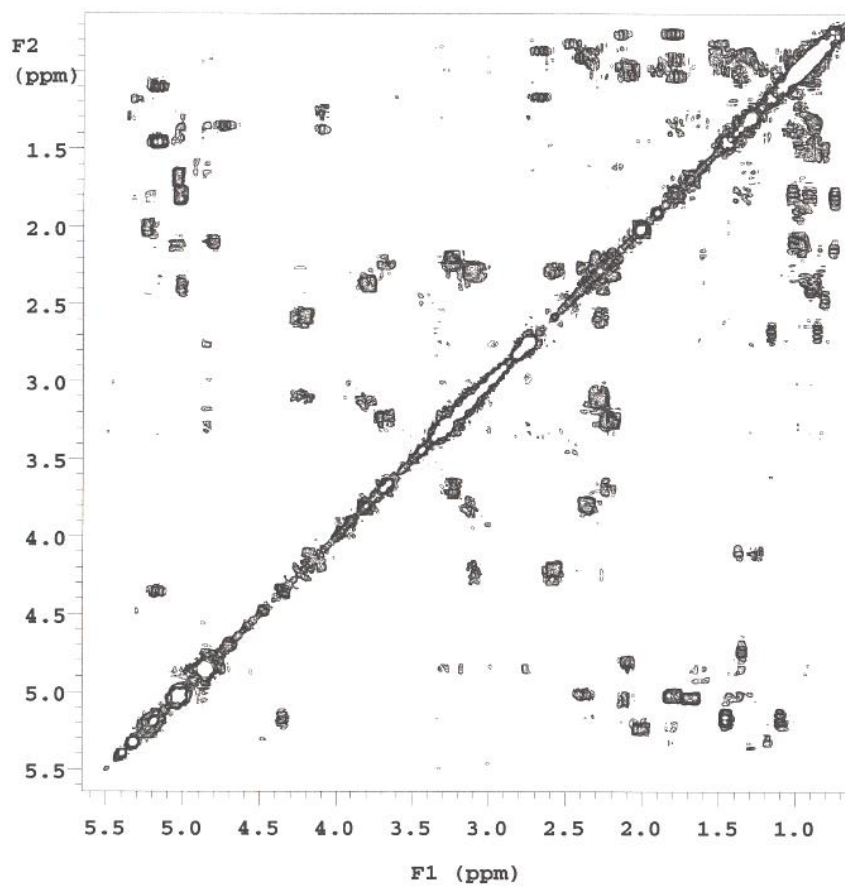


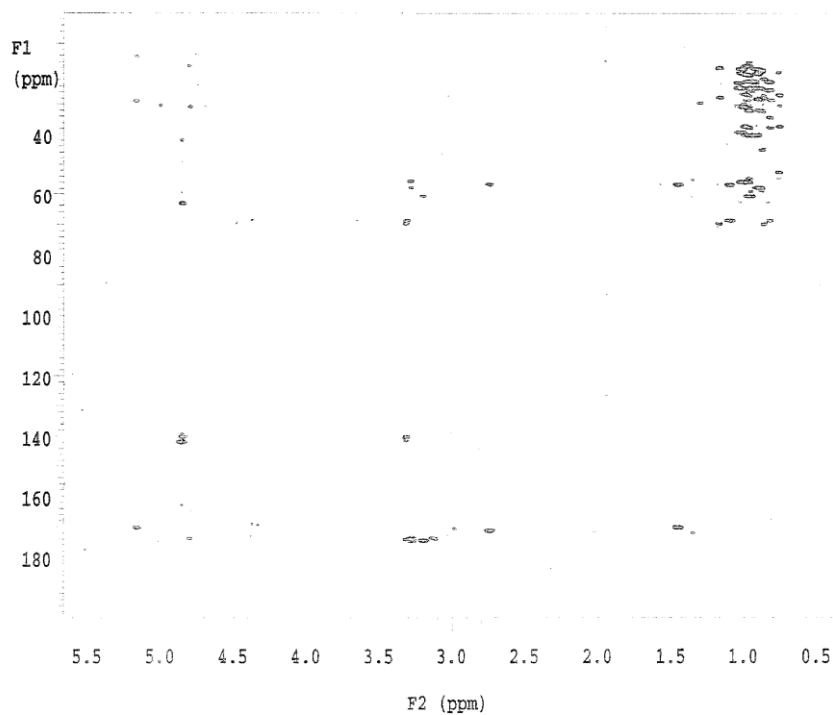
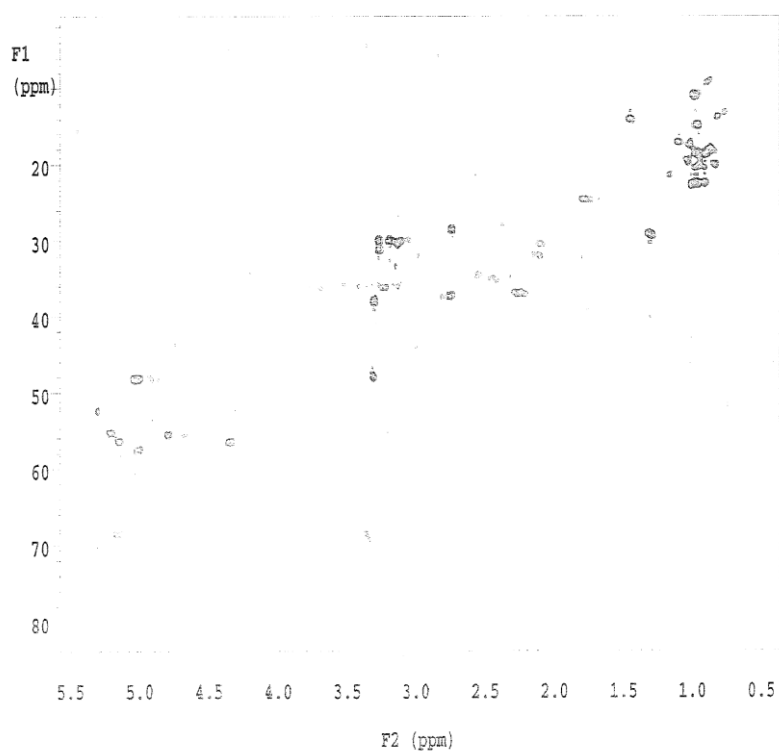
$^1\text{H}$  spectrum (700 MHz) of swinholide K (**6**) in  $\text{CD}_3\text{OD}$ 

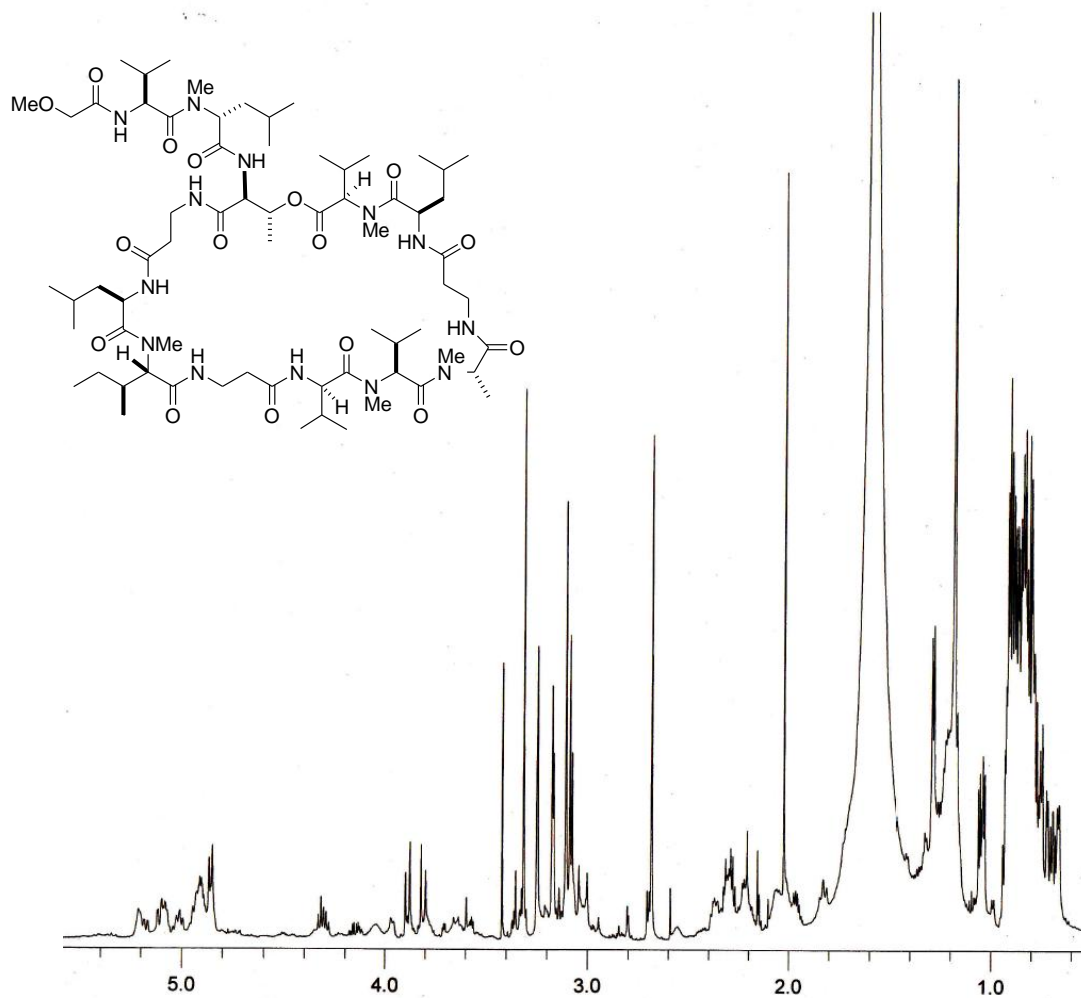
COSY spectrum (700 MHz) of swinholide K (**6**) in CD<sub>3</sub>OD

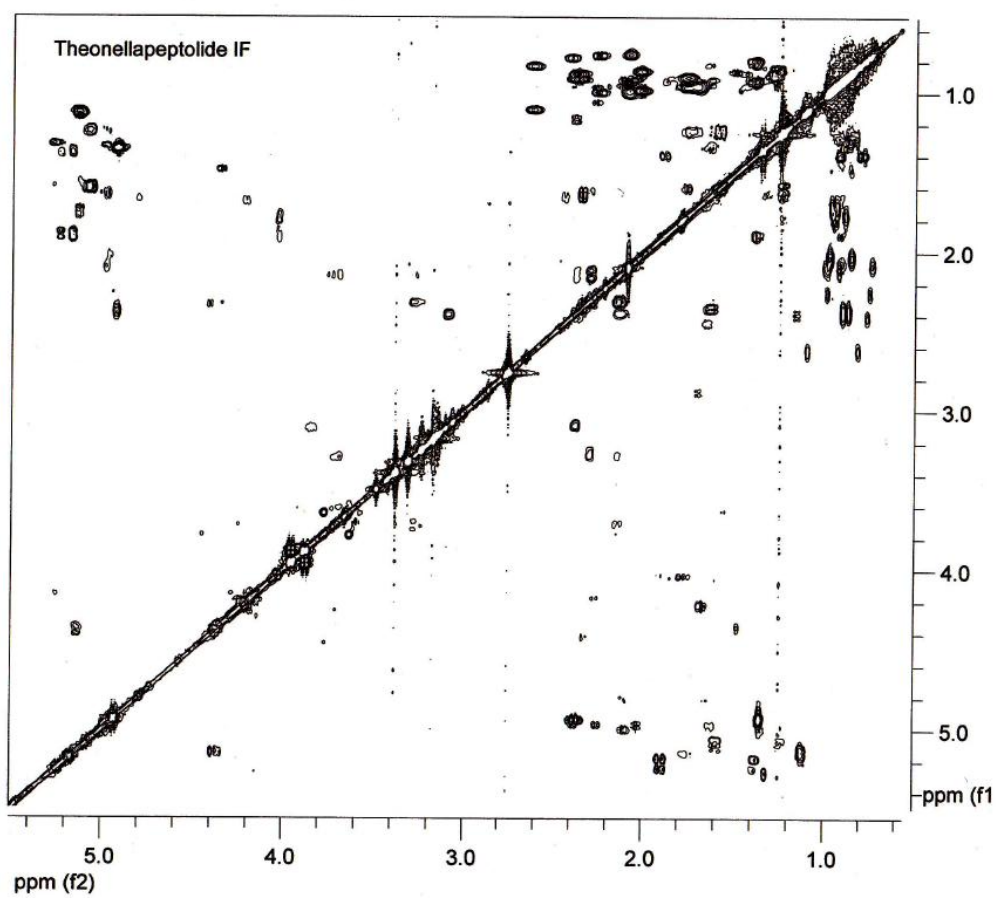
HMBC spectrum (700 MHz) of swinholide K (6) in CD<sub>3</sub>ODHSQC spectrum (700 MHz) of swinholide K (6) in CD<sub>3</sub>OD

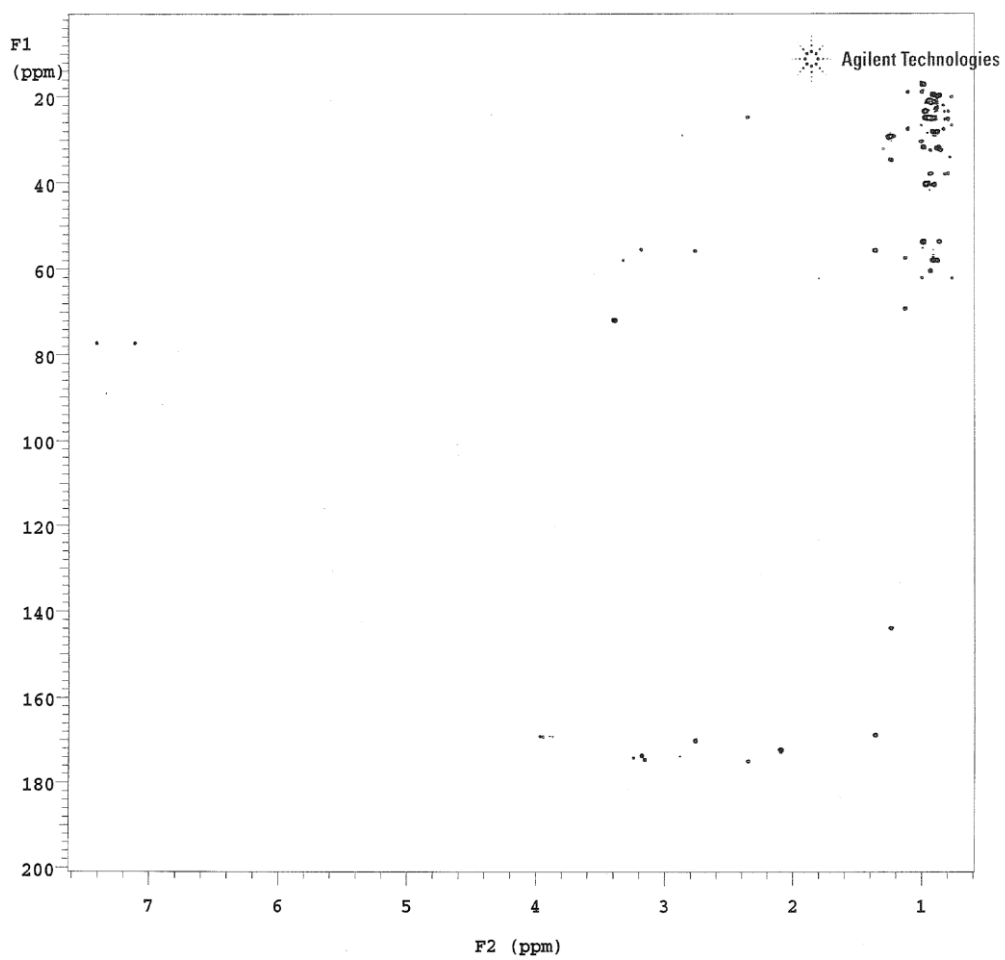
$^1\text{H}$  spectrum (500 MHz) of sulfinyltheonellapeptolide (**8**) in  $\text{CD}_3\text{OD}$ 

COSY spectrum (500 MHz) of sulfinyltheonellapeptolide (**8**) in CD<sub>3</sub>OD

HMBC spectrum (500 MHz) of sulfinyltheonellapeptolide (**8**) in CD<sub>3</sub>ODHSQC spectrum (500 MHz) of sulfinyltheonellapeptolide (**8**) in CD<sub>3</sub>OD

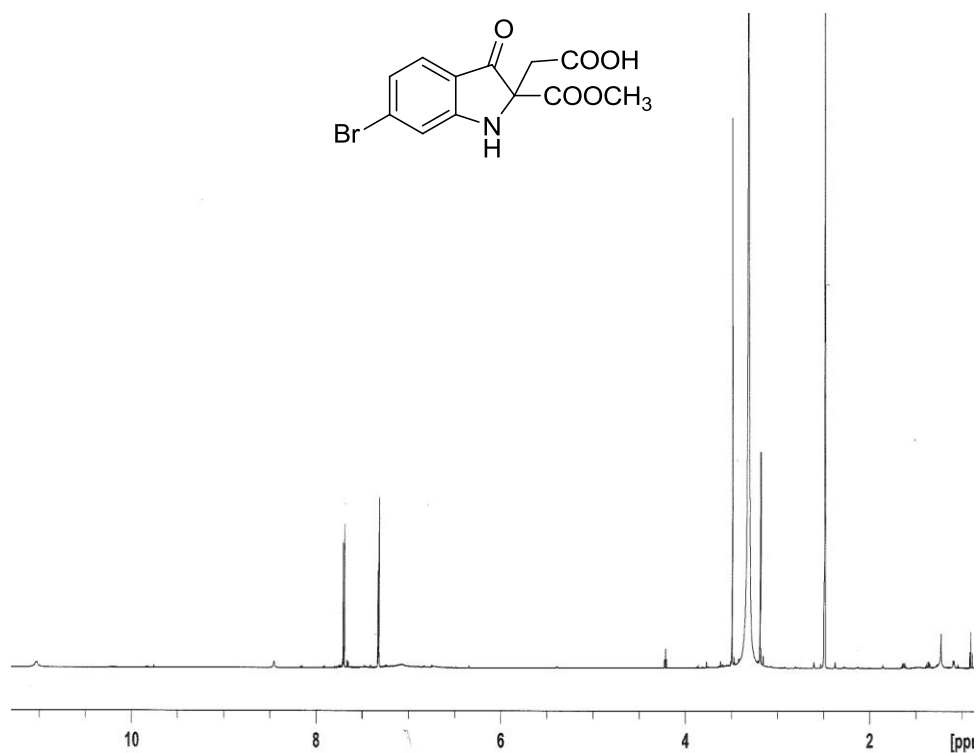
$^1\text{H}$  spectrum (500 MHz) of theonellapeptolide If (**9**) in  $\text{CD}_3\text{OD}$ 

COSY spectrum (500 MHz) of theonellapeptolide If (9) in CD<sub>3</sub>OD

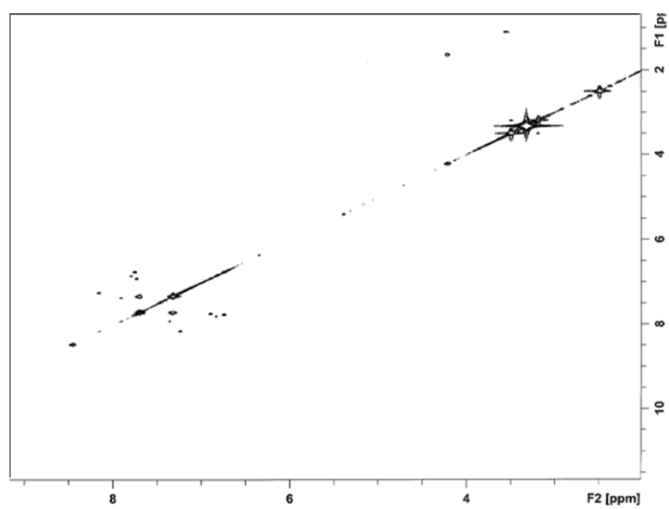
HMBC spectrum (500 MHz) of theonellapeptolide If (**9**) in CD<sub>3</sub>OD

**Spectral data for CHAPTER 3**

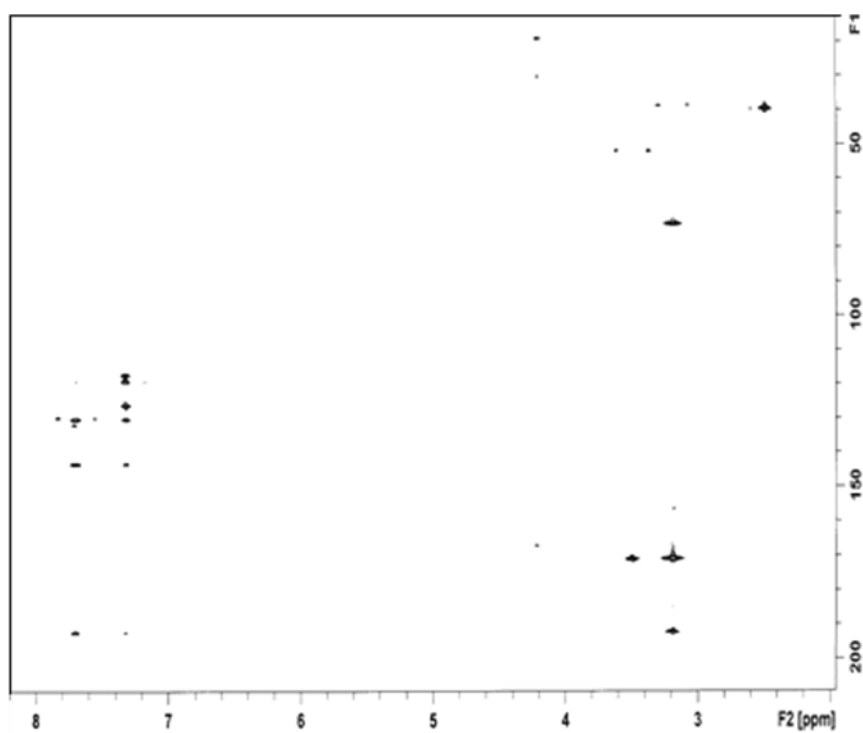
<sup>1</sup>H spectrum (600 MHz) of compound (9) in DMSO



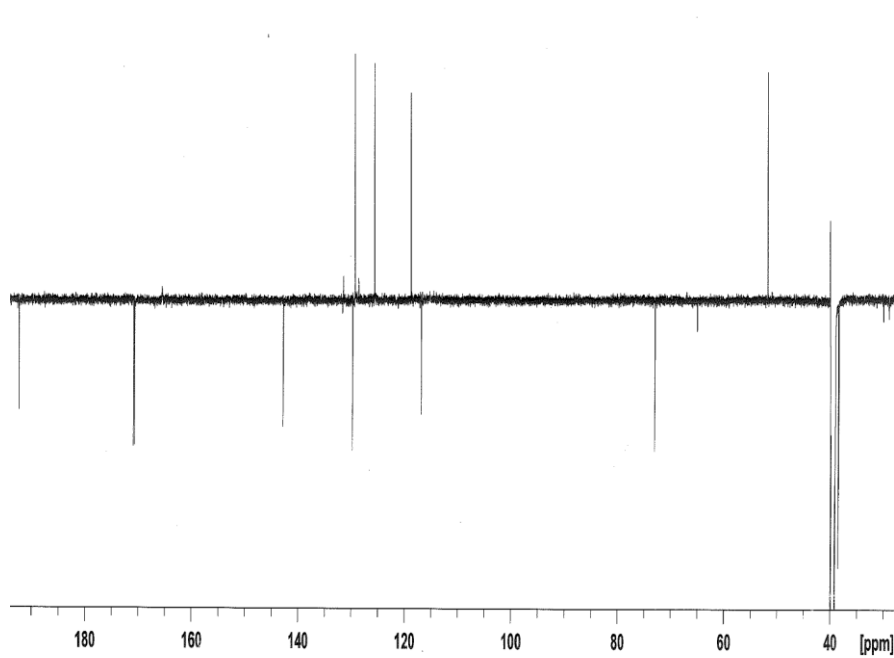
COSY spectrum (600 MHz) of compound (9) in DMSO



HMBC spectrum (600 MHz) of compound (9) in DMSO

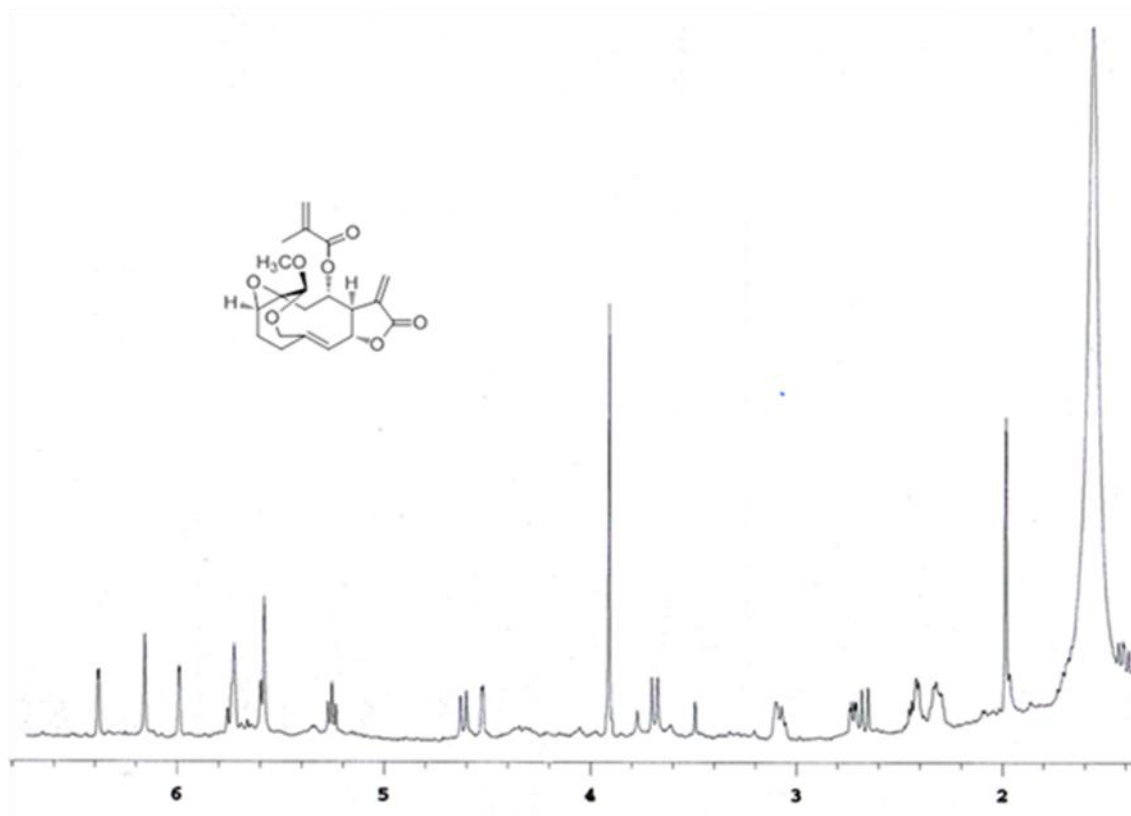


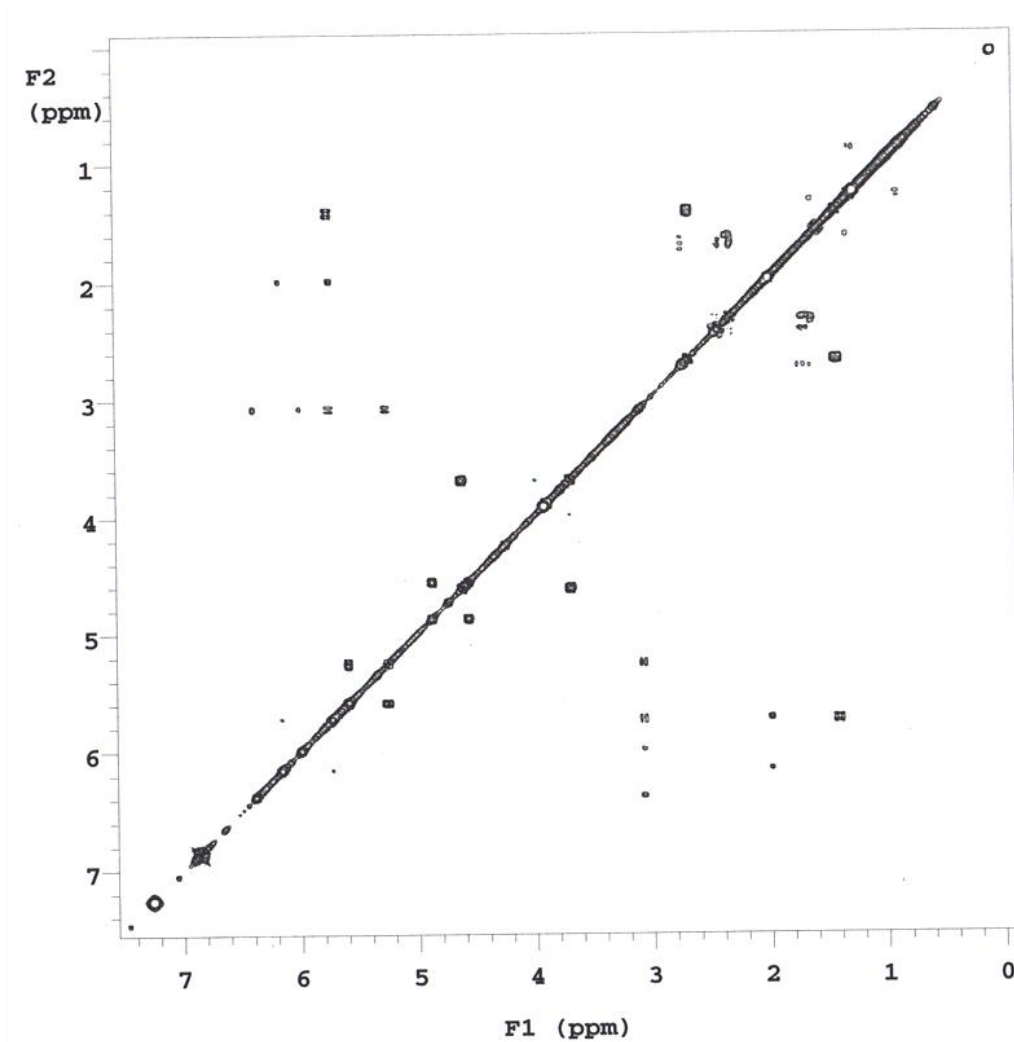
DEPT-Q spectrum (600 MHz) of compound (9) in DMSO

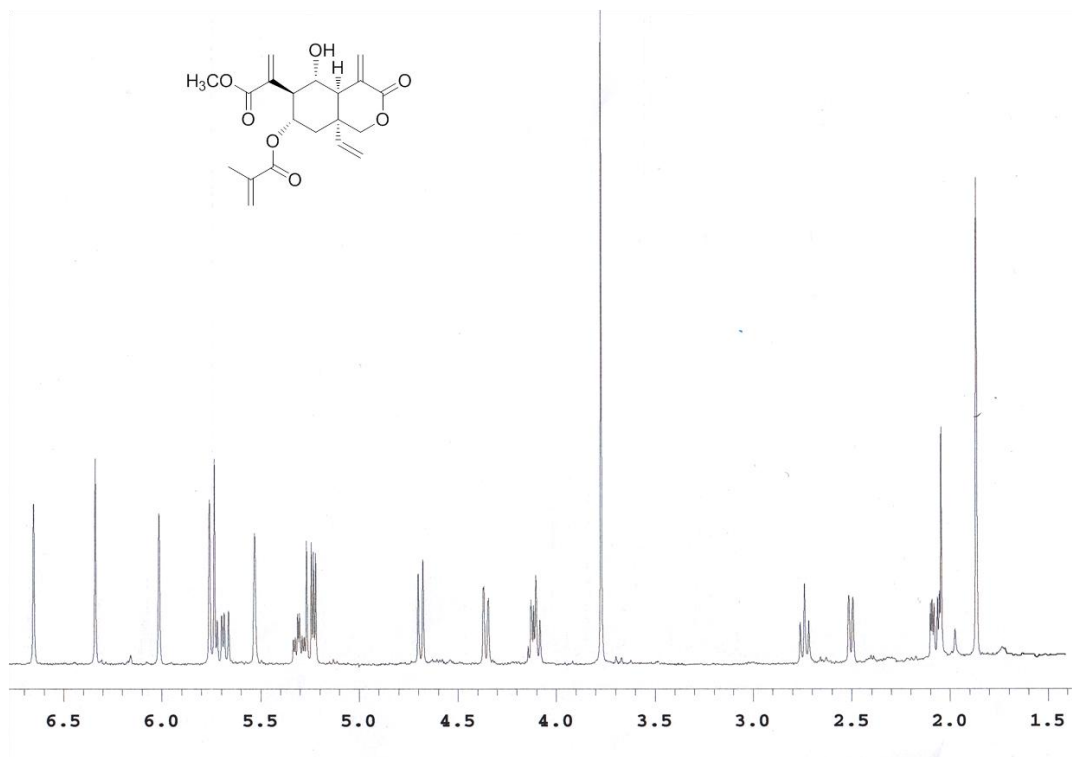


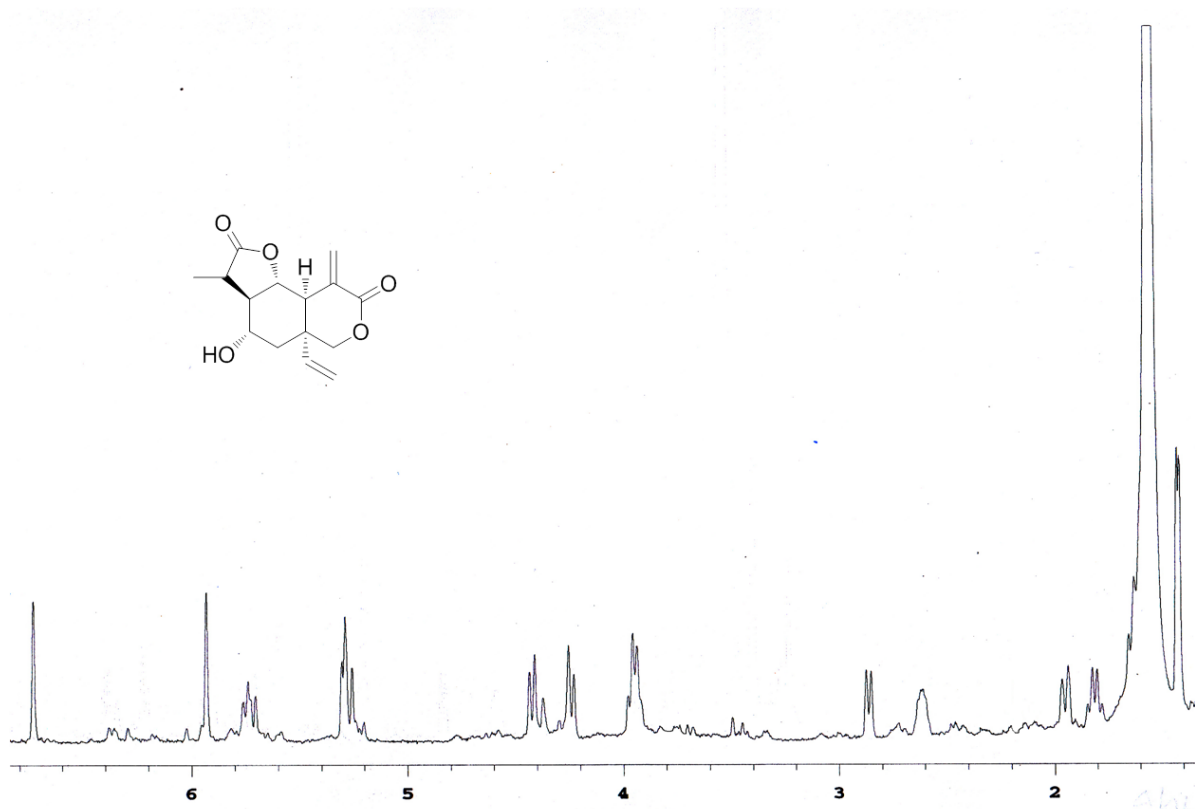
**Spectral data for CHAPTER 4**

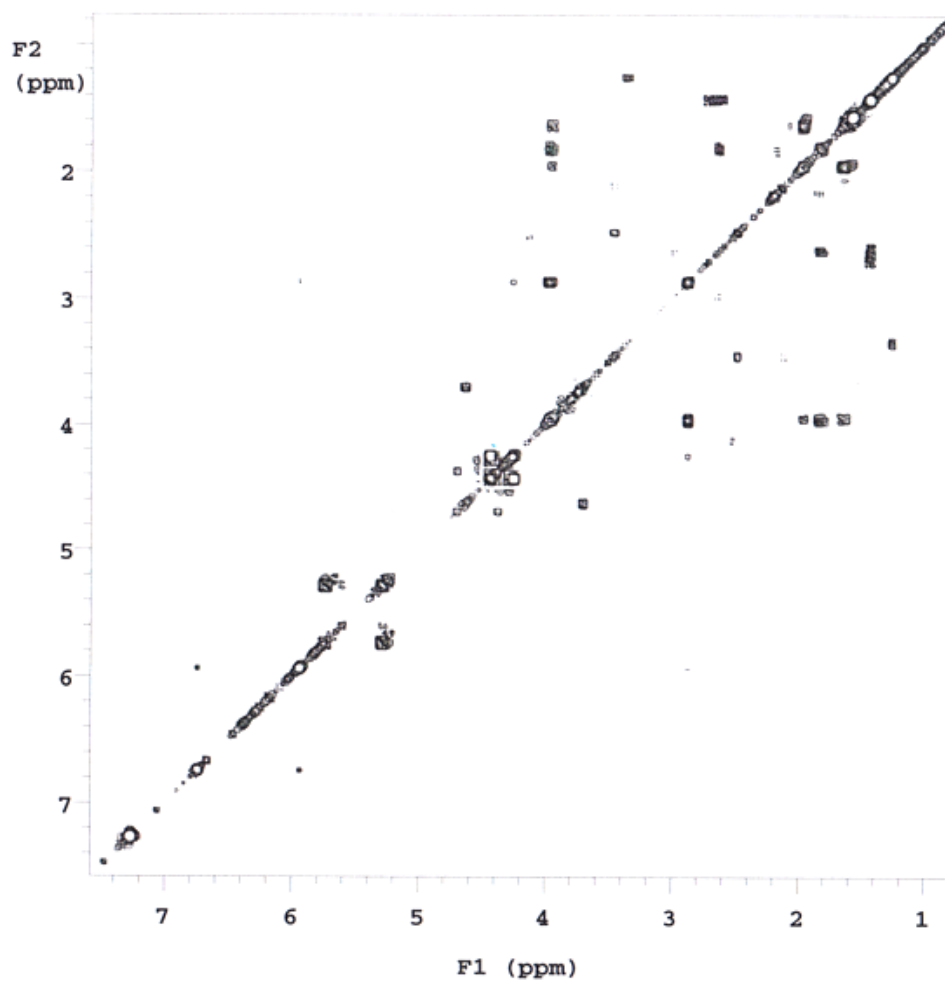
$^1\text{H}$  spectrum (500 MHz) of methylvernoilide (**13**) in  $\text{CDCl}_3$

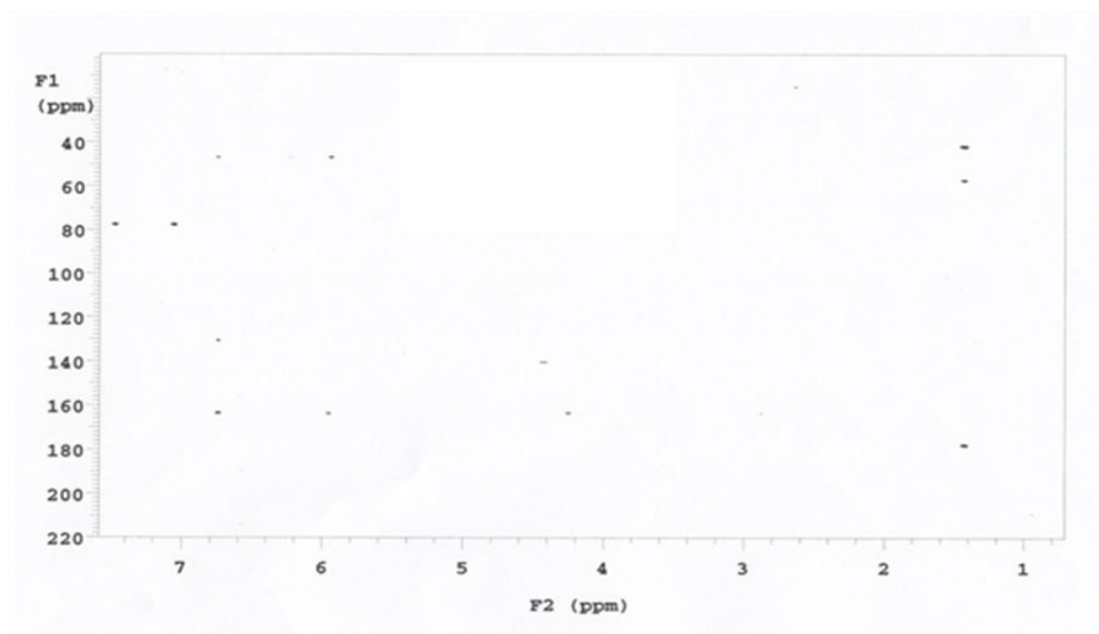


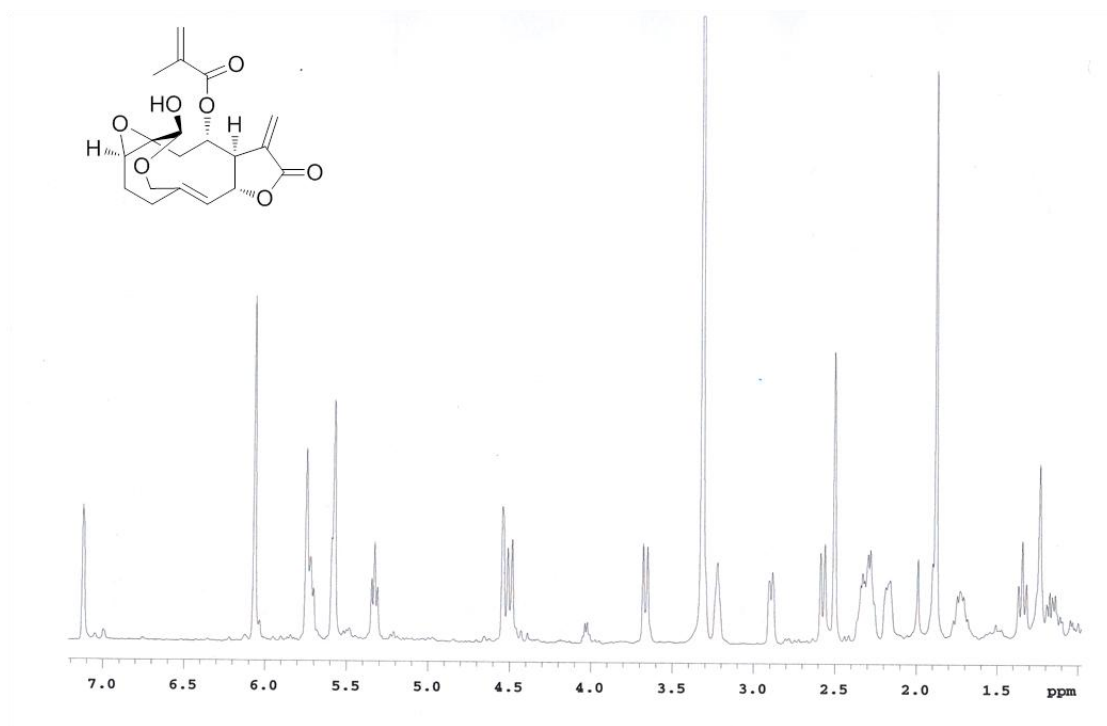
COSY spectrum (500 MHz) of methylvernoilide (**13**) in CDCl<sub>3</sub>

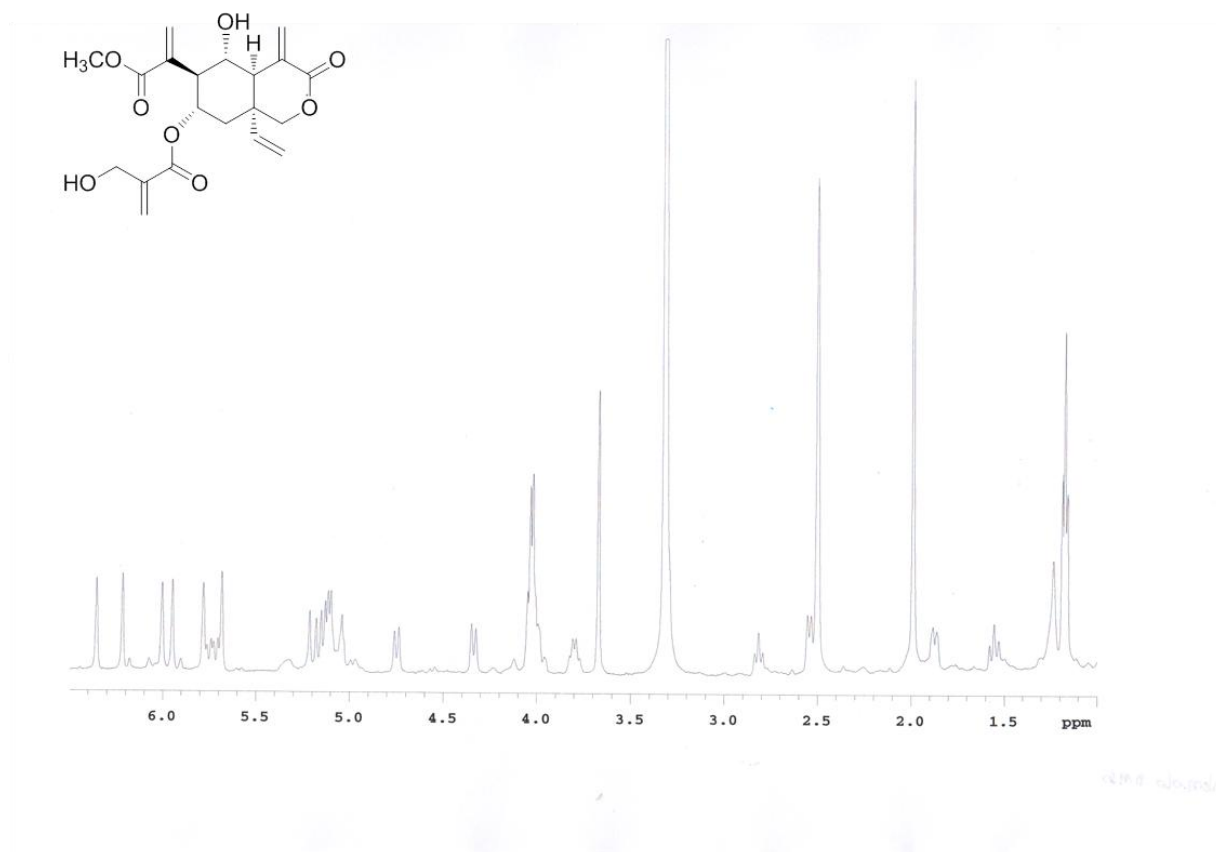
$^1\text{H}$  spectrum (500 MHz) of deoxyvernodalol (**14**) in  $\text{CDCl}_3$ 

$^1\text{H}$  spectrum (500 MHz) of vernomygdalin (**15**) in  $\text{CDCl}_3$ 

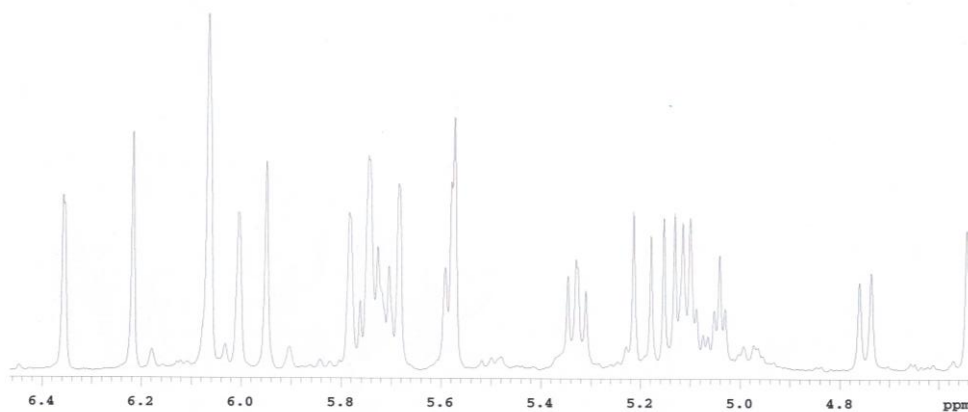
COSY spectrum (500 MHz) of vernomygdalin (**15**) in CDCl<sub>3</sub>

HMBC spectrum (500 MHz) of vernomygdalin (**15**) in CDCl<sub>3</sub>

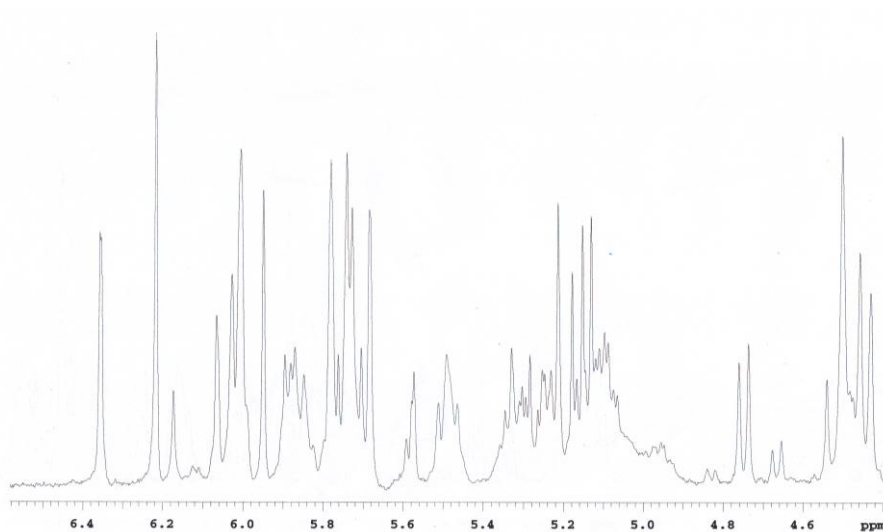
$^1\text{H}$  spectrum (500 MHz) of vernolide (**8**) in DMSO

$^1\text{H}$  spectrum (500 MHz) of vernodalol (9) in DMSO

Low-field region of the  $^1\text{H}$  NMR spectrum (500 MHz) of a 1:1 mixture of vernolide (**8**) and vernodalol (**9**) in  $\text{DMSO-d}_6$ .



Low-field region of the  $^1\text{H}$  NMR spectrum (500 MHz) of a 1:1 mixture of vernolide (**8**) and vernodalol (**9**) in  $\text{DMSO-d}_6$  15 min. after addition of 1 equiv. of cysteamine





## **Acknowledgements**

---

*This work is the result of a multidisciplinary research project. I would like to acknowledge the following researchers, whose contribution has been of key importance:*

- *Prof. Maria Valeria D'Auria and Prof. Angela Zampella (Dipartimento di Farmacia, Università degli Studi di Napoli Federico II, Italy) for the collaboration on the projects on *Theonella swinhoei*.*
- *Prof. Stefano Fiorucci (Dipartimento di Medicina Clinica e Sperimentale, Università di Perugia, Italy) for pharmacological tests in the project on *Theonella swinhoei*.*
- *Dr. Marie-Lise Bourguet-Kondracki and Dr. Arlette Longeon (Unité "Molécules de Communication et Adaptation des Microorganismes", Muséum National d'Histoire Naturelle, Paris, France) for collaboration on the project and for the sample of *Iotrochota purpurea*.*
- *Dr. Laurent Meijer (Man Ros Therapeutics, Roscoff, France) for antikinase tests.*
- *Prof. Annette Habluetzel and Dr. Solomon Abay (Scuola di Scienze del Farmaco e dei Prodotti della Salute, Università di Camerino, Italy) for antimalarial tests and for the sample of *Vernonia amygdalina*.*
- *Prof. Giovanni Appendino (Dipartimento di Scienze Chimiche, Alimentari, Farmaceutiche e Farmacologiche, Università del Piemonte Orientale, Novara, Italy) and Prof. Eduardo Muñoz (Maimónides Institute for Research in Biomedicine of Córdoba, University of Córdoba, Spain) for the collaboration on the project on *V. amygdalina*.*

*It was an honor and a pleasure to collaborate with them.*

*I would like to express my particular thanks to my tutor, Prof. Orazio Taglialatela-Scafati, for essential scientific support and academic guidance during all my research work.*

*My PhD period has been a long and surprising journey. I have to say thank you to people that took this trip with me:*

*Dr. Pina Chianese, for human and professional support, and for friendship.*

*All professors, researchers and PhDs of Department of Pharmacy. In particular, I wish to thank my colleagues Roberta, Gerardo, Antonia, Mila, Emma, Germana, Alessia, for hearty laughs and funny moments.*

*All students and guests (italians and foreign), past and present, in the lab. N13: it was beautiful to teach you and learn from you.*

*All components of Unité MCAM of Muséum National d'Histoire Naturelle of Paris, for welcome and for scientific help during my stay in France; in particular Lihn, Françoise and Johan, for material support, kindness and patience.*

*My "Neapolitan family", Sara and all my flatmates, past and present.*

*My little "Parisian family" Irene, friend and sister too, and all people I met in Paris.*

*All my friends from Potenza, in particular "pink friends": I know that you are always with me.*

*My mother Emanuela, my father Giuseppe and my brother Canio: they always believe in me and in my dreams.*

*Mario, for everything he is doing every day for me and for our projects.*

*In closing, thank you to Naples and thank you to Paris, for unforgettable memories I will have for ever.*